David Hicks * Stefano Curtarolo

Symmetry of Crystals Supplemental

- "Symmetry Relationships Between Crystal Structures" by U. Müller
- "AFLOW Library of Crystallographic Prototypes : Part 1" by M. Mehl et al.
- "International Tables for Crystallography: Volume A" (ITC-A) ed. T. Hahn
- "AFLOW Library of Crystallographic Prototypes : Part 2" by D. Hicks et al.
- "AFLOW-SYM : platform for the complete, automatic and self-consistent symmetry analysis of crystals" by D. Hicks et al.

In crystallography, the types of crystallographic symmetry operations are designated by their **Hermann–Mauguin symbols** (Figs. 4.1 and 4.2). These are:

- 1 for the identical mapping.
- $\overline{1}$ ('one bar') for the inversion.
- Rotations: A number N, $N = 2, 3, 4, 6$. This corresponds to the order of the rotation. If needed, the power of the rotation is mentioned; for example, $6^{-1} = 6^5$, rotation by $-60° = 300°$.
- Screw rotations: N_p designates a screw rotation consisting of a rotation N coupled with a translation parallel to the axis of rotation by p/N of the shortest lattice distance in this direction. The possible symbols are: 2_1 ('two sub one'), 3_1, 3_2, 4_1, 4_2, 4_3, 6_1, 6_2, 6_3, 6_4, and 6_5.
- Rotoinversions: $\overline{3}$, $\overline{4}$ and $\overline{6}$.
- Reflections: m (like *mirror*). m is identical to $\overline{2}$.

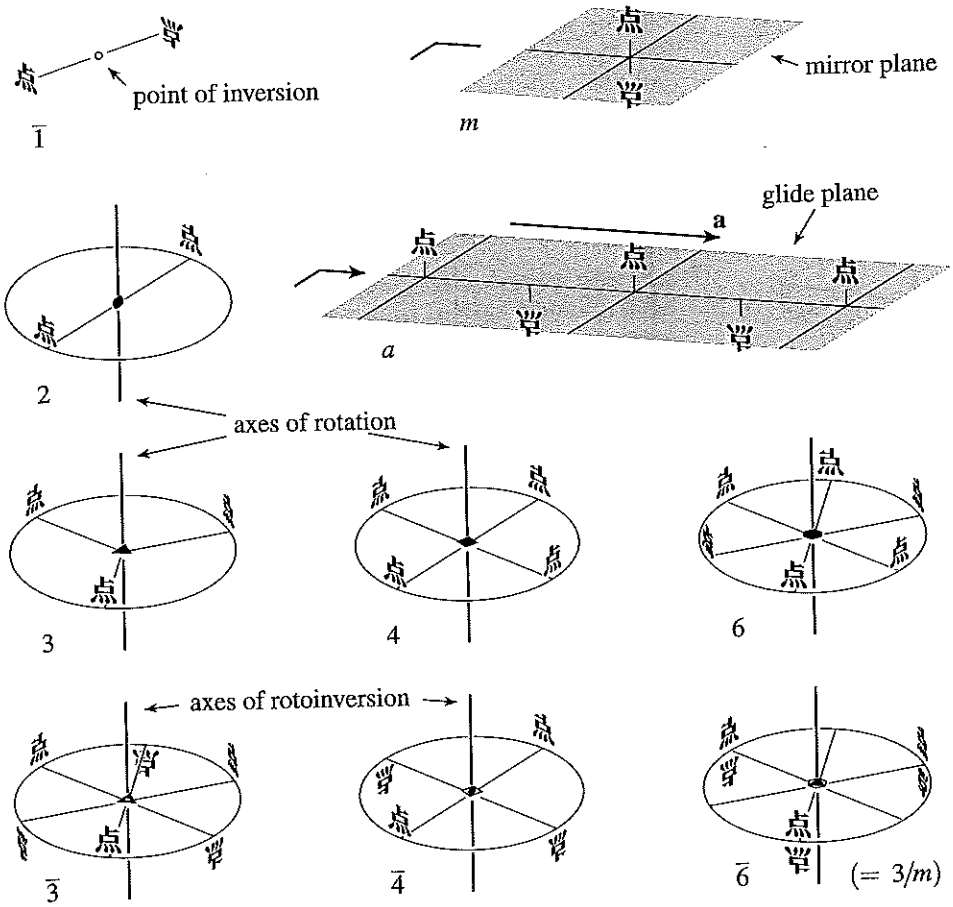

Fig. 4.1 The effect of different symmetry operations on the point 点 (Chinese symbol for point, pronounced diǎn in Chinese, hoshee in Japanese). The symmetry operations are designated by their Hermann–Mauguin symbols and by their graphical symbols.

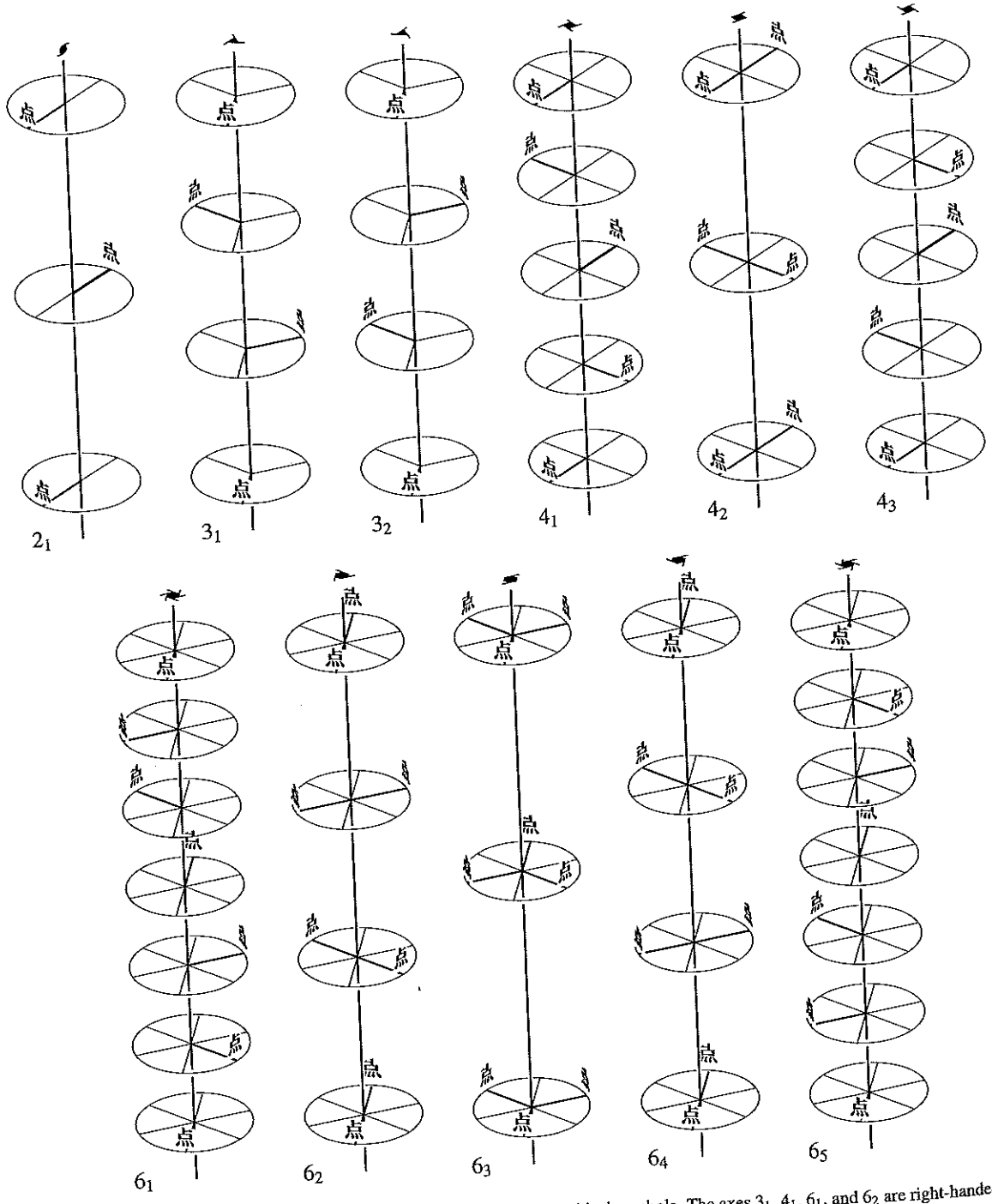

Fig. 4.2 The crystallographic screw axes with their Hermann–Mauguin and graphical symbols. The axes 3_1, 4_1, 6_1, and 6_2 are right-handed, 3_2, 4_3, 6_5, and 6_4 left-handed. One length of translation in the axis direction is depicted.

XX3

Example 6.4
$P2/m2/n2_1/a$, $P2/m2_1/a2/n$, $P2_1/b2/m2/n$, $P2/n2/m2_1/b$, $P2/n2_1/c2/m$, and $P2_1/c2/n2/m$ denote the same orthorhombic space group type No. 53 ($Pmna$).
$P2_1/n2_1/m2_1/a$, $P2_1/n2_1/a2_1/m$, $P2_1/m2_1/n2_1/b$, $P2_1/b2_1/n2_1/m$, $P2_1/m2_1/c2_1/n$, and $P2_1/c2_1/m2_1/n$ are the (full) Hermann–Mauguin symbols of another orthorhombic space group type, No. 62 ($Pnma$).
The symbols mentioned first refer to the conventional settings. The other five are non-conventional settings, with differently oriented bases. More details on non-conventional settings are the subject of Section 9.3.

The point group symbol corresponding to a space group can be obtained from the Hermann–Mauguin symbol in the following way:

(1) the lattice symbol is deleted (P, A, B, C, F, I or R);

(2) all screw components are deleted (the subscript ciphers are deleted);

(3) the letters for glide reflections (a, b, c, n, d, e) are replaced by m.

Examples: $C2/c \rightarrow 2/m$
$P2/m2/n2_1/a$ (short $Pmna$) $\rightarrow 2/m2/m2/m$ (short mmm)
$I\bar{4}2d \rightarrow \bar{4}2m$
$I4_1/a\bar{3}2/d$ (short $Ia\bar{3}d$) $\rightarrow 4/m\bar{3}2/m$ (short $m\bar{3}m$)

6.3.2 Schoenflies symbols

Schoenflies symbols were developed 35 years before the Hermann–Mauguin symbols. Compared to their original form, some of them have been slightly altered.

Rotoreflections are used instead of rotoinversions. A rotoreflection results from a coupling of a rotation with a reflection through a plane perpendicular to the rotation axis. Rotoreflections and rotoinversions state identical facts, but the orders of their rotations differ in pairs if they are not divisible by 4:

rotoreflection (Schoenflies)	S_1	S_2	S_3	S_6	S_4
rotoinversion (Hermann–Mauguin)	$\bar{2} = m$	$\bar{1}$	$\bar{6}^5$	$\bar{3}^2$	$\bar{4}^3$

In Section 6.1.2 the space groups are assigned to crystal classes according to their point groups. SCHOENFLIES introduced symbols for these crystal classes (point-group types) in the following way:

C_1 no symmetry.
C_i a centre of inversion is the only symmetry element.
C_s a plane of reflection is the only symmetry element.
C_N an N-fold rotation axis is the only symmetry element.
S_N an N-fold rotoreflection axis is the only symmetry element; only S_4 is used; for symbols replacing S_3 and S_6 see the following.

XX4

C_{Ni} there is an N-fold rotation axis (N odd) and a centre of inversion on the axis. Identical to S_M with $M = 2 \times N$.

D_N there are N twofold rotation axes perpendicular to an N-fold rotation axis.

C_{Nh} there is a vertical N-fold rotation axis and a horizontal reflection plane. C_{3h} is identical to S_3. There is also an inversion centre if N is even.

C_{Nv} an N-fold vertical rotation axis is situated at the intersection line of N vertical reflection planes.

D_{Nh} there is an N-fold vertical rotation axis, N horizontal twofold rotation axes, N vertical reflection planes, and a horizontal reflection plane. There is also an inversion centre if N is even.

D_{Nd} an N-fold vertical rotation axis contains a $2N$-fold rotoreflection axis and N horizontal twofold axes have bisecting directions between N vertical reflection planes. There is also an inversion centre if N is odd. Identical to S_{Mv} with $M = 2 \times N$.

O_h symmetry of an octahedron and a cube.

O as O_h without reflection planes (rotations of an octahedron).

T_d symmetry of a tetrahedron.

T_h symmetry of an octahedron with twofold instead of fourfold axes.

T as T_d and T_h without reflection planes (rotations of a tetrahedron).

Special non-crystallographic point groups:

I_h symmetry of an icosahedron and pentagonal dodecahedron.

I as I_h without reflection planes (rotations of an icosahedron).

$C_{\infty v}$ symmetry of a cone.

$D_{\infty h}$ symmetry of a cylinder.

K_h symmetry of a sphere.

The space-group types belonging to a crystal class were simply numbered consecutively by SCHOENFLIES; they are distinguished by superscript numbers. The sequence of the crystal classes has not always been kept the same in the space-group tables. Since 1952 the space-group types have been numbered in *International Tables* from 1 to 230, with the consequence that this sequence can hardly be changed.

Some Schoenflies symbols are compared with the corresponding Hermann–Mauguin symbols in Table 6.4 .

Schoenflies space-group symbols have the advantage that they designate the space-group types in a unique way and independent of the selection (setting) of a basis. They have the disadvantage that they only give direct information about the point-group symmetry. They lack information about the lattice type, which is expressed only indirectly by the superscript number.

Schoenflies symbols are concise, but contain less information than Hermann–Mauguin symbols. Schoenflies symbols continue to be very popular in spectroscopy, quantum chemistry, and to designate the symmetry of molecules. In crystallography they are hardly used anymore.

XX5

The primitive cell of a crystal is uniquely specified by these values (up to an arbitrary rotation), and crystallographic articles report the structures in this form.

3. Crystal Systems, Lattices, Space Groups and Standard Lattice Vectors

Having defined what we mean by a lattice, we now discuss the possible lattices that can exist in a three dimensional space, and some of their properties. Here we define our terms following Lax [37], paraphrasing his discussion.

1. A *Crystal* is a periodic array of physical objects. In this article we discuss crystals made of periodic arrays of atoms and their associated electrons.
2. A *Crystal Structure* is the complete description of the crystal including its periodic structure and the contents of the unit cell. In our case, we obtain a complete description of the crystal by specifying the primitive vectors of the periodic lattice $\mathbf{a}_i, (i = 1,2,3)$ and the positions $\mathbf{B}_j, (j = 1,2,3,\ldots,N)$ of the N atoms in a unit cell. The ground state electronic charge density, if desired, can then be computed from these atomic positions.
3. A *Space Group* is the set of all operations (translations, rotations, and reflections) that restore a crystal to itself. In three dimensional space there are 230 space groups.
4. A *Crystal Class* is the point group of the crystal. This includes all possible rotations and reflections (but not translations) that leave the shape of the crystal unchanged. This does not mean that the crystal is transformed into itself, only the point group. In three dimensions there are 32 crystal classes.
5. A *Bravais Lattice* is a collection of points
$$\{t_1\,\mathbf{a}_1 + t_2\,\mathbf{a}_2 + t_3\,\mathbf{a}_3\}, \tag{15}$$
where the t_i are integers and the $\mathbf{a}_i$ are not co-planar, *i.e.* the volume (6) is non-zero. Equation (4) allows some freedom in the choice of $\mathbf{a}_i$, but all choices lead to the same points for a given Bravais lattice. In three dimensions a given crystal class has at least one and a maximum of four Bravais lattices.
6. The *holohedry* of a Bravais lattice is the point group that describes its rotational symmetry.
7. A *Crystal System* is the set of all Bravais lattices that have the same holohedry. In three dimensions there are seven crystal systems, many of which contain multiple Bravais lattices.

In 1891 E. S. Federov [38] and A. Schönflies [39] determined the 230 space groups allowed in three dimensions. Wyckoff [40] tabulated all of these groups, and determined the special atomic coordinates (the Wyckoff positions) allowed for each space group. Here we briefly describe the properties of each crystal system and its associated Bravais lattices, and list the space groups associated with each lattice. In general we will start with the lowest symmetry and go to increasingly higher symmetries. Each space group will be labeled by the International symbol associated with its standard orientation as defined in the International Tables [16]. Alternative orientations of the space groups will lead to different labels. Cockcroft [41] has a complete list of these online.

In the following, we will frequently refer to conventional lattices and primitive, or Bravais, lattices. The basic definition of a Bravais lattice is that it describes the periodicity of a particular system. A conventional lattice, on the other hand, describes the holohedry of all of the Bravais lattices in a given crystal system. Each crystal system has a Bravais lattice that is identical with the conventional lattice.

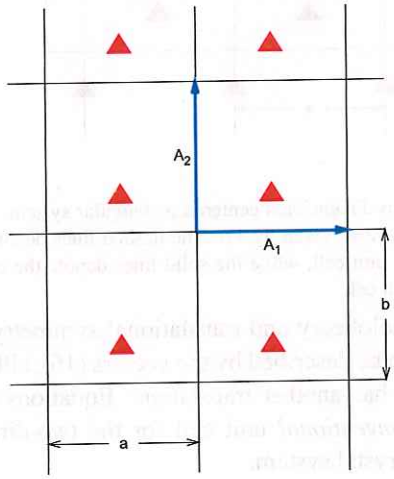

Figure 1: A two-dimensional rectangular system, with primitive vectors $\mathbf{A}_1$ and $\mathbf{A}_2$ given by (16). The solid lines denote the edges of the unit cell.

This is most easily seen in two dimensions. Figure 1 shows a rectangular periodic structure. The periodicity can be described by the primitive vectors

$$\begin{aligned} \mathbf{A}_1 &= a\,\hat{\mathbf{x}} \\ \mathbf{A}_2 &= b\,\hat{\mathbf{y}}. \end{aligned} \tag{16}$$

The solid lines mark the edges of the unit cell for this system.

Next consider the structure shown in Figure 2. It can obviously be described as a periodic structure with primitive vectors (16) and a unit cell bounded by the solid lines. However, it can also be described by the primitive vectors

$$\begin{aligned} \mathbf{a}_1 &= \frac{a}{2}\,\hat{\mathbf{x}} - \frac{b}{2}\,\hat{\mathbf{y}} \\ \mathbf{a}_2 &= \frac{a}{2}\,\hat{\mathbf{x}} + \frac{b}{2}\,\hat{\mathbf{y}}. \end{aligned} \tag{17}$$

XX6

These primitive vectors are shown in Figure 2, and the unit cells associated with these vectors are bounded by the dashed lines.

Both of these structures have the same holohedry, belonging to the two-dimensional rectangular crystal system. They have different Bravais lattices. We can call these lattices *simple* rectangular, shown in Figure 1, and *centered* rectangular, shown in Figure 2.[3]

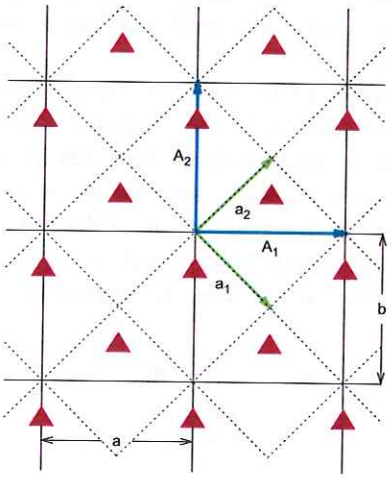

Figure 2: A two-dimensional centered rectangular system, with primitive vectors $\mathbf{a}_1$ and $\mathbf{a}_2$ given by 17. The dashed lines denote the edges of the primitive unit cell, while the solid lines denote the edges of the conventional unit cell.

Both the holohedry and translational symmetry of these structures can be described by the vectors (16), although the centered cell has another translation. Equations (16) then define the *conventional* unit cell for the two-dimensional rectangular crystal system.

The area of the conventional Bravais lattice, ab, is twice that of the centered Bravais lattice, as can be seen from Figure 2, which also shows that the conventional lattice has twice as many triangles (atoms) per unit cell as the Bravais lattice. In three dimensions, as we will see, the conventional lattice can hold one, two, three or four times as many atoms as the underlying Bravais lattice.

Going back to three dimensions, standard crystallographic practice is to report the lattice parameters (a, b, c, α, β, γ) of (13-14) using the conventional lattice, rather than the Bravais lattice. While this may seem arbitrary, the primitive vectors

$$\begin{aligned} \mathbf{a}_1 &= a\,\hat{\mathbf{x}} \\ \mathbf{a}_2 &= \frac{a}{2}\,\hat{\mathbf{x}} + \frac{b}{2}\,\hat{\mathbf{y}} \end{aligned}$$

describe Figure 2 just as well as (17), but have different lengths and angles, and there are a multitude of other possible sets. There is, however, only one logical way to describe the conventional cell, (16). This happens in three dimensions as well. As a general rule,[4] (a, b, c, α, β, γ), and even the number of atoms in a unit cell, are given for the conventional lattice. The size of the primitive cell has to be inferred from knowledge of the space group.

We now consider the seven crystal systems, including the Bravais lattice, and the space groups associated with each Bravais lattice.

As noted above, there are an infinite number of choices for a set of primitive vectors describing a unit cell. In general we follow the choices made by Setyawan and Curtarolo [42]. Differences occur in the monoclinic, base-centered orthorhombic, and rhombohedral lattices, and are discussed in the footnotes.

4. The Triclinic Crystal System

The triclinic is the most general crystal system. All of the other crystal systems can be considered special cases of the triclinic. The primitive vectors are also completely general: their lengths (a, b, c) and angles (α, β, γ) may have arbitrary values. The triclinic system has one Bravais lattice, which is also the conventional lattice for this system.

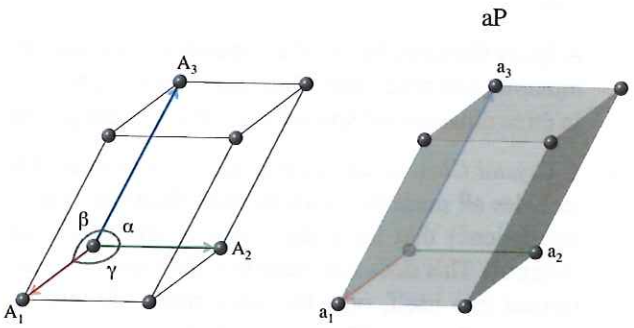

Figure 3: The conventional and simple unit cells for the triclinic crystal system.

4.1. Lattice 1: Triclinic

There are many choices for the primitive vectors in the triclinic system. We make the choice

$$\begin{aligned} \mathbf{a}_1 &= a\,\hat{\mathbf{x}} \\ \mathbf{a}_2 &= b\cos\gamma\,\hat{\mathbf{x}} + b\sin\gamma\,\hat{\mathbf{y}} \\ \mathbf{a}_3 &= c_x\,\hat{\mathbf{x}} + c_y\,\hat{\mathbf{y}} + c_z\,\hat{\mathbf{z}}, \end{aligned} \tag{18}$$

where

$$\begin{aligned} c_x &= c\cos\beta \\ c_y &= \frac{c\,(\cos\alpha - \cos\beta\,\cos\gamma)}{\sin\gamma} \end{aligned}$$

[3] This is called a centered lattice because the primitive vectors (17) point to the center of the rectangular unit cell.

[4] The one exception to this rule is the rhombohedral lattice, which we shall discuss below.

XX7

and

$$c_z = \sqrt{c^2 - c_x^2 - c_y^2}.$$

The volume of the triclinic unit cell is

$$V = a\,b\,c_z\,\sin\gamma. \tag{19}$$

The space groups associated with the triclinic lattice are given in Table 1.

Table 1: The space groups associated with the triclinic Bravais lattice (18) are

1. $P1$	2. $P\bar{1}$

5. The Monoclinic Crystal System

In the monoclinic crystal system, the conventional unit cell is defined by primitive vectors of arbitrary length, where one of the vectors is perpendicular to the other two. Modern convention chooses this vector to be the one with length b (or "unique axis b" in the literature), so that $\alpha = \gamma = \pi/2$ and $\beta \neq \pi/2$.[5]

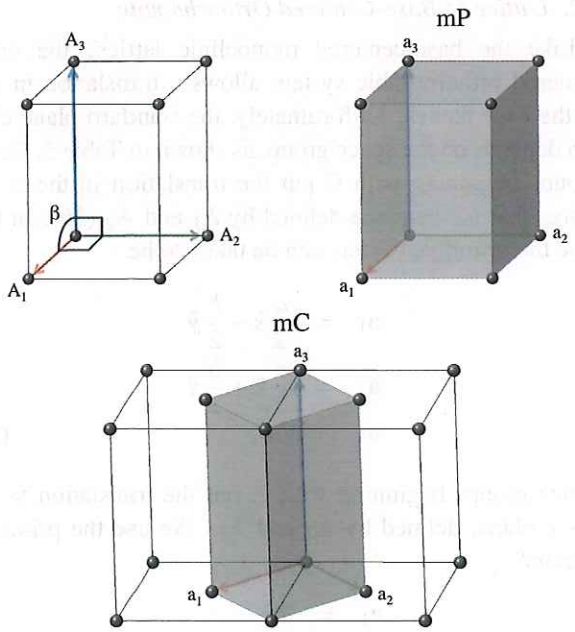

Figure 4: The conventional, simple, and base-centered unit cells for the monoclinic crystal system.

The conventional unit cell can be described by the vectors

$$\begin{aligned}\mathbf{A}_1 &= a\,\hat{\mathbf{x}}\\ \mathbf{A}_2 &= b\,\hat{\mathbf{y}}\\ \mathbf{A}_3 &= c\,\cos\beta\,\hat{\mathbf{x}} + c\,\sin\beta\,\hat{\mathbf{z}},\end{aligned} \tag{20}$$

and the volume of a conventional unit cell is

$$V = a\,b\,c\,\sin\beta. \tag{21}$$

[5]Note that this orientation differs from that of Setyawan and Curtarolo [42], who used an unique axis "a" setting. Their angle α would be γ in our notation.

5.1. Lattice 2: Simple Monoclinic

The simple monoclinic cell is identical to the conventional cell. Its primitive vectors are identical to (20)

$$\begin{aligned}\mathbf{a}_1 &= a\,\hat{\mathbf{x}}\\ \mathbf{a}_2 &= b\,\hat{\mathbf{y}}\\ \mathbf{a}_3 &= c\,\cos\beta\,\hat{\mathbf{x}} + c\,\sin\beta\,\hat{\mathbf{z}},\end{aligned} \tag{22}$$

and the cell volume is just

$$V = a\,b\,c\,\sin\beta. \tag{23}$$

The space groups associated with the simple monoclinic lattice are given in Table 2.

Table 2: The space groups associated with the simple monoclinic Bravais lattice (22) are

3. $P2$	4. $P2_1$	6. Pm
7. Pc	10. $P2/m$	11. $P2_1/m$
13. $P2/c$	14. $P2_1/c$	

5.2. Lattice 3: Base-Centered Monoclinic

The base-centered monoclinic lattice is in the same crystal system as the monoclinic lattice, but its periodicity allows an additional translation in the plane defined by $\mathbf{a}_1$ and $\mathbf{a}_2$, much as in (17). The primitive vectors for the base-centered monoclinic lattice can be written

$$\begin{aligned}\mathbf{a}_1 &= \frac{a}{2}\,\hat{\mathbf{x}} - \frac{b}{2}\,\hat{\mathbf{y}}\\ \mathbf{a}_2 &= \frac{a}{2}\,\hat{\mathbf{x}} + \frac{b}{2}\,\hat{\mathbf{y}}\\ \mathbf{a}_3 &= c\,\cos\beta\,\hat{\mathbf{x}} + c\,\sin\beta\,\hat{\mathbf{z}}.\end{aligned} \tag{24}$$

The volume of the base-centered monoclinic unit cell is

$$V = \left(\frac{1}{2}\right) a\,b\,c\,\sin\beta, \tag{25}$$

half that of the conventional unit cell.

The space groups associated with the base-centered monoclinic lattice are given in Table 3. The labels for these space groups all begin with C, indicating the base-centered translation associated with these groups. This differs from the labels for space groups in Table 1 and Table 2, which begin with P, indicating that the primitive lattice is the conventional lattice.

The *International Tables* offer two representations of the base-centered monoclinic space groups, one for "unique axis b" and one for "unique axis c," where $\alpha \neq \pi/2$ and $\beta = \pi/2$. Space group 5 is then listed as "B2" or "C2" depending on this choice. Most authors ignore this distinction, as will we.

Table 3: The space groups associated with the base-centered monoclinic Bravais lattice (24) are

5. $C2$	8. Cm	9. Cc
12. $C2/m$	15. $C2/c$	

XX8

6. The Orthorhombic Crystal System

In the orthorhombic system, the conventional unit cell is a parallelepiped, defined by three mutually orthogonal vectors of unequal length:

$$\begin{aligned} \mathbf{A}_1 &= a\,\hat{\mathbf{x}} \\ \mathbf{A}_2 &= b\,\hat{\mathbf{y}} \\ \mathbf{A}_3 &= c\,\hat{\mathbf{z}}, \end{aligned} \tag{26}$$

so that $a \neq b \neq c$, but $\alpha = \beta = \gamma = \pi/2$. It is a limiting case of the conventional monoclinic crystal with $\beta \to \pi/2$. The volume of the conventional unit cell is

$$V = a\,b\,c. \tag{27}$$

There are four Bravais lattices in the orthorhombic system.

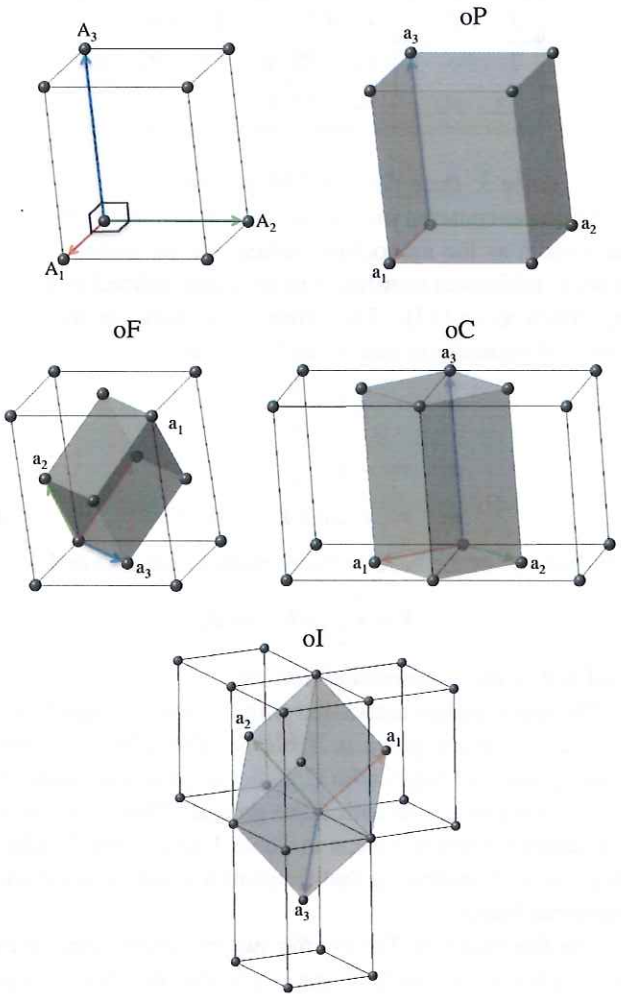

Figure 5: The conventional, simple, face-centered, base-centered, and body-centered unit cells for the orthorhombic crystal system.

6.1. Lattice 4: Simple Orthorhombic

The simple orthorhombic Bravais lattice is identical to the conventional cell

$$\begin{aligned} \mathbf{a}_1 &= a\,\hat{\mathbf{x}} \\ \mathbf{a}_2 &= b\,\hat{\mathbf{y}} \\ \mathbf{a}_3 &= c\,\hat{\mathbf{z}}, \end{aligned} \tag{28}$$

with volume

$$V = a\,b\,c\,. \tag{29}$$

The space groups associated with the simple orthorhombic lattice are given in Table 4.

Table 4: The space groups associated with the simple orthorhombic lattice (28) are

16. *P*222	17. $P222_1$	18. $P2_12_12$
19. $P2_12_12_1$	25. *Pmm*2	26. $Pmc2_1$
27. *Pcc*2	28. *Pma*2	29. $Pca2_1$
30. *Pnc*2	31. $Pmn2_1$	32. *Pba*2
33. $Pna2_1$	34. *Pnn*2	47. *Pmmm*
48. *Pnnn*	49. *Pccm*	50. *Pban*
51. *Pmma*	52. *Pnna*	53. *Pmna*
54. *Pcca*	55. *Pbam*	56. *Pccn*
57. *Pbcm*	58. *Pnnm*	59. *Pmmn*
60. *Pbcn*	61. *Pbca*	62. *Pnma*

6.2. Lattice 5: Base-Centered Orthorhombic

Like the base-centered monoclinic lattice, the base-centered orthorhombic system allows a translation in one of the base planes. Unfortunately, the standard plane chosen depends on the space group, as shown in Table 5. Space groups beginning with C put the translation in the $a - b$ plane, that is, the plane defined by $\mathbf{A}_1$ and $\mathbf{A}_2$ (26). In this case the primitive vectors can be taken to be

$$\begin{aligned} \mathbf{a}_1 &= \frac{a}{2}\,\hat{\mathbf{x}} - \frac{b}{2}\,\hat{\mathbf{y}} \\ \mathbf{a}_2 &= \frac{a}{2}\,\hat{\mathbf{x}} + \frac{b}{2}\,\hat{\mathbf{y}} \\ \mathbf{a}_3 &= c\,\hat{\mathbf{z}}\,. \end{aligned} \tag{30}$$

Space groups beginning with A put the translation in the $b - c$ plane, defined by $\mathbf{A}_2$ and $\mathbf{A}_3$. We use the primitive vectors[6]

$$\begin{aligned} \mathbf{a}_1 &= a\,\hat{\mathbf{x}} \\ \mathbf{a}_2 &= \frac{b}{2}\,\hat{\mathbf{y}} - \frac{c}{2}\,\hat{\mathbf{z}} \\ \mathbf{a}_3 &= \frac{b}{2}\,\hat{\mathbf{y}} + \frac{c}{2}\,\hat{\mathbf{z}}. \end{aligned} \tag{31}$$

In both cases the volume of the primitive unit cell is

$$V = \frac{a\,b\,c}{2}. \tag{32}$$

There are two primitive base-centered orthorhombic unit cells in the conventional orthorhombic unit cell.

[6]Orientation (31) is not used by Setyawan and Curtarolo [42], who only considered centering in the "C" plane defined by $\mathbf{a}_2$ and $\mathbf{a}_3$. A simple rotation brings the vectors into agreement.

Table 5: The space groups associated with the base-centered orthorhombic lattice. Space groups beginning with C place the base-translation in the $a-b$ plane and use primitive vectors (30), while space groups beginning with A put the translation in the $b-c$ plane and use the primitive vectors (31).

20. $C222_1$	21. $C222$	35. $Cmm2$
36. $Cmc2_1$	37. $Ccc2$	38. $Amm2$
39. $Abm2$	40. $Ama2$	41. $Aba2$
63. $Cmcm$	64. $Cmca$	65. $Cmmm$
66. $Cccm$	67. $Cmma$	68. $Ccca$

6.3. Lattice 6: Body-Centered Orthorhombic

The body-centered orthorhombic lattice has the same point group and translational symmetry as the simple orthorhombic system, with the addition of a translation to the center of the parallelepiped defined by the vectors (26). Our standard form of the primitive vectors is

$$\begin{aligned} \mathbf{a}_1 &= -\frac{a}{2}\hat{\mathbf{x}} + \frac{b}{2}\hat{\mathbf{y}} + \frac{c}{2}\hat{\mathbf{z}} \\ \mathbf{a}_2 &= \frac{a}{2}\hat{\mathbf{x}} - \frac{b}{2}\hat{\mathbf{y}} + \frac{c}{2}\hat{\mathbf{z}} \\ \mathbf{a}_3 &= \frac{a}{2}\hat{\mathbf{x}} + \frac{b}{2}\hat{\mathbf{y}} - \frac{c}{2}\hat{\mathbf{z}}. \end{aligned} \tag{33}$$

The volume of the primitive body-centered orthorhombic unit cell is

$$V = \frac{a\,b\,c}{2}. \tag{34}$$

There are two primitive body-centered orthorhombic unit cells in the conventional orthorhombic unit cell. The space groups associated with this lattice, all of which begin with I in standard notation, are given in Table 6.

Table 6: The space groups associated with the body-centered orthorhombic lattice (33).

23. $I222$	24. $I2_12_12_1$	44. $Imm2$
45. $Iba2$	46. $Ima2$	71. $Immm$
72. $Ibam$	73. $Ibca$	74. $Imma$

6.4. Lattice 7: Face-Centered Orthorhombic

While the base-centered monoclinic lattice allows translations to one base plane, the face-centered orthorhombic lattice allows translations to any of the base planes. Our standard choice for the primitive vectors of this system are given by

$$\mathbf{a}_1 = \frac{b}{2}\hat{\mathbf{y}} + \frac{c}{2}\hat{\mathbf{z}} \tag{35}$$

$$\mathbf{a}_2 = \frac{a}{2}\hat{\mathbf{x}} + \frac{c}{2}\hat{\mathbf{z}} \tag{36}$$

$$\mathbf{a}_3 = \frac{a}{2}\hat{\mathbf{x}} + \frac{b}{2}\hat{\mathbf{y}}. \tag{37}$$

The volume of the primitive face-centered orthorhombic unit cell is

$$V = \frac{a\,b\,c}{4}, \tag{38}$$

so that there are four primitive body-centered orthorhombic unit cells in the conventional orthorhombic unit cell. The space groups associated with this lattice, all of which begin with F in standard notation, are given in Table 7.

Table 7: The space groups associated with the face-centered orthorhombic lattice (37).

22. $F222$	42. $Fmm2$	43. $Fdd2$
69. $Fmmm$	70. $Fddd$	

7. The Tetragonal Crystal System

In the tetragonal system, like the orthorhombic, the conventional unit cell is a parallelepiped, but two sides are equal, so that $a = b$ and $c \neq a$, while $\alpha = \beta = \gamma = \pi/2$, and this is a special case of the orthorhombic system. The primitive vectors of the conventional unit cell are

$$\begin{aligned} \mathbf{A}_1 &= a\hat{\mathbf{x}} \\ \mathbf{A}_2 &= a\hat{\mathbf{y}} \\ \mathbf{A}_3 &= c\hat{\mathbf{z}}. \end{aligned} \tag{39}$$

The volume of the conventional unit cell is

$$V = a^2\,c. \tag{40}$$

Given the similarity between the tetragonal and orthorhombic crystal system, we might expect that the tetragonal system would have four Bravais lattices as well, but the additional symmetry generated because $b = a$ reduces this to two. When $b \to a$, the base-centered orthorhombic Bravais lattice (30) becomes a simple tetragonal lattice, while the face-centered orthorhombic lattice (37) can be shown to be identical to a body-centered tetragonal cell [43].

7.1. Lattice 8: Simple Tetragonal

The simple tetragonal Bravais lattice is identical to the conventional cell

$$\begin{aligned} \mathbf{a}_1 &= a\hat{\mathbf{x}} \\ \mathbf{a}_2 &= a\hat{\mathbf{y}} \\ \mathbf{a}_3 &= c\hat{\mathbf{z}}, \end{aligned} \tag{41}$$

with volume

$$V = a^2\,c. \tag{42}$$

The space groups associated with the simple tetragonal lattice are given in Table 8.

XX10

Table 8: The space groups associated with the simple tetragonal lattice (41).

75. $P4$	76. $P4_1$	77. $P4_2$
78. $P4_3$	81. $P\bar{4}$	83. $P4/m$
84. $P4_2/m$	85. $P4/n$	86. $P4_2/n$
89. $P422$	90. $P42_12$	91. $P4_122$
92. $P4_12_12$	93. $P4_222$	94. $P4_22_12$
95. $P4_322$	96. $P4_32_12$	99. $P4mm$
100. $P4bm$	101. $P4_2cm$	102. $P4_2nm$
103. $P4cc$	104. $P4nc$	105. $P4_2mc$
106. $P4_2bc$	111. $P\bar{4}2m$	112. $P\bar{4}2c$
113. $P\bar{4}2_1m$	114. $P\bar{4}2_1c$	115. $P\bar{4}m2$
116. $P\bar{4}c2$	117. $P\bar{4}b2$	118. $P\bar{4}n2$
123. $P4/mmm$	124. $P4/mcc$	125. $P4/nbm$
126. $P4/nnc$	127. $P4/mbm$	128. $P4/mnc$
129. $P4/nmm$	130. $P4/ncc$	131. $P4_2/mmc$
132. $P4_2/mcm$	133. $P4_2/nbc$	134. $P4_2/nnm$
135. $P4_2/mbc$	136. $P4_2/mnm$	137. $P4_2/nmc$
138. $P4_2/ncm$		

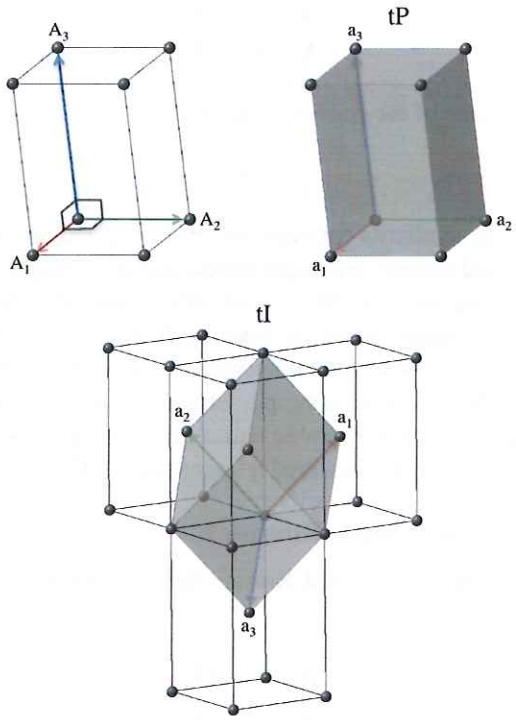

Figure 6: The conventional, simple, and body-centered unit cells for the tetragonal crystal system.

7.2. Lattice 9: Body-Centered Tetragonal

The body-centered tetragonal system has the same point group and translational symmetry as the simple tetragonal system, with the addition of a translation to the center of the parallelepiped defined by the vectors (39). Our standard form of the primitive vectors is

$$\begin{aligned} \mathbf{a}_1 &= -\frac{a}{2}\hat{\mathbf{x}} + \frac{a}{2}\hat{\mathbf{y}} + \frac{c}{2}\hat{\mathbf{z}} \\ \mathbf{a}_2 &= \frac{a}{2}\hat{\mathbf{x}} - \frac{a}{2}\hat{\mathbf{y}} + \frac{c}{2}\hat{\mathbf{z}} \\ \mathbf{a}_3 &= \frac{a}{2}\hat{\mathbf{x}} + \frac{a}{2}\hat{\mathbf{y}} - \frac{c}{2}\hat{\mathbf{z}}. \end{aligned} \tag{43}$$

The volume of the primitive body-centered tetragonal unit cell is

$$V = \frac{a^2 c}{2}. \tag{44}$$

There are two primitive body-centered tetragonal unit cells in the conventional tetragonal unit cell. The space groups associated with this lattice, all of which begin with I in standard notation, are given in Table 9.

Table 9: The space groups associated with the body-centered tetragonal lattice (43).

79. $I4$	80. $I4_1$	82. $I\bar{4}$
87. $I4/m$	88. $I4_1/a$	97. $I422$
98. $I4_122$	107. $I4mm$	108. $I4cm$
109. $I4_1md$	110. $I4_1cd$	119. $I\bar{4}m2$
120. $I\bar{4}c2$	121. $I\bar{4}2m$	122. $I\bar{4}2d$
139. $I4/mmm$	140. $I4/mcm$	141. $I4_1/amd$
142. $I4_1/acd$		

8. The Trigonal Crystal System

The trigonal crystal system is defined by a three-fold rotation axis, and can be generated from the cubic crystal system (Section 10) by stretching the cube along its diagonal. The symmetry requires the primitive vectors to have the form $a = b$, $\alpha = \beta = \pi/2$, $\gamma = 120°$.[7] The trigonal system is a limiting case of the simple monoclinic Bravais lattice (22), with $\beta = 120°$. It can also be obtained from the base-centered orthorhombic Bravais lattice (30) with $b = \sqrt{3}a$. The conventional unit cell is described by the vectors

$$\begin{aligned} \mathbf{A}_1 &= \frac{a}{2}\hat{\mathbf{x}} - \frac{\sqrt{3}}{2}a\hat{\mathbf{y}} \\ \mathbf{A}_2 &= \frac{a}{2}\hat{\mathbf{x}} + \frac{\sqrt{3}}{2}a\hat{\mathbf{y}} \\ \mathbf{A}_3 &= c\hat{\mathbf{z}}. \end{aligned} \tag{45}$$

There are two Bravais lattices in the trigonal system.

[7] We could take $\gamma = 60°$, but in that case the three-fold rotation axis is not obvious from the primitive vectors.

XXII

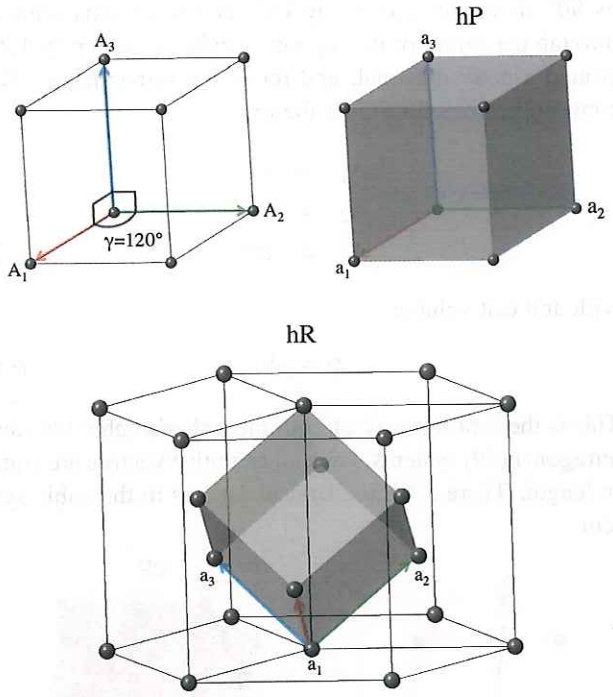

Figure 7: The conventional, simple (hexagonal), and rhombohedral unit cells for the trigonal crystal system.

8.1. Lattice 10: Hexagonal

Somewhat confusingly, what might be called the simple trigonal Bravais lattice is known as the hexagonal lattice. It shares the same primitive vectors, but not point operations, as the hexagonal crystal system (9). The primitive vectors are identical to those of the conventional cell,

$$\begin{aligned} \mathbf{a}_1 &= \frac{a}{2}\,\hat{\mathbf{x}} - \frac{\sqrt{3}}{2}\,a\,\hat{\mathbf{y}} \\ \mathbf{a}_2 &= \frac{a}{2}\,\hat{\mathbf{x}} + \frac{\sqrt{3}}{2}\,a\,\hat{\mathbf{y}} \\ \mathbf{a}_3 &= c\,\hat{\mathbf{z}}. \end{aligned} \tag{46}$$

The volume of the primitive cell is

$$V = \left(\frac{\sqrt{3}}{2}\right) a^2\,c. \tag{47}$$

The space groups associated with the (trigonal) hexagonal lattice are given in Table 10.

Table 10: The space groups associated with the (trigonal) hexagonal lattice (46).

143. $P3$	144. $P3_1$	145. $P3_2$
147. $P\bar{3}$	149. $P312$	150. $P321$
151. $P3_112$	152. $P3_121$	153. $P3_212$
154. $P3_221$	156. $P3m1$	157. $P31m$
158. $P3c1$	159. $P31c$	162. $P\bar{3}1m$
163. $P\bar{3}1c$	164. $P\bar{3}m1$	165. $P\bar{3}c1$

8.2. Lattice 11: Rhombohedral

The rhombohedral Bravais lattice has the periodicity of the conventional trigonal cell (45), with the addition of two translation vectors, $2/3\mathbf{A}_1 + 1/3\mathbf{A}_2 + 1/3\mathbf{A}_3$ and $1/3\mathbf{A}_1 + 2/3\mathbf{A}_2 + 2/3\mathbf{A}_3$.

The primitive vectors can be taken in the form

$$\begin{aligned} \mathbf{a}_1 &= \frac{a}{2}\,\hat{\mathbf{x}} - \frac{a}{\left(2\sqrt{3}\right)}\,\hat{\mathbf{y}} + \frac{c}{3}\,\hat{\mathbf{z}} \\ \mathbf{a}_2 &= \frac{a}{\sqrt{3}}\,\hat{\mathbf{y}} + \frac{c}{3}\,\hat{\mathbf{z}} \\ \mathbf{a}_3 &= -\frac{a}{2}\,\hat{\mathbf{x}} - \frac{a}{\left(2\sqrt{3}\right)}\,\hat{\mathbf{y}} + \frac{c}{3}\,\hat{\mathbf{z}}, \end{aligned} \tag{48}$$

and the volume of the primitive cell is one-third that of the conventional cell,

$$V = \left(\frac{2}{\sqrt{3}}\right) a^2\,c. \tag{49}$$

The vectors (48) are all of identical length,

$$|\mathbf{a}_1| = |\mathbf{a}_2| = |\mathbf{a}_3| = \sqrt{\frac{a^2}{3} + \frac{c^2}{9}} \equiv a', \tag{50}$$

or, equivalently, $a = b = c \equiv a'$, where we designate the common length as a' to distinguish it from the length of the first two vectors in the conventional lattice. The vectors also make equal angles with each other

$$\alpha = \beta = \gamma = \cos^{-1}\left(\frac{2c^2 - 3a^2}{2\left(c^2 + 3a^2\right)}\right). \tag{51}$$

Equations (50) and (51) provide another definition of the rhombohedral lattice. We can show this by writing the primitive vectors in a form that depends only on the common length and separation angle,[8]

$$\begin{aligned} \mathbf{a}_1 &= a'\begin{pmatrix} \sin\frac{\alpha}{2}\,\hat{\mathbf{x}} \\ -\left(\frac{1}{\sqrt{3}}\right)\sin\frac{\alpha}{2}\,\hat{\mathbf{y}} \\ +\sqrt{\frac{1}{3}\left(4\cos^2\frac{\alpha}{2} - 1\right)}\,\hat{\mathbf{z}} \end{pmatrix} \\ \mathbf{a}_2 &= a'\begin{pmatrix} \left(2/\sqrt{3}\right)\sin\frac{\alpha}{2}\,\hat{\mathbf{y}} \\ +\sqrt{\frac{1}{3}\left(4\cos^2\frac{\alpha}{2} - 1\right)}\,\hat{\mathbf{z}} \end{pmatrix} \\ \mathbf{a}_3 &= a'\begin{pmatrix} -\sin\frac{\alpha}{2}\,\hat{\mathbf{x}} \\ -\left(\frac{1}{\sqrt{3}}\right)\sin\frac{\alpha}{2}\,\hat{\mathbf{y}} \\ +\sqrt{\frac{1}{3}\left(4\cos^2\frac{\alpha}{2} - 1\right)}\,\hat{\mathbf{z}} \end{pmatrix}. \end{aligned} \tag{52}$$

We can define the rhombohedral lattice in two ways: as a trigonal lattice with additional translational vectors, or as a

[8] An alternative orientation is given by Setyawan and Curtarolo [42], who only give the primitive vectors in this (a', α) setting. The primitive vectors used for their rhombohedral cell (section A.11) differ from (52) only by the orientation of the vectors relative to the Cartesian axes. Their choice is simpler for computational purposes, but does not show the relationship between (48) and (52).

XX12

"simple" lattice with equal primitive vectors making equal angles with one another. The *International Tables* addresses this ambiguity by listing atomic positions for the rhombohedral lattice in a "hexagonal setting," where all coordinates are referenced to the conventional cell (45), and in a "rhombohedral setting," where the coordinates are referenced to (52). To further confuse matters, the unit cell's dimensions might be reported in terms of (a, c) from (45), or in terms of (a', α) from (52). An article might say that there were N atoms in the rhombohedral cell, or 3N atoms in the conventional cell. One has to pay attention to the context.

In the database, we will report the lattice parameters of the system by giving a and c, since that is the usual crystallographic practice. However, we will record atomic positions using the primitive vectors (48), since computer calculations work best with the smallest number of atoms needed to describe the system.

The space groups associated with the rhombohedral lattice are given in Table 11.

Table 11: The space groups associated with the rhombohedral lattice (48).

146. $R3$	148. $R\bar{3}$	155. $R32$
160. $R3m$	161. $R3c$	166. $R\bar{3}m$
167. $R\bar{3}c$		

9. The Hexagonal Crystal System

The hexagonal crystal system has a six-fold rotation axis. There is only one Bravais lattice in this system, the hexagonal Bravais lattice given by (45) and (46), so the conventional and primitive lattices are equivalent.

The space groups associated with the hexagonal crystal system and lattice are given in Table 12.

Table 12: The space groups associated with the hexagonal crystal system and lattice.

168. $P6$	169. $P6_1$	170. $P6_5$
171. $P6_2$	172. $P6_4$	173. $P6_3$
174. $P\bar{6}$	175. $P6/m$	176. $P6_3/m$
177. $P622$	178. $P6_122$	179. $P6_522$
180. $P6_222$	181. $P6_422$	182. $P6_322$
183. $P6mm$	184. $P6cc$	185. $P6_3cm$
186. $P6_3mc$	187. $P\bar{6}m2$	188. $P\bar{6}c2$
189. $P\bar{6}2m$	190. $P\bar{6}2c$	191. $P6/mmm$
192. $P6/mcc$	193. $P6_3/mcm$	194. $P6_3/mmc$

10. The Cubic Crystal System

The cubic crystal system is defined as having the symmetry of a cube: the conventional unit cell can be rotated by 90° about any axis, or by 180° around an axis running through the center of two opposing cube edges, or by 120° around a body diagonal, and retain the same shape. The conventional cell then takes the form

$$\begin{aligned} \mathbf{A}_1 &= a\,\hat{\mathbf{x}} \\ \mathbf{A}_2 &= a\,\hat{\mathbf{y}} \\ \mathbf{A}_3 &= a\,\hat{\mathbf{z}}, \end{aligned} \tag{53}$$

with unit cell volume

$$V = a^3. \tag{54}$$

This is the limiting case of both the orthorhombic (26) and tetragonal (39) systems when all primitive vectors are equal in length. There are three Bravais lattices in the cubic system.

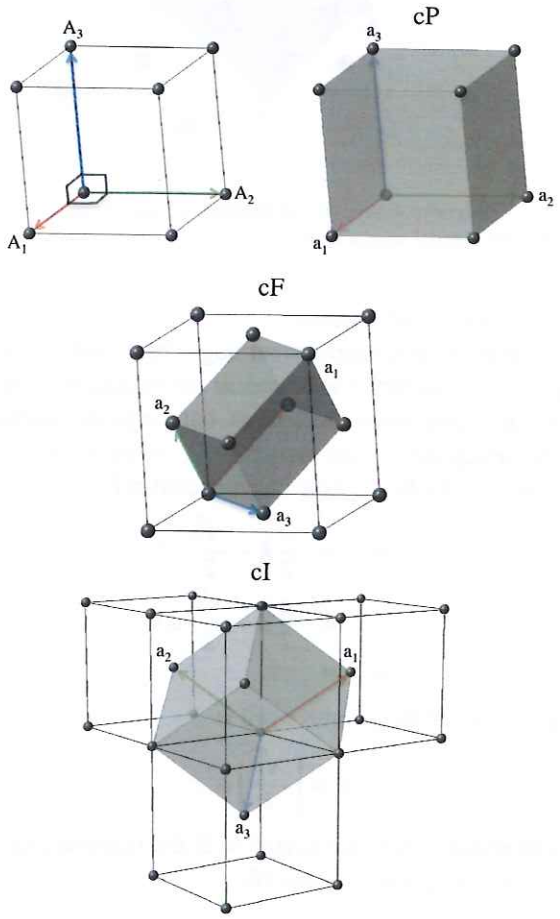

Figure 8: The conventional, simple, face-centered, and and body-centered unit cells for the cubic crystal system.

10.1. Lattice 12: Simple Cubic

The simple cubic system is identical to the conventional cubic unit cell

$$\begin{aligned} \mathbf{a}_1 &= a\,\hat{\mathbf{x}} \\ \mathbf{a}_2 &= a\,\hat{\mathbf{y}} \\ \mathbf{a}_3 &= a\,\hat{\mathbf{z}}, \end{aligned} \tag{55}$$

XX13

with volume

$$V = a^3. \tag{56}$$

This can also be considered as a rhombohedral lattice (48) with $\alpha = \pi/2$. The space groups associated with this lattice are given in Table 13.

Table 13: The space groups associated with the simple cubic lattice (55).

195. $P23$	198. $P2_13$	200. $Pm\bar{3}$
201. $Pn\bar{3}$	205. $Pa\bar{3}$	207. $P432$
208. $P4_232$	212. $P4_332$	213. $P4_132$
215. $P\bar{4}3m$	218. $P\bar{4}3n$	221. $Pm\bar{3}m$
222. $Pn\bar{3}n$	223. $Pm\bar{3}n$	224. $Pn\bar{3}m$

10.2. Lattice 13: Face-Centered Cubic

The face-centered cubic lattice can be derived from its predecessors in the orthorhombic and tetragonal systems, having the same periodicity as its simple cubic parent with the addition of a translation from one corner of the cube to the center of any face. Our standard face-centered cubic primitive vectors have the form

$$\mathbf{a}_1 = \frac{a}{2}\hat{\mathbf{y}} + \frac{a}{2}\hat{\mathbf{z}} \tag{57}$$

$$\mathbf{a}_2 = \frac{a}{2}\hat{\mathbf{x}} + \frac{a}{2}\hat{\mathbf{z}} \tag{58}$$

$$\mathbf{a}_3 = \frac{a}{2}\hat{\mathbf{x}} + \frac{a}{2}\hat{\mathbf{y}}, \tag{59}$$

and the primitive cell volume is

$$V = \frac{a^3}{4}. \tag{60}$$

There are four face-centered cubic primitive cells in the conventional cubic cell. The face-centered cubic lattice can be considered as a rhombohedral lattice where $\alpha = 60°$. The space groups associated with this lattice are given in Table 14.

Table 14: The space groups associated with the face-centered cubic lattice (57).

196. $F23$	202. $Fm\bar{3}$	203. $Fd\bar{3}$
209. $F432$	210. $F4_132$	216. $F\bar{4}3m$
219. $F4\bar{3}c$	225. $Fm\bar{3}m$	226. $Fm\bar{3}c$
227. $Fd\bar{3}m$	228. $Fd\bar{3}c$	

10.3. Lattice 14: Body-Centered Cubic

Like its predecessors in the orthorhombic and tetragonal systems, the body-centered cubic crystal has the same periodicity as its parent with the addition of a translation from one corner of the cube to its center. Our standard body-centered cubic primitive vectors have the form

$$\mathbf{a}_1 = -\frac{a}{2}\hat{\mathbf{x}} + \frac{a}{2}\hat{\mathbf{y}} + \frac{a}{2}\hat{\mathbf{z}} \tag{61}$$

$$\mathbf{a}_2 = \frac{a}{2}\hat{\mathbf{x}} - \frac{a}{2}\hat{\mathbf{y}} + \frac{a}{2}\hat{\mathbf{z}} \tag{62}$$

$$\mathbf{a}_3 = \frac{a}{2}\hat{\mathbf{x}} + \frac{a}{2}\hat{\mathbf{y}} - \frac{a}{2}\hat{\mathbf{z}}, \tag{63}$$

and the primitive cell volume is

$$V = \frac{a^3}{2}. \tag{64}$$

There are two body-centered cubic primitive cells in the conventional cubic cell. The body-centered cubic lattice can be considered as a rhombohedral lattice where $\alpha = \cos^{-1}(-1/3) \approx 109.47°$. The space groups associated with this lattice are given in Table 15.

Table 15: The space groups associated with the body-centered cubic lattice (61).

197. $I23$	199. $I2_13$	204. $Im\bar{3}$
206. $Ia\bar{3}$	211. $I432$	214. $I4_132$
217. $I\bar{4}3m$	220. $I\bar{4}3d$	229. $Im\bar{3}m$
230. $Ia\bar{3}d$		

11. Locating the atoms in the unit cell

Section 3 describes the Bravais lattices that occur in three dimensional space. Just describing the lattice, however, does not describe the complete crystal system. We must also find the positions of the atoms in the primitive (or conventional) unit cell. These positions are restricted by the crystal system, Bravais lattice, and space group that the system is in.

We will illustrate this using our two-dimensional centered rectangular lattice (17). There are seventeen plane groups in two dimensions [44]. Two are centered rectangular plane groups, $c1m1$ (#5) and $c2mm$ (#9). If we look at the International Tables [16] or Bilbao server [17], we will find a table that looks much like Table 16.

Table 16: The Wyckoff positions for the plane group $c1m1$ (#5). This is a somewhat simplified version of the table, as we neglect the site symmetries of each point. See Refs. [16] and [17] for complete information.

Wyckoff Position	Coordinates +(1/2, 1/2)
(4b)	(x,y) (-x, y)
(2a)	(0,y)

This table gives a set of Wyckoff positions, so called because Wyckoff denoted all possible positions for the 230

XX14

International Tables for Crystallography (2006). Vol. A, Chapter 1.4, pp. 7–11.

1.4. Graphical symbols for symmetry elements in one, two and three dimensions

BY TH. HAHN

1.4.1. Symmetry planes normal to the plane of projection (three dimensions) and symmetry lines in the plane of the figure (two dimensions)

Symmetry plane or symmetry line	Graphical symbol	Glide vector in units of lattice translation vectors parallel and normal to the projection plane	Printed symbol
Reflection plane, mirror plane Reflection line, mirror line (two dimensions)		None	*m*
'Axial' glide plane Glide line (two dimensions)		$\frac{1}{2}$ lattice vector along line in projection plane $\frac{1}{2}$ lattice vector along line in figure plane	*a*, *b* or *c* *g*
'Axial' glide plane		$\frac{1}{2}$ lattice vector normal to projection plane	*a*, *b* or *c*
'Double' glide plane* (in centred cells only)		*Two* glide vectors: $\frac{1}{2}$ along line parallel to projection plane and $\frac{1}{2}$ normal to projection plane	*e*
'Diagonal' glide plane		*One* glide vector with *two* components: $\frac{1}{2}$ along line parallel to projection plane, $\frac{1}{2}$ normal to projection plane	*n*
'Diamond' glide plane† (pair of planes; in centred cells only)		$\frac{1}{4}$ along line parallel to projection plane, combined with $\frac{1}{4}$ normal to projection plane (arrow indicates direction parallel to the projection plane for which the normal component is positive)	*d*

* For further explanations of the 'double' glide plane *e* see Note (iv) below and Note (x) in Section 1.3.2.
† See footnote § to Section 1.3.1.

1.4.2. Symmetry planes parallel to the plane of projection

Symmetry plane	Graphical symbol*	Glide vector in units of lattice translation vectors parallel to the projection plane	Printed symbol
Reflection plane, mirror plane	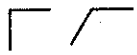	None	*m*
'Axial' glide plane	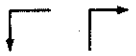	$\frac{1}{2}$ lattice vector in the direction of the arrow	*a*, *b* or *c*
'Double' glide plane† (in centred cells only)		*Two* glide vectors: $\frac{1}{2}$ in either of the directions of the two arrows	*e*
'Diagonal' glide plane		*One* glide vector with *two* components $\frac{1}{2}$ in the direction of the arrow	*n*
'Diamond' glide plane‡ (pair of planes; in centred cells only)		$\frac{1}{2}$ in the direction of the arrow; the glide vector is always half of a centring vector, *i.e.* one quarter of a diagonal of the conventional face-centred cell	*d*

* The symbols are given at the upper left corner of the space-group diagrams. A fraction *h* attached to a symbol indicates two symmetry planes with 'heights' *h* and $h+\frac{1}{2}$ above the plane of projection; *e.g.* $\frac{1}{8}$ stands for $h=\frac{1}{8}$ and $\frac{5}{8}$. No fraction means $h=0$ and $\frac{1}{2}$ (*cf.* Section 2.2.6).
† For further explanations of the 'double' glide plane *e* see Note (iv) below and Note (x) in Section 1.3.2.
‡ See footnote § to Section 1.3.1.

XX 15

1.4.3. Symmetry planes inclined to the plane of projection (in cubic space groups of classes $\bar{4}3m$ and $m\bar{3}m$ only)

Symmetry plane	Graphical symbol* for planes normal to [011] and [01$\bar{1}$]	Graphical symbol* for planes normal to [101] and [10$\bar{1}$]	Glide vector in units of lattice translation vectors for planes normal to [011] and [01$\bar{1}$]	Glide vector in units of lattice translation vectors for planes normal to [101] and [10$\bar{1}$]	Printed symbol
Reflection plane, mirror plane	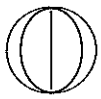		None	None	*m*
'Axial' glide plane		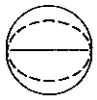	$\frac{1}{2}$ lattice vector along [100]	$\frac{1}{2}$ lattice vector along [010]	*a* or *b*
'Axial' glide plane	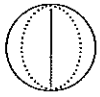		$\frac{1}{2}$ lattice vector along [01$\bar{1}$] or along [011]	$\frac{1}{2}$ lattice vector along [10$\bar{1}$] or along [101]	
'Double' glide plane† [in space groups $I\bar{4}3m$ (217) and $Im\bar{3}m$ (229) only]			*Two* glide vectors: $\frac{1}{2}$ along [100] *and* $\frac{1}{2}$ along [01$\bar{1}$] or $\frac{1}{2}$ along [011]	*Two* glide vectors: $\frac{1}{2}$ along [010] *and* $\frac{1}{2}$ along [10$\bar{1}$] or $\frac{1}{2}$ along [101]	*e*
'Diagonal' glide plane	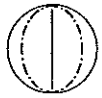	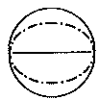	*One* glide vector: $\frac{1}{2}$ along [11$\bar{1}$] or along [111]‡	*One* glide vector: $\frac{1}{2}$ along [11$\bar{1}$] or along [111]‡	*n*
'Diamond' glide plane¶ (pair of planes; in centred cells only)	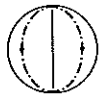	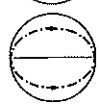	$\frac{1}{2}$ along [1$\bar{1}$1] or along [111]§	$\frac{1}{2}$ along [$\bar{1}$11] or along [111]§	*d*
	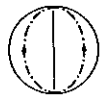	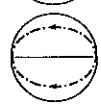	$\frac{1}{2}$ along [$\bar{1}\bar{1}$1] or along [$\bar{1}$11]§	$\frac{1}{2}$ along [$\bar{1}\bar{1}$1] or along [1$\bar{1}$1]§	

* The symbols represent orthographic projections. In the cubic space-group diagrams, complete orthographic projections of the symmetry elements around high-symmetry points, such as $0,0,0;\ \frac{1}{2},0,0;\ \frac{1}{4},\frac{1}{4},0$, are given as 'inserts'.

† For further explanations of the 'double' glide plane *e* see Note (iv) below and Note (x) in Section 1.3.2.

‡ In the space groups $F\bar{4}3m$ (216), $Fm\bar{3}m$ (225) and $Fd\bar{3}m$ (227), the shortest lattice translation vectors in the glide directions are $\mathbf{t}(1,\frac{1}{2},\frac{\bar{1}}{2})$ or $\mathbf{t}(1,\frac{1}{2},\frac{1}{2})$ and $\mathbf{t}(\frac{1}{2},1,\frac{\bar{1}}{2})$ or $\mathbf{t}(\frac{1}{2},1,\frac{1}{2})$, respectively.

§ The glide vector is half of a centring vector, *i.e.* one quarter of the diagonal of the conventional body-centred cell in space groups $I\bar{4}3d$ (220) and $Ia\bar{3}d$ (230).

¶ See footnote § to Section 1.3.1.

1.4.4. Notes on graphical symbols of symmetry planes

(i) The *graphical* symbols and their explanations (columns 2 and 3) are independent of the projection direction and the labelling of the basis vectors. They are, therefore, applicable to any projection diagram of a space group. The *printed* symbols of *glide planes* (column 4), however, may change with a change of the basis vectors, as shown by the following example.

In the rhombohedral space groups $R3c$ (161) and $R\bar{3}c$ (167), the dotted line refers to a *c* glide when described with 'hexagonal axes' and projected along [001]; for a description with 'rhombohedral axes' and projection along [111], the same dotted glide plane would be called *n*. The dash-dotted *n* glide in the hexagonal description becomes an *a*, *b* or *c* glide in the rhombohedral description; *cf.* footnote † to Section 1.3.1.

(ii) The graphical symbols for glide planes in column 2 are not only used for the glide planes defined in Chapter 1.3, but also for the further glide planes *g* which are mentioned in Section 1.3.2 (Note x) and listed in Table 4.3.2.1; they are explained in Sections 2.2.9 and 11.1.2.

(iii) In monoclinic space groups, the 'parallel' glide vector of a glide plane may be along a lattice translation vector which is inclined to the projection plane.

(iv) In 1992, the International Union of Crystallography introduced the 'double' glide plane *e* and the graphical symbol ·–·–· for *e* glide planes oriented 'normal' and 'inclined' to the plane of projection (de Wolff *et al.*, 1992); for details of *e* glide planes see Chapter 1.3. Note that the graphical symbol $\overrightarrow{\downarrow}$ for *e* glide planes oriented 'parallel' to the projection plane has already been used in *IT* (1935) and *IT* (1952).

XX16

1.4.5. Symmetry axes normal to the plane of projection and symmetry points in the plane of the figure

Symmetry axis or symmetry point	Graphical symbol*	Screw vector of a right-handed screw rotation in units of the shortest lattice translation vector parallel to the axis	Printed symbol (partial elements in parentheses)
Identity	None	None	1
Twofold rotation axis Twofold rotation point (two dimensions)		None	2
Twofold screw axis: '2 sub 1'		$\frac{1}{2}$	2_1
Threefold rotation axis Threefold rotation point (two dimensions)		None	3
Threefold screw axis: '3 sub 1'		$\frac{1}{3}$	3_1
Threefold screw axis: '3 sub 2'		$\frac{2}{3}$	3_2
Fourfold rotation axis Fourfold rotation point (two dimensions)		None	4 (2)
Fourfold screw axis: '4 sub 1'	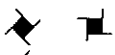	$\frac{1}{4}$	4_1 (2_1)
Fourfold screw axis: '4 sub 2'		$\frac{1}{2}$	4_2 (2)
Fourfold screw axis: '4 sub 3'		$\frac{3}{4}$	4_3 (2_1)
Sixfold rotation axis Sixfold rotation point (two dimensions)		None	6 (3,2)
Sixfold screw axis: '6 sub 1'		$\frac{1}{6}$	6_1 ($3_1, 2_1$)
Sixfold screw axis: '6 sub 2'		$\frac{1}{3}$	6_2 (3_2, 2)
Sixfold screw axis: '6 sub 3'		$\frac{1}{2}$	6_3 (3, 2_1)
Sixfold screw axis: '6 sub 4'		$\frac{2}{3}$	6_4 (3_1, 2)
Sixfold screw axis: '6 sub 5'		$\frac{5}{6}$	6_5 ($3_2, 2_1$)
Centre of symmetry, inversion centre: '1 bar' Reflection point, mirror point (one dimension)		None	$\bar{1}$
Inversion axis: '3 bar'		None	$\bar{3}$ (3, $\bar{1}$)
Inversion axis: '4 bar'		None	$\bar{4}$ (2)
Inversion axis: '6 bar'		None	$\bar{6} \equiv 3/m$
Twofold rotation axis with centre of symmetry		None	$2/m$ ($\bar{1}$)
Twofold screw axis with centre of symmetry		$\frac{1}{2}$	$2_1/m$ ($\bar{1}$)
Fourfold rotation axis with centre of symmetry		None	$4/m$ ($\bar{4}$, 2, $\bar{1}$)
'4 sub 2' screw axis with centre of symmetry		$\frac{1}{2}$	$4_2/m$ ($\bar{4}$, 2, $\bar{1}$)
Sixfold rotation axis with centre of symmetry		None	$6/m$ ($\bar{6}, \bar{3}$, 3, 2, $\bar{1}$)
'6 sub 3' screw axis with centre of symmetry		$\frac{1}{2}$	$6_3/m$ ($\bar{6}, \bar{3}$, 3, 2_1, $\bar{1}$)

* Notes on the 'heights' h of symmetry points $\bar{1}$, $\bar{3}$, $\bar{4}$ and $\bar{6}$:

(1) Centres of symmetry $\bar{1}$ and $\bar{3}$, as well as inversion points $\bar{4}$ and $\bar{6}$ on $\bar{4}$ and $\bar{6}$ axes parallel to [001], occur in pairs at 'heights' h and $h+\frac{1}{2}$. In the space-group diagrams, only one fraction h is given, *e.g.* $\frac{1}{4}$ stands for $h=\frac{1}{4}$ and $\frac{3}{4}$. No fraction means $h=0$ and $\frac{1}{2}$. In *cubic* space groups, however, because of their complexity, *both* fractions are given for vertical $\bar{4}$ axes, including $h=0$ and $\frac{1}{2}$.

(2) Symmetries $4/m$ and $6/m$ contain vertical $\bar{4}$ and $\bar{6}$ axes; their $\bar{4}$ and $\bar{6}$ inversion points coincide with the centres of symmetry. This is not indicated in the space-group diagrams.

(3) Symmetries $4_2/m$ and $6_3/m$ also contain vertical $\bar{4}$ and $\bar{6}$ axes, but their $\bar{4}$ and $\bar{6}$ inversion points alternate with the centres of symmetry; *i.e.* $\bar{1}$ points at h and $h+\frac{1}{2}$ interleave with $\bar{4}$ or $\bar{6}$ points at $h+\frac{1}{4}$ and $h+\frac{3}{4}$. In the tetragonal and hexagonal space-group diagrams, only *one* fraction for $\bar{1}$ and one for $\bar{4}$ or $\bar{6}$ is given. In the cubic diagrams, *all four* fractions are listed for $4_2/m$; *e.g.* $Pm\bar{3}n$ (No. 223): $\bar{1}$: 0, $\frac{1}{2}$; $\bar{4}$: $\frac{1}{4}$, $\frac{3}{4}$.

XXM

1.4.6. Symmetry axes parallel to the plane of projection

Symmetry axis	Graphical symbol*	Screw vector of a right-handed screw rotation in units of the shortest lattice translation vector parallel to the axis	Printed symbol (partial elements in parentheses)
Twofold rotation axis		None	2
Twofold screw axis: '2 sub 1'		$\frac{1}{2}$	2_1
Fourfold rotation axis		None	4 (2)
Fourfold screw axis: '4 sub 1'		$\frac{1}{4}$	4_1 (2_1)
Fourfold screw axis: '4 sub 2'		$\frac{1}{2}$	4_2 (2)
Fourfold screw axis: '4 sub 3'		$\frac{3}{4}$	4_3 (2_1)
Inversion axis: '4 bar'		None	$\bar{4}$ (2)
Inversion point on '4 bar'-axis		–	$\bar{4}$ point

in cubic space groups only

* The symbols for horizontal symmetry axes are given outside the unit cell of the space-group diagrams. *Twofold* axes always occur in pairs, at 'heights' h and $h+\frac{1}{2}$ above the plane of projection; here, a fraction h attached to such a symbol indicates two axes with heights h and $h+\frac{1}{2}$. No fraction stands for $h=0$ and $\frac{1}{2}$. The rule of pairwise occurrence, however, is not valid for the horizontal *fourfold* axes in cubic space groups; here, *all* heights are given, including $h=0$ and $\frac{1}{2}$. This applies also to the horizontal $\bar{4}$ axes and the $\bar{4}$ inversion points located on these axes.

1.4.7. Symmetry axes inclined to the plane of projection (in cubic space groups only)

Symmetry axis	Graphical symbol*	Screw vector of a right-handed screw rotation in units of the shortest lattice translation vector parallel to the axis	Printed symbol (partial elements in parentheses)
Twofold rotation axis	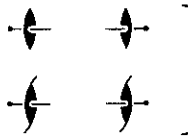	None	2
Twofold screw axis: '2 sub 1'		$\frac{1}{2}$	2_1
Threefold rotation axis	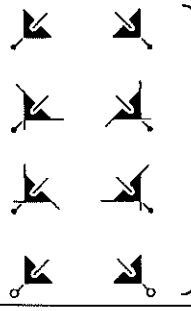	None	3
Threefold screw axis: '3 sub 1'		$\frac{1}{3}$	3_1
Threefold screw axis: '3 sub 2'		$\frac{2}{3}$	3_2
Inversion axis: '3 bar'		None	$\bar{3}$ ($3, \bar{1}$)

Parallel to a face diagonal of the cube

Parallel to a body diagonal of the cube

* The dots mark the intersection points of axes with the plane at $h=0$. In some cases, the intersection points are obscured by symbols of symmetry elements with height $h \geq 0$; examples: $Fd\bar{3}$ (203), origin choice 2; $Pn\bar{3}n$ (222), origin choice 2; $Pm\bar{3}n$ (223); $Im\bar{3}m$ (229); $Ia\bar{3}d$ (230).

XX 18

(3) The *short international* (Hermann–Mauguin) *symbol* for the point group to which the plane or space group belongs (*cf.* Chapter 12.1).
(4) The name of the *crystal system* (*cf.* Table 2.1.2.1).

Second line

(5) The sequential *number of the plane or space group*, as introduced in *IT* (1952).
(6) The *full international* (Hermann–Mauguin) *symbol* for the plane or space group.

For monoclinic space groups, the headline of every description contains the full symbol appropriate to that description.

(7) The *Patterson symmetry* (see Section 2.2.5).

Third line

This line is used, where appropriate, to indicate origin choices, settings, cell choices and coordinate axes (see Section 2.2.2). For five orthorhombic space groups, an entry 'Former space-group symbol' is given; *cf.* Chapter 1.3, Note (x).

2.2.4. International (Hermann–Mauguin) symbols for plane groups and space groups (*cf.* Chapter 12.2)

2.2.4.1. *Present symbols*

Both the short and the full Hermann–Mauguin symbols consist of two parts: (i) a letter indicating the centring type of the conventional cell, and (ii) a set of characters indicating symmetry elements of the space group (modified point-group symbol).

(i) The letters for the centring types of cells are listed in Chapter 1.2. Lower-case letters are used for two dimensions (nets), capital letters for three dimensions (lattices).

(ii) The one, two or three entries after the centring letter refer to the one, two or three kinds of *symmetry directions* of the lattice belonging to the space group. These symmetry directions were called *blickrichtungen* by Heesch (1929). Symmetry directions occur either as singular directions (as in the monoclinic and orthorhombic crystal systems) or as sets of symmetrically equivalent symmetry directions (as in the higher-symmetrical crystal systems). Only one representative of each set is required. The (sets of) symmetry directions and their sequence for the different lattices are summarized in Table 2.2.4.1. According to their position in this sequence, the symmetry directions are referred to as 'primary', 'secondary' and 'tertiary' directions.

This sequence of lattice symmetry directions is transferred to the sequence of positions in the corresponding Hermann–Mauguin space-group symbols. Each position contains one or two characters designating symmetry elements (axes and planes) of the space group (*cf.* Chapter 1.3) that occur for the corresponding lattice symmetry direction. Symmetry planes are represented by their normals; if a symmetry axis and a normal to a symmetry plane are parallel, the two characters (symmetry symbols) are separated by a slash, as in $P6_3/m$ or $P2/m$ ('two over m').

For the different crystal lattices, the Hermann–Mauguin space-group symbols have the following form:

(i) *Triclinic* lattices have no symmetry direction because they have, in addition to translations, only centres of symmetry, $\bar{1}$. Thus, only two triclinic space groups, $P1$ (1) and $P\bar{1}$ (2), exist.

(ii) *Monoclinic* lattices have one symmetry direction. Thus, for monoclinic space groups, only one position after the centring letter is needed. This is used in the *short* Hermann–Mauguin symbols, as in $P2_1$. Conventionally, the symmetry direction is labelled either b ('unique axis b') or c ('unique axis c').

In order to distinguish between the different settings, the *full* Hermann–Mauguin symbol contains two extra entries '1'. They indicate those two axial directions that are not symmetry directions of the lattice. Thus, the symbols $P121$, $P112$ and $P211$ show that the b axis, c axis and a axis, respectively, is the unique axis. Similar considerations apply to the three *rectangular* plane groups *pm, pg* and *cm* (*e.g.* plane group No. 5: short symbol *cm*, full symbol $c1m1$ or $c11m$).

(iii) *Rhombohedral* lattices have two kinds of symmetry directions. Thus, the symbols of the seven rhombohedral space groups contain only two entries after the letter R, as in $R3m$ or $R3c$.

(iv) *Orthorhombic, tetragonal, hexagonal* and *cubic* lattices have three kinds of symmetry directions. Hence, the corresponding space-group symbols have three entries after the centring letter, as in *Pmna*, $P3m1$, *P6cc* or $Ia\bar{3}d$.

Lattice symmetry directions that carry no symmetry elements for the space group under consideration are represented by the symbol '1', as in $P3m1$ and $P31m$. If no misinterpretation is possible, entries '1' at the end of a space-group symbol are omitted, as in $P6$ (instead of $P611$), $R\bar{3}$ (instead of $R\bar{3}1$), $I4_1$ (instead of $I4_111$), $F23$ (instead of $F231$); similarly for the plane groups.

Table 2.2.4.1. *Lattice symmetry directions for two and three dimensions*

Directions that belong to the same set of equivalent symmetry directions are collected between braces. The first entry in each set is taken as the representative of that set.

Lattice	Symmetry direction (position in Hermann–Mauguin symbol)		
	Primary	Secondary	Tertiary
Two dimensions			
Oblique	Rotation point in plane		
Rectangular		[10]	[01]
Square		{[10], [01]}	{[1$\bar{1}$], [11]}
Hexagonal		{[10], [01], [$\bar{1}\bar{1}$]}	{[1$\bar{1}$], [12], [$\bar{2}$1]}
Three dimensions			
Triclinic	None		
Monoclinic*	[010] ('unique axis b') [001] ('unique axis c')		
Orthorhombic	[100]	[010]	[001]
Tetragonal	[001]	{[100], [010]}	{[1$\bar{1}$0], [110]}
Hexagonal	[001]	{[100], [010], [$\bar{1}\bar{1}$0]}	{[1$\bar{1}$0], [120], [$\bar{2}\bar{1}$0]}
Rhombohedral (hexagonal axes)	[001]	{[100], [010], [$\bar{1}\bar{1}$0]}	
Rhombohedral (rhombohedral axes)	[111]	{[1$\bar{1}$0], [01$\bar{1}$], [$\bar{1}$01]}	
Cubic	{[100], [010], [001]}	{[111], [1$\bar{1}\bar{1}$], [$\bar{1}$1$\bar{1}$], [$\bar{1}\bar{1}$1]}	{[1$\bar{1}$0] [110], [01$\bar{1}$] [011], [$\bar{1}$01] [101]}

* For the full Hermann–Mauguin symbols see Section 2.2.4.1.

XX 19

(1) $P2_1/c$ (2) C_{2h}^5 (3) $2/m$ (4) Monoclinic

(5) No. 14 (6) $P12_1/c1$ (7) Patterson symmetry $P12/m1$

UNIQUE AXIS b, CELL CHOICE 1

(8)

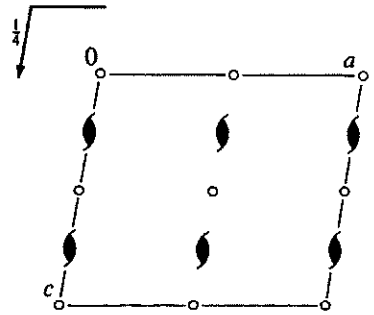

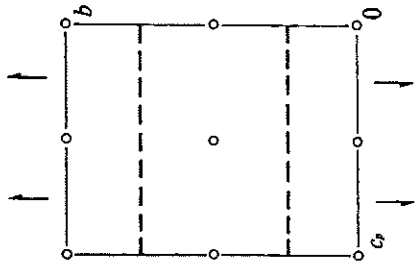

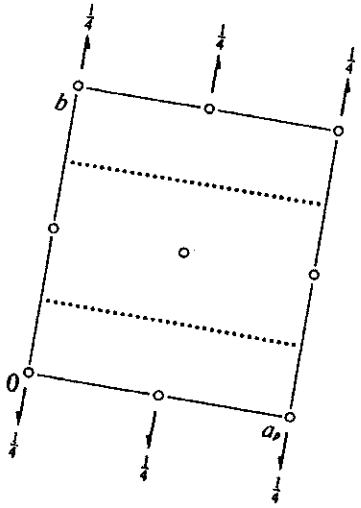

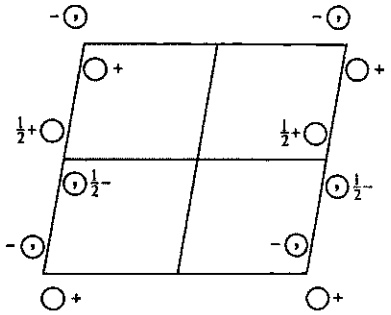

(9) **Origin** at $\bar{1}$

(10) **Asymmetric unit** $0 \le x \le 1; \quad 0 \le y \le \frac{1}{4}; \quad 0 \le z \le 1$

(11) **Symmetry operations**

(1) 1 (2) $2(0,\frac{1}{2},0)$ $0,y,\frac{1}{4}$ (3) $\bar{1}$ 0,0,0 (4) c $x,\frac{1}{4},z$

XX20

(12) **Generators selected** (1); $t(1,0,0)$; $t(0,1,0)$; $t(0,0,1)$; (2); (3)

(13) **Positions**

(14)

Multiplicity, Wyckoff letter, Site symmetry			Coordinates				Reflection conditions
							General:
4	e	1	(1) x,y,z	(2) $\bar{x},y+\frac{1}{2},\bar{z}+\frac{1}{2}$	(3) $\bar{x},\bar{y},\bar{z}$	(4) $x,\bar{y}+\frac{1}{2},z+\frac{1}{2}$	$h0l$: $l=2n$ $0k0$: $k=2n$ $00l$: $l=2n$
							Special: as above, plus
2	d	$\bar{1}$	$\frac{1}{2},0,\frac{1}{2}$	$\frac{1}{2},\frac{1}{2},0$			hkl : $k+l=2n$
2	c	$\bar{1}$	$0,0,\frac{1}{2}$	$0,\frac{1}{2},0$			hkl : $k+l=2n$
2	b	$\bar{1}$	$\frac{1}{2},0,0$	$\frac{1}{2},\frac{1}{2},\frac{1}{2}$			hkl : $k+l=2n$
2	a	$\bar{1}$	$0,0,0$	$0,\frac{1}{2},\frac{1}{2}$			hkl : $k+l=2n$

(15) **Symmetry of special projections**

Along [001] $p2gm$
$\mathbf{a}' = \mathbf{a}_p$ $\mathbf{b}' = \mathbf{b}$
Origin at $0,0,z$

Along [100] $p2gg$
$\mathbf{a}' = \mathbf{b}$ $\mathbf{b}' = \mathbf{c}_p$
Origin at $x,0,0$

Along [010] $p2$
$\mathbf{a}' = \frac{1}{2}\mathbf{c}$ $\mathbf{b}' = \mathbf{a}$
Origin at $0,y,0$

(16) **Maximal non-isomorphic subgroups**

I [2] $P1c1$ (Pc, 7) 1; 4
[2] $P12_11$ ($P2_1$, 4) 1; 2
[2] $P\bar{1}$ (2) 1; 3

IIa none

IIb none

(17) **Maximal isomorphic subgroups of lowest index**

IIc [2] $P12_1/c1$ ($\mathbf{a}' = 2\mathbf{a}$ or $\mathbf{a}' = 2\mathbf{a}, \mathbf{c}' = 2\mathbf{a}+\mathbf{c}$) ($P2_1/c$, 14); [3] $P12_1/c1$ ($\mathbf{b}' = 3\mathbf{b}$) ($P2_1/c$, 14)

(18) **Minimal non-isomorphic supergroups**

I [2] $Pnna$ (52); [2] $Pmna$ (53); [2] $Pcca$ (54); [2] $Pbam$ (55); [2] $Pccn$ (56); [2] $Pbcm$ (57); [2] $Pnnm$ (58); [2] $Pbcn$ (60); [2] $Pbca$ (61); [2] $Pnma$ (62); [2] $Cmce$ (64)

II [2] $A12/m1$ ($C2/m$, 12); [2] $C12/c1$ ($C2/c$, 15); [2] $I12/c1$ ($C2/c$, 15); [2] $P12_1/m1$ ($\mathbf{c}' = \frac{1}{2}\mathbf{c}$) ($P2_1/m$, 11); [2] $P12/c1$ ($\mathbf{b}' = \frac{1}{2}\mathbf{b}$) ($P2/c$, 13)

XX21

$P2_1/c$ C_{2h}^5 $2/m$ Monoclinic

No. 14

UNIQUE AXIS b, DIFFERENT CELL CHOICES

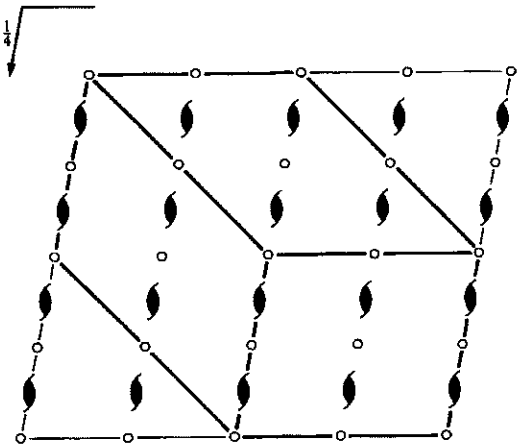

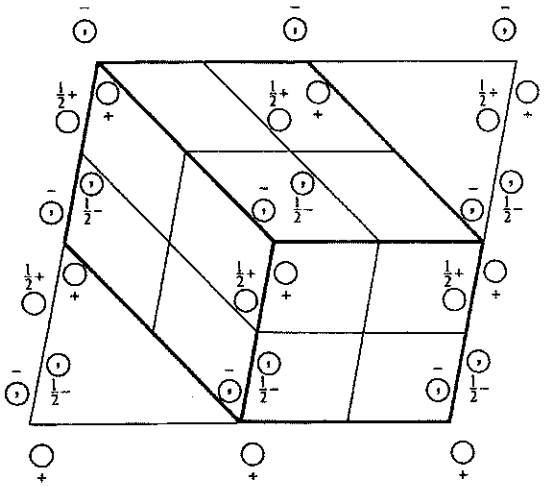

$P12_1/c1$

UNIQUE AXIS b, CELL CHOICE 1

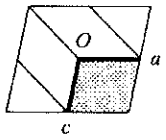

Origin at $\bar{1}$

Asymmetric unit $0 \le x \le 1;\quad 0 \le y \le \frac{1}{4};\quad 0 \le z \le 1$

Generators selected (1); $t(1,0,0)$; $t(0,1,0)$; $t(0,0,1)$; (2); (3)

Positions

Multiplicity, Wyckoff letter, Site symmetry			Coordinates				Reflection conditions
							General:
4	e	1	(1) x,y,z	(2) $\bar{x},y+\frac{1}{2},\bar{z}+\frac{1}{2}$	(3) $\bar{x},\bar{y},\bar{z}$	(4) $x,\bar{y}+\frac{1}{2},z+\frac{1}{2}$	$h0l$: $l=2n$ $0k0$: $k=2n$ $00l$: $l=2n$
							Special: as above, plus
2	d	$\bar{1}$	$\frac{1}{2},0,\frac{1}{2}$	$\frac{1}{2},\frac{1}{2},0$			hkl : $k+l=2n$
2	c	$\bar{1}$	$0,0,\frac{1}{2}$	$0,\frac{1}{2},0$			hkl : $k+l=2n$
2	b	$\bar{1}$	$\frac{1}{2},0,0$	$\frac{1}{2},\frac{1}{2},\frac{1}{2}$			hkl : $k+l=2n$
2	a	$\bar{1}$	$0,0,0$	$0,\frac{1}{2},\frac{1}{2}$			hkl : $k+l=2n$

XX22

$P12_1/n1$

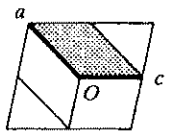

UNIQUE AXIS b, CELL CHOICE 2

Origin at $\bar{1}$

Asymmetric unit $0 \le x \le 1;\quad 0 \le y \le \frac{1}{4};\quad 0 \le z \le 1$

Generators selected (1); $t(1,0,0)$; $t(0,1,0)$; $t(0,0,1)$; (2); (3)

Positions

Multiplicity, Wyckoff letter, Site symmetry			Coordinates				Reflection conditions
							General:
4	e	1	(1) x,y,z	(2) $\bar{x}+\frac{1}{2},y+\frac{1}{2},\bar{z}+\frac{1}{2}$	(3) $\bar{x},\bar{y},\bar{z}$	(4) $x+\frac{1}{2},\bar{y}+\frac{1}{2},z+\frac{1}{2}$	$h0l$: $h+l=2n$ $0k0$: $k=2n$ $h00$: $h=2n$ $00l$: $l=2n$
							Special: as above, plus
2	d	$\bar{1}$	$\frac{1}{2},0,0$	$0,\frac{1}{2},\frac{1}{2}$			hkl : $h+k+l=2n$
2	c	$\bar{1}$	$\frac{1}{2},0,\frac{1}{2}$	$0,\frac{1}{2},0$			hkl : $h+k+l=2n$
2	b	$\bar{1}$	$0,0,\frac{1}{2}$	$\frac{1}{2},\frac{1}{2},0$			hkl : $h+k+l=2n$
2	a	$\bar{1}$	$0,0,0$	$\frac{1}{2},\frac{1}{2},\frac{1}{2}$			hkl : $h+k+l=2n$

$P12_1/a1$

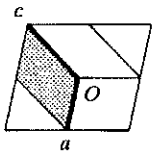

UNIQUE AXIS b, CELL CHOICE 3

Origin at $\bar{1}$

Asymmetric unit $0 \le x \le 1;\quad 0 \le y \le \frac{1}{4};\quad 0 \le z \le 1$

Generators selected (1); $t(1,0,0)$; $t(0,1,0)$; $t(0,0,1)$; (2); (3)

Positions

Multiplicity, Wyckoff letter, Site symmetry			Coordinates				Reflection conditions
							General:
4	e	1	(1) x,y,z	(2) $\bar{x}+\frac{1}{2},y+\frac{1}{2},\bar{z}$	(3) $\bar{x},\bar{y},\bar{z}$	(4) $x+\frac{1}{2},\bar{y}+\frac{1}{2},z$	$h0l$: $h=2n$ $0k0$: $k=2n$ $h00$: $h=2n$
							Special: as above, plus
2	d	$\bar{1}$	$0,0,\frac{1}{2}$	$\frac{1}{2},\frac{1}{2},\frac{1}{2}$			hkl : $h+k=2n$
2	c	$\bar{1}$	$\frac{1}{2},0,0$	$0,\frac{1}{2},0$			hkl : $h+k=2n$
2	b	$\bar{1}$	$\frac{1}{2},0,\frac{1}{2}$	$0,\frac{1}{2},\frac{1}{2}$			hkl : $h+k=2n$
2	a	$\bar{1}$	$0,0,0$	$\frac{1}{2},\frac{1}{2},0$			hkl : $h+k=2n$

XX23

$P2_1/c$ C_{2h}^5 $2/m$ Monoclinic

No. 14 $P112_1/a$ Patterson symmetry $P112/m$

UNIQUE AXIS c, CELL CHOICE 1

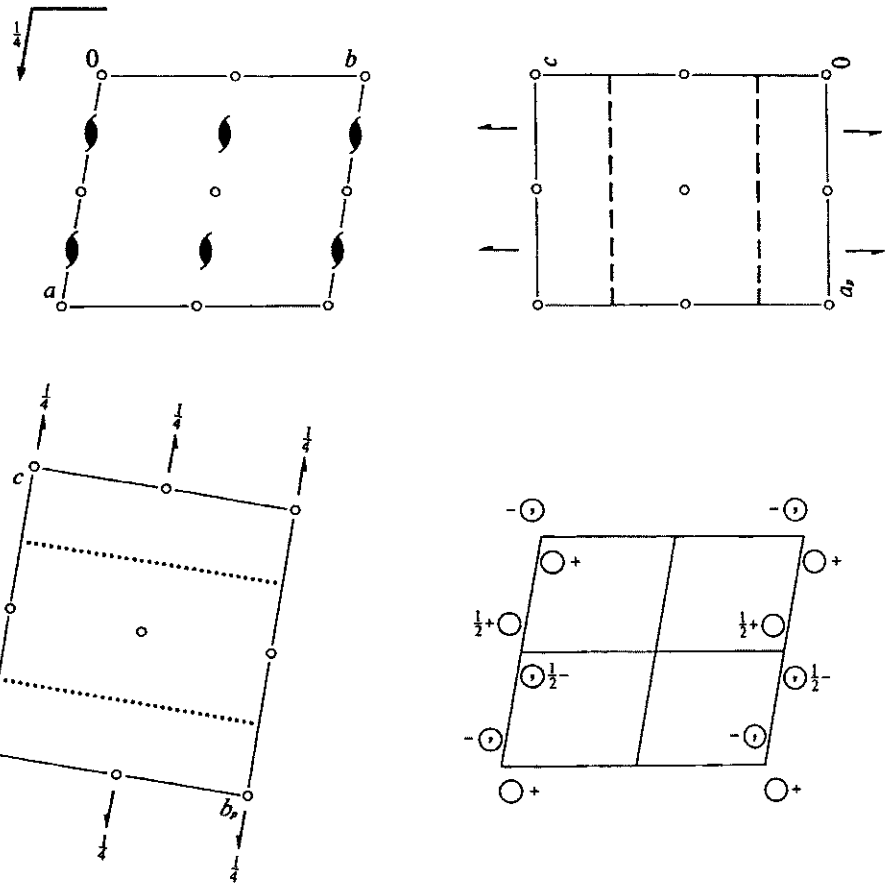

Origin at $\bar{1}$

Asymmetric unit $0 \le x \le 1; \quad 0 \le y \le 1; \quad 0 \le z \le \frac{1}{4}$

Symmetry operations

(1) 1 (2) $2(0,0,\frac{1}{2})$ $\frac{1}{4},0,z$ (3) $\bar{1}$ 0,0,0 (4) a $x,y,\frac{1}{4}$

XX24

Generators selected (1); $t(1,0,0)$; $t(0,1,0)$; $t(0,0,1)$; (2); (3)

Positions

Multiplicity, Wyckoff letter, Site symmetry			Coordinates				Reflection conditions
							General:
4	e	1	(1) x,y,z	(2) $\bar{x}+\frac{1}{2},\bar{y},z+\frac{1}{2}$	(3) $\bar{x},\bar{y},\bar{z}$	(4) $x+\frac{1}{2},y,\bar{z}+\frac{1}{2}$	$hk0$: $h=2n$ $00l$: $l=2n$ $h00$: $h=2n$
							Special: as above, plus
2	d	$\bar{1}$	$\frac{1}{2},\frac{1}{2},0$	$0,\frac{1}{2},\frac{1}{2}$			hkl : $h+l=2n$
2	c	$\bar{1}$	$\frac{1}{2},0,0$	$0,0,\frac{1}{2}$			hkl : $h+l=2n$
2	b	$\bar{1}$	$0,\frac{1}{2},0$	$\frac{1}{2},\frac{1}{2},\frac{1}{2}$			hkl : $h+l=2n$
2	a	$\bar{1}$	$0,0,0$	$\frac{1}{2},0,\frac{1}{2}$			hkl : $h+l=2n$

Symmetry of special projections

Along [001] $p2$
$\mathbf{a}'=\frac{1}{2}\mathbf{a}$ $\mathbf{b}'=\mathbf{b}$
Origin at $0,0,z$

Along [100] $p2gm$
$\mathbf{a}'=\mathbf{b}_p$ $\mathbf{b}'=\mathbf{c}$
Origin at $x,0,0$

Along [010] $p2gg$
$\mathbf{a}'=\mathbf{c}$ $\mathbf{b}'=\mathbf{a}_p$
Origin at $0,y,0$

Maximal non-isomorphic subgroups

I [2] $P1\,1\,a$ (Pc, 7) 1; 4
[2] $P1\,1\,2_1$ ($P2_1$, 4) 1; 2
[2] $P\,\bar{1}$ (2) 1; 3

IIa none

IIb none

Maximal isomorphic subgroups of lowest index

IIc [2] $P1\,1\,2_1/a$ ($\mathbf{b}'=2\mathbf{b}$ or $\mathbf{a}'=\mathbf{a}+2\mathbf{b},\mathbf{b}'=2\mathbf{b}$) ($P2_1/c$, 14); [3] $P1\,1\,2_1/a$ ($\mathbf{c}'=3\mathbf{c}$) ($P2_1/c$, 14)

Minimal non-isomorphic supergroups

I [2] $Pnna$ (52); [2] $Pmna$ (53); [2] $Pcca$ (54); [2] $Pbam$ (55); [2] $Pccn$ (56); [2] $Pbcm$ (57); [2] $Pnnm$ (58); [2] $Pbcn$ (60); [2] $Pbca$ (61); [2] $Pnma$ (62); [2] $Cmce$ (64)

II [2] $A\,1\,1\,2/a$ ($C2/c$, 15); [2] $B\,1\,1\,2/m$ ($C2/m$, 12); [2] $I\,1\,1\,2/a$ ($C2/c$, 15); [2] $P\,1\,1\,2_1/m$ ($\mathbf{a}'=\frac{1}{2}\mathbf{a}$) ($P2_1/m$, 11); [2] $P\,1\,1\,2/a$ ($\mathbf{c}'=\frac{1}{2}\mathbf{c}$) ($P2/c$, 13)

XX25

$P2_1/c$ C_{2h}^5 $2/m$ Monoclinic

No. 14

UNIQUE AXIS c, DIFFERENT CELL CHOICES

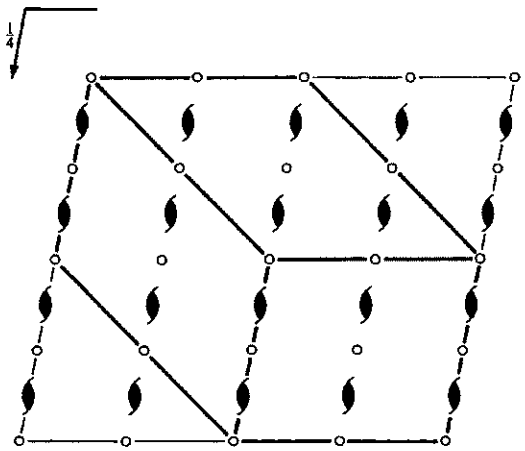

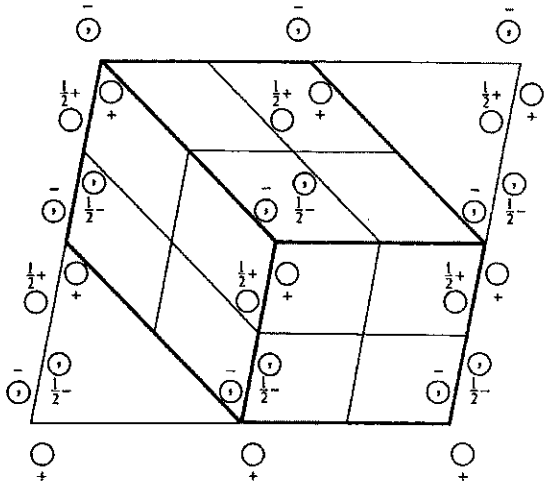

$P112_1/a$

UNIQUE AXIS c, CELL CHOICE 1

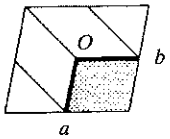

Origin at $\bar{1}$

Asymmetric unit $0 \le x \le 1;\quad 0 \le y \le 1;\quad 0 \le z \le \frac{1}{4}$

Generators selected (1); $t(1,0,0)$; $t(0,1,0)$; $t(0,0,1)$; (2); (3)

Positions

Multiplicity, Wyckoff letter, Site symmetry			Coordinates				Reflection conditions
							General:
4	e	1	(1) x,y,z	(2) $\bar{x}+\frac{1}{2},\bar{y},z+\frac{1}{2}$	(3) $\bar{x},\bar{y},\bar{z}$	(4) $x+\frac{1}{2},y,\bar{z}+\frac{1}{2}$	$h0l$: $h=2n$ $00l$: $l=2n$ $h00$: $h=2n$
							Special: as above, plus
2	d	$\bar{1}$	$\frac{1}{2},\frac{1}{2},0$	$0,\frac{1}{2},\frac{1}{2}$			hkl : $h+l=2n$
2	c	$\bar{1}$	$\frac{1}{2},0,0$	$0,0,\frac{1}{2}$			hkl : $h+l=2n$
2	b	$\bar{1}$	$0,\frac{1}{2},0$	$\frac{1}{2},\frac{1}{2},\frac{1}{2}$			hkl : $h+l=2n$
2	a	$\bar{1}$	$0,0,0$	$\frac{1}{2},0,\frac{1}{2}$			hkl : $h+l=2n$

XX26

$P112_1/n$

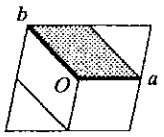

UNIQUE AXIS c, CELL CHOICE 2

Origin at $\bar{1}$

Asymmetric unit $0 \le x \le 1;\quad 0 \le y \le 1;\quad 0 \le z \le \frac{1}{4}$

Generators selected (1); $t(1,0,0)$; $t(0,1,0)$; $t(0,0,1)$; (2); (3)

Positions

Multiplicity, Wyckoff letter, Site symmetry	Coordinates				Reflection conditions
					General:
4 e 1	(1) x,y,z	(2) $\bar{x}+\frac{1}{2},\bar{y}+\frac{1}{2},z+\frac{1}{2}$	(3) $\bar{x},\bar{y},\bar{z}$	(4) $x+\frac{1}{2},y+\frac{1}{2},\bar{z}+\frac{1}{2}$	$hk0$: $h+k=2n$ $00l$: $l=2n$ $h00$: $h=2n$ $0k0$: $k=2n$
					Special: as above, plus
2 d $\bar{1}$	$0,\frac{1}{2},0$	$\frac{1}{2},0,\frac{1}{2}$			hkl : $h+k+l=2n$
2 c $\bar{1}$	$\frac{1}{2},\frac{1}{2},0$	$0,0,\frac{1}{2}$			hkl : $h+k+l=2n$
2 b $\bar{1}$	$\frac{1}{2},0,0$	$0,\frac{1}{2},\frac{1}{2}$			hkl : $h+k+l=2n$
2 a $\bar{1}$	$0,0,0$	$\frac{1}{2},\frac{1}{2},\frac{1}{2}$			hkl : $h+k+l=2n$

$P112_1/b$

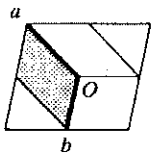

UNIQUE AXIS c, CELL CHOICE 3

Origin at $\bar{1}$

Asymmetric unit $0 \le x \le 1;\quad 0 \le y \le 1;\quad 0 \le z \le \frac{1}{4}$

Generators selected (1); $t(1,0,0)$; $t(0,1,0)$; $t(0,0,1)$; (2); (3)

Positions

Multiplicity, Wyckoff letter, Site symmetry	Coordinates				Reflection conditions
					General:
4 e 1	(1) x,y,z	(2) $\bar{x},\bar{y}+\frac{1}{2},z+\frac{1}{2}$	(3) $\bar{x},\bar{y},\bar{z}$	(4) $x,y+\frac{1}{2},\bar{z}+\frac{1}{2}$	$hk0$: $k=2n$ $00l$: $l=2n$ $0k0$: $k=2n$
					Special: as above, plus
2 d $\bar{1}$	$\frac{1}{2},0,0$	$\frac{1}{2},\frac{1}{2},\frac{1}{2}$			hkl : $k+l=2n$
2 c $\bar{1}$	$0,\frac{1}{2},0$	$0,0,\frac{1}{2}$			hkl : $k+l=2n$
2 b $\bar{1}$	$\frac{1}{2},\frac{1}{2},0$	$\frac{1}{2},0,\frac{1}{2}$			hkl : $k+l=2n$
2 a $\bar{1}$	$0,0,0$	$0,\frac{1}{2},\frac{1}{2}$			hkl : $k+l=2n$

XX27

$C2/c$ C_{2h}^6 $2/m$ Monoclinic

No. 15 $C12/c1$ Patterson symmetry $C12/m1$

UNIQUE AXIS b, CELL CHOICE 1

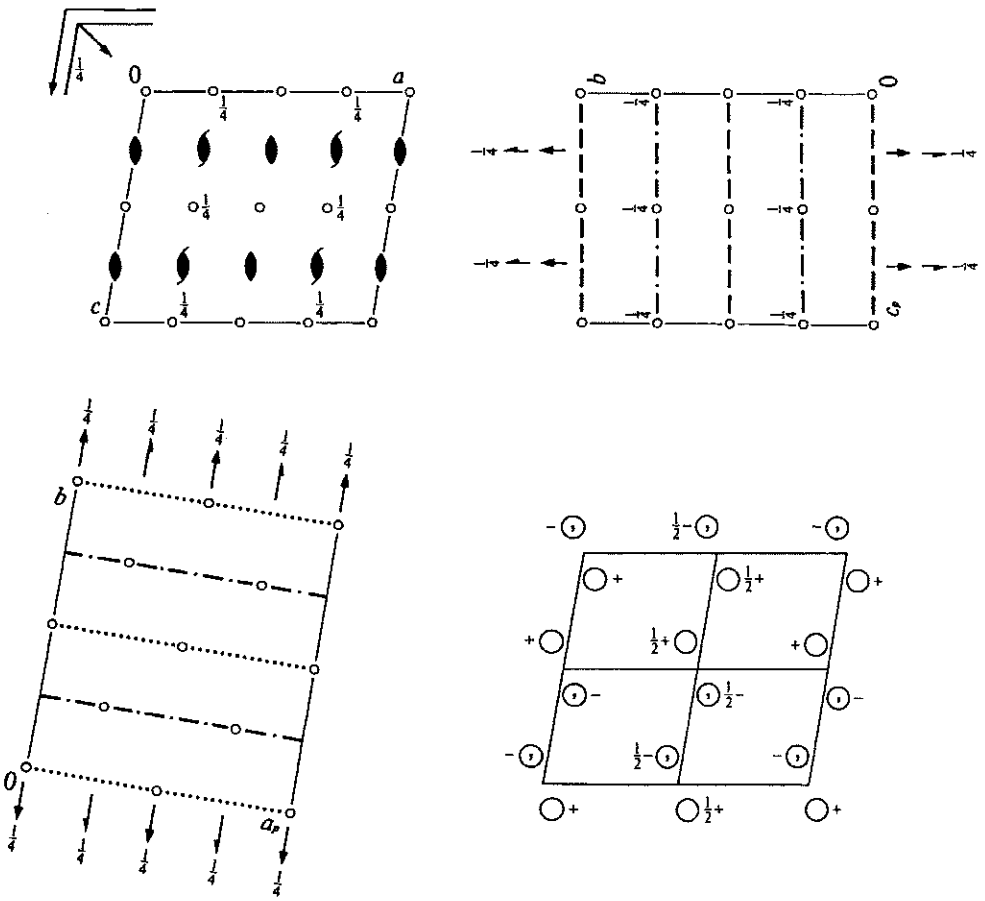

Origin at $\bar{1}$ on glide plane c

Asymmetric unit $0 \le x \le \frac{1}{2}$; $0 \le y \le \frac{1}{2}$; $0 \le z \le \frac{1}{2}$

Symmetry operations

For $(0,0,0)+$ set

(1) 1 (2) 2 $0,y,\frac{1}{4}$ (3) $\bar{1}$ $0,0,0$ (4) c $x,0,z$

For $(\frac{1}{2},\frac{1}{2},0)+$ set

(1) $t(\frac{1}{2},\frac{1}{2},0)$ (2) $2(0,\frac{1}{2},0)$ $\frac{1}{4},y,\frac{1}{4}$ (3) $\bar{1}$ $\frac{1}{4},\frac{1}{4},0$ (4) $n(\frac{1}{2},0,\frac{1}{2})$ $x,\frac{1}{4},z$

XX28

Generators selected (1); $t(1,0,0)$; $t(0,1,0)$; $t(0,0,1)$; $t(\frac{1}{2},\frac{1}{2},0)$; (2); (3)

Positions

Multiplicity, Wyckoff letter, Site symmetry			Coordinates				Reflection conditions
			(0,0,0)+ $(\frac{1}{2},\frac{1}{2},0)$+				General:
8	f	1	(1) x,y,z	(2) $\bar{x},y,\bar{z}+\frac{1}{2}$	(3) $\bar{x},\bar{y},\bar{z}$	(4) $x,\bar{y},z+\frac{1}{2}$	hkl : $h+k=2n$ $h0l$: $h,l=2n$ $0kl$: $k=2n$ $hk0$: $h+k=2n$ $0k0$: $k=2n$ $h00$: $h=2n$ $00l$: $l=2n$
							Special: as above, plus
4	e	2	$0,y,\frac{1}{4}$	$0,\bar{y},\frac{3}{4}$			no extra conditions
4	d	$\bar{1}$	$\frac{1}{4},\frac{1}{4},\frac{1}{2}$	$\frac{3}{4},\frac{1}{4},0$			hkl : $k+l=2n$
4	c	$\bar{1}$	$\frac{1}{4},\frac{1}{4},0$	$\frac{3}{4},\frac{1}{4},\frac{1}{2}$			hkl : $k+l=2n$
4	b	$\bar{1}$	$0,\frac{1}{2},0$	$0,\frac{1}{2},\frac{1}{2}$			hkl : $l=2n$
4	a	$\bar{1}$	0,0,0	$0,0,\frac{1}{2}$			hkl : $l=2n$

Symmetry of special projections

Along [001] $c2mm$
$\mathbf{a}' = \mathbf{a}_p$ $\mathbf{b}' = \mathbf{b}$
Origin at $0,0,z$

Along [100] $p2gm$
$\mathbf{a}' = \frac{1}{2}\mathbf{b}$ $\mathbf{b}' = \mathbf{c}_p$
Origin at $x,0,0$

Along [010] $p2$
$\mathbf{a}' = \frac{1}{2}\mathbf{c}$ $\mathbf{b}' = \frac{1}{2}\mathbf{a}$
Origin at $0,y,0$

Maximal non-isomorphic subgroups

I
[2] $C1c1$ (Cc, 9) (1; 4)+
[2] $C121$ ($C2$, 5) (1; 2)+
[2] $C\bar{1}$ ($P\bar{1}$, 2) (1; 3)+

IIa
[2] $P12_1/n1$ ($P2_1/c$, 14) 1; 3; (2; 4) + $(\frac{1}{2},\frac{1}{2},0)$
[2] $P12_1/c1$ ($P2_1/c$, 14) 1; 4; (2; 3) + $(\frac{1}{2},\frac{1}{2},0)$
[2] $P12/c1$ ($P2/c$, 13) 1; 2; 3; 4
[2] $P12/n1$ ($P2/c$, 13) 1; 2; (3; 4) + $(\frac{1}{2},\frac{1}{2},0)$

IIb none

Maximal isomorphic subgroups of lowest index

IIc [3] $C12/c1$ ($\mathbf{b}' = 3\mathbf{b}$) ($C2/c$, 15); [3] $C12/c1$ ($\mathbf{c}' = 3\mathbf{c}$) ($C2/c$, 15);
[3] $C12/c1$ ($\mathbf{a}' = 3\mathbf{a}$ or $\mathbf{a}' = 3\mathbf{a}, \mathbf{c}' = -\mathbf{a}+\mathbf{c}$ or $\mathbf{a}' = 3\mathbf{a}, \mathbf{c}' = \mathbf{a}+\mathbf{c}$) ($C2/c$, 15)

Minimal non-isomorphic supergroups

I [2] $Cmcm$ (63); [2] $Cmce$ (64); [2] $Cccm$ (66); [2] $Ccce$ (68); [2] $Fddd$ (70); [2] $Ibam$ (72); [2] $Ibca$ (73); [2] $Imma$ (74); [2] $I4_1/a$ (88); [3] $P\bar{3}1c$ (163); [3] $P\bar{3}c1$ (165); [3] $R\bar{3}c$ (167)

II [2] $F12/m1$ ($C2/m$, 12); [2] $C12/m1$ ($\mathbf{c}' = \frac{1}{2}\mathbf{c}$) ($C2/m$, 12); [2] $P12/c1$ ($\mathbf{a}' = \frac{1}{2}\mathbf{a}, \mathbf{b}' = \frac{1}{2}\mathbf{b}$) ($P2/c$, 13)

XX29

No. 15

UNIQUE AXIS b, DIFFERENT CELL CHOICES

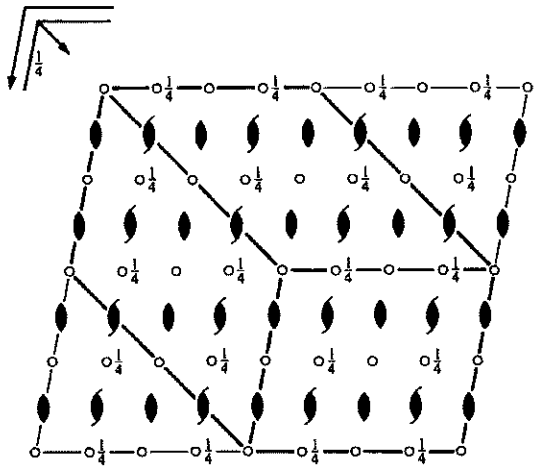

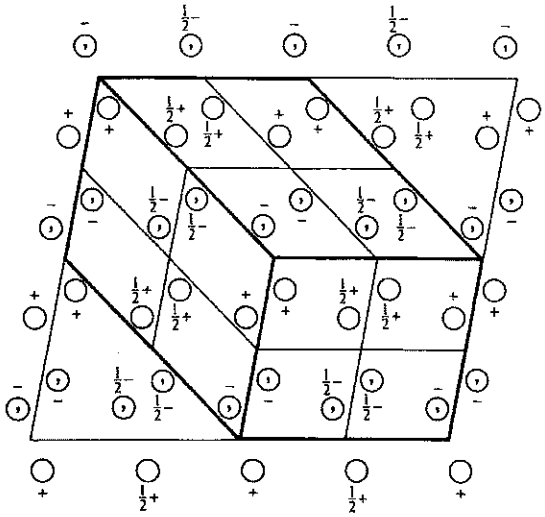

$C12/c1$

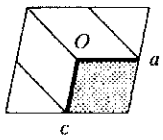

UNIQUE AXIS b, CELL CHOICE 1

Origin at $\bar{1}$ on glide plane c

Asymmetric unit $0 \le x \le \frac{1}{2}$; $0 \le y \le \frac{1}{2}$; $0 \le z \le \frac{1}{2}$

Generators selected (1); $t(1,0,0)$; $t(0,1,0)$; $t(0,0,1)$; $t(\frac{1}{2},\frac{1}{2},0)$; (2); (3)

Positions

Multiplicity, Wyckoff letter, Site symmetry	Coordinates				Reflection conditions
	(0,0,0)+ $(\frac{1}{2},\frac{1}{2},0)$+				General:
8 f 1	(1) x,y,z	(2) $\bar{x},y,\bar{z}+\frac{1}{2}$	(3) $\bar{x},\bar{y},\bar{z}$	(4) $x,\bar{y},z+\frac{1}{2}$	hkl : $h+k=2n$ $0k0$: $k=2n$ $h0l$: $h,l=2n$ $h00$: $h=2n$ $0kl$: $k=2n$ $00l$: $l=2n$ $hk0$: $h+k=2n$
					Special: as above, plus
4 e 2	$0,y,\frac{1}{4}$	$0,\bar{y},\frac{3}{4}$			no extra conditions
4 d $\bar{1}$	$\frac{1}{4},\frac{1}{4},\frac{1}{2}$	$\frac{3}{4},\frac{1}{4},0$	4 c $\bar{1}$	$\frac{1}{4},\frac{1}{4},0$ $\frac{3}{4},\frac{1}{4},\frac{1}{2}$	hkl : $k+l=2n$
4 b $\bar{1}$	$0,\frac{1}{2},0$	$0,\frac{1}{2},\frac{1}{2}$	4 a $\bar{1}$	$0,0,0$ $0,0,\frac{1}{2}$	hkl : $l=2n$

XX30

$A12/n1$

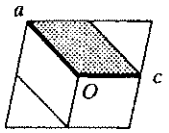

UNIQUE AXIS b, CELL CHOICE 2

Origin at $\bar{1}$ on glide plane n

Asymmetric unit $0 \le x \le \frac{1}{2}$; $0 \le y \le 1$; $0 \le z \le \frac{1}{4}$

Generators selected (1); $t(1,0,0)$; $t(0,1,0)$; $t(0,0,1)$; $t(0,\frac{1}{2},\frac{1}{2})$; (2); (3)

Positions

Multiplicity, Wyckoff letter, Site symmetry			Coordinates				Reflection conditions
			$(0,0,0)+$	$(0,\frac{1}{2},\frac{1}{2})+$			General:
8	f	1	(1) x,y,z	(2) $\bar{x}+\frac{1}{2},y,\bar{z}+\frac{1}{2}$	(3) $\bar{x},\bar{y},\bar{z}$	(4) $x+\frac{1}{2},\bar{y},z+\frac{1}{2}$	hkl : $k+l=2n$ $0kl$: $k+l=2n$ $hk0$: $k=2n$ $h0l$: $h,l=2n$ $0kl$: $k+l=2n$ $hk0$: $k=2n$ $0k0$: $k=2n$ $h00$: $h=2n$ $00l$: $l=2n$
							Special: as above, plus
4	e	2	$\frac{3}{4},y,\frac{3}{4}$	$\frac{1}{4},\bar{y},\frac{1}{4}$			no extra conditions
4	d	$\bar{1}$	$\frac{1}{2},\frac{1}{4},\frac{3}{4}$	$0,\frac{1}{4},\frac{3}{4}$			hkl : $h=2n$
4	b	$\bar{1}$	$0,\frac{1}{2},0$	$\frac{1}{2},\frac{1}{2},\frac{1}{2}$			hkl : $h+k=2n$
4	c	$\bar{1}$	$0,\frac{1}{4},\frac{1}{4}$	$\frac{1}{2},\frac{1}{4},\frac{1}{4}$			
4	a	$\bar{1}$	$0,0,0$	$\frac{1}{2},0,\frac{1}{2}$			

$I12/a1$

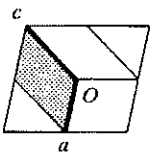

UNIQUE AXIS b, CELL CHOICE 3

Origin at $\bar{1}$ on glide plane a

Asymmetric unit $0 \le x \le 1$; $0 \le y \le \frac{1}{2}$; $0 \le z \le \frac{1}{4}$

Generators selected (1); $t(1,0,0)$; $t(0,1,0)$; $t(0,0,1)$; $t(\frac{1}{2},\frac{1}{2},\frac{1}{2})$; (2); (3)

Positions

Multiplicity, Wyckoff letter, Site symmetry			Coordinates				Reflection conditions
			$(0,0,0)+$	$(\frac{1}{2},\frac{1}{2},\frac{1}{2})+$			General:
8	f	1	(1) x,y,z	(2) $\bar{x}+\frac{1}{2},y,\bar{z}$	(3) $\bar{x},\bar{y},\bar{z}$	(4) $x+\frac{1}{2},\bar{y},z$	hkl : $h+k+l=2n$ $0kl$: $k+l=2n$ $hk0$: $h+k=2n$ $h0l$: $h,l=2n$ $0kl$: $k+l=2n$ $hk0$: $h+k=2n$ $0k0$: $k=2n$ $h00$: $h=2n$ $00l$: $l=2n$
							Special: as above, plus
4	e	2	$\frac{1}{4},y,0$	$\frac{3}{4},\bar{y},0$			no extra conditions
4	d	$\bar{1}$	$\frac{1}{4},\frac{1}{4},\frac{3}{4}$	$\frac{1}{4},\frac{1}{4},\frac{1}{4}$			hkl : $l=2n$
4	b	$\bar{1}$	$0,\frac{1}{2},0$	$\frac{1}{2},\frac{1}{2},0$			hkl : $h=2n$
4	c	$\bar{1}$	$\frac{3}{4},\frac{1}{4},\frac{3}{4}$	$\frac{3}{4},\frac{1}{4},\frac{1}{4}$			
4	a	$\bar{1}$	$0,0,0$	$\frac{1}{2},0,0$			

XX31

$P4_22_12$ D_4^6 422 Tetragonal

No. 94 $P4_22_12$ Patterson symmetry $P4/mmm$

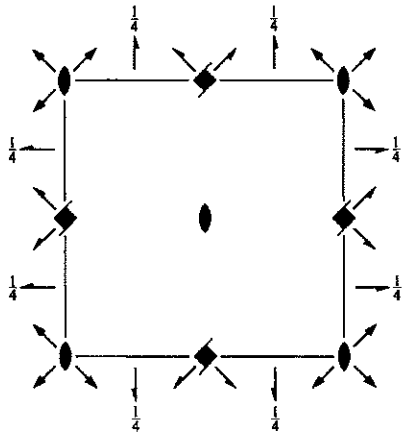

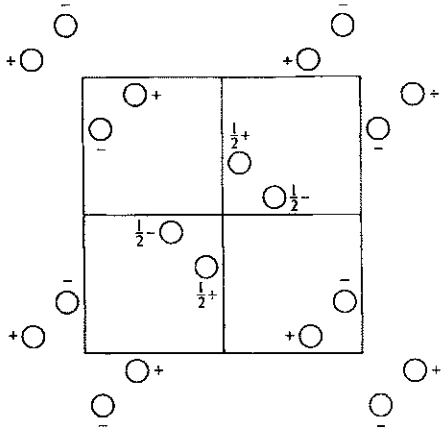

Origin at 222 at 212

Asymmetric unit $0 \le x \le \frac{1}{2}$; $0 \le y \le \frac{1}{2}$; $0 \le z \le \frac{1}{2}$

Symmetry operations

(1) 1
(2) 2 0,0,z
(3) $4^+(0,0,\frac{1}{2})$ $0,\frac{1}{2},z$
(4) $4^-(0,0,\frac{1}{2})$ $\frac{1}{2},0,z$
(5) $2(0,\frac{1}{2},0)$ $\frac{1}{4},y,\frac{1}{4}$
(6) $2(\frac{1}{2},0,0)$ $x,\frac{1}{4},\frac{1}{4}$
(7) 2 $x,x,0$
(8) 2 $x,\bar{x},0$

XX32

Generators selected (1); $t(1,0,0)$; $t(0,1,0)$; $t(0,0,1)$; (2); (3); (5)

Positions

Multiplicity, Wyckoff letter, Site symmetry			Coordinates				Reflection conditions
							General:
8	g	1	(1) x,y,z	(2) $\bar{x},\bar{y},z$	(3) $\bar{y}+\frac{1}{2},x+\frac{1}{2},z+\frac{1}{2}$	(4) $y+\frac{1}{2},\bar{x}+\frac{1}{2},z+\frac{1}{2}$	$00l$: $l=2n$ $h00$: $h=2n$
			(5) $\bar{x}+\frac{1}{2},y+\frac{1}{2},\bar{z}+\frac{1}{2}$	(6) $x+\frac{1}{2},\bar{y}+\frac{1}{2},\bar{z}+\frac{1}{2}$	(7) $y,x,\bar{z}$	(8) $\bar{y},\bar{x},\bar{z}$	
							Special: as above, plus
4	f	..2	$x,x,\frac{1}{2}$	$\bar{x},\bar{x},\frac{1}{2}$	$\bar{x}+\frac{1}{2},x+\frac{1}{2},0$	$x+\frac{1}{2},\bar{x}+\frac{1}{2},0$	$0kl$: $k+l=2n$
4	e	..2	$x,x,0$	$\bar{x},\bar{x},0$	$\bar{x}+\frac{1}{2},x+\frac{1}{2},\frac{1}{2}$	$x+\frac{1}{2},\bar{x}+\frac{1}{2},\frac{1}{2}$	$0kl$: $k+l=2n$
4	d	2..	$0,\frac{1}{2},z$	$0,\frac{1}{2},z+\frac{1}{2}$	$\frac{1}{2},0,\bar{z}+\frac{1}{2}$	$\frac{1}{2},0,\bar{z}$	hkl : $l=2n$ $hk0$: $h+k=2n$
4	c	2..	$0,0,z$	$\frac{1}{2},\frac{1}{2},z+\frac{1}{2}$	$\frac{1}{2},\frac{1}{2},\bar{z}+\frac{1}{2}$	$0,0,\bar{z}$	hkl : $h+k+l=2n$
2	b	2.22	$0,0,\frac{1}{2}$	$\frac{1}{2},\frac{1}{2},0$			hkl : $h+k+l=2n$
2	a	2.22	$0,0,0$	$\frac{1}{2},\frac{1}{2},\frac{1}{2}$			hkl : $h+k+l=2n$

Symmetry of special projections

Along [001] $p4gm$
$\mathbf{a}'=\mathbf{a}$ $\mathbf{b}'=\mathbf{b}$
Origin at $0,\frac{1}{2},z$

Along [100] $p2mg$
$\mathbf{a}'=\mathbf{b}$ $\mathbf{b}'=\mathbf{c}$
Origin at $x,\frac{1}{4},\frac{1}{4}$

Along [110] $p2mm$
$\mathbf{a}'=\frac{1}{2}(-\mathbf{a}+\mathbf{b})$ $\mathbf{b}'=\mathbf{c}$
Origin at $x,x,0$

Maximal non-isomorphic subgroups

I [2] $P4_211$ ($P4_2$, 77) 1; 2; 3; 4
[2] $P212$ ($C222$, 21) 1; 2; 7; 8
[2] $P22_11$ ($P2_12_12$, 18) 1; 2; 5; 6

IIa none

IIb [2] $P4_32_12$ ($\mathbf{c}'=2\mathbf{c}$) (96); [2] $P4_12_12$ ($\mathbf{c}'=2\mathbf{c}$) (92)

Maximal isomorphic subgroups of lowest index

IIc [3] $P4_22_12$ ($\mathbf{c}'=3\mathbf{c}$) (94); [9] $P4_22_12$ ($\mathbf{a}'=3\mathbf{a},\mathbf{b}'=3\mathbf{b}$) (94)

Minimal non-isomorphic supergroups

I [2] $P4_2/mbc$ (135); [2] $P4_2/mnm$ (136); [2] $P4_2/nmc$ (137); [2] $P4_2/ncm$ (138)

II [2] $C4_222$ ($P4_222$, 93); [2] $I422$ (97); [2] $P42_12$ ($\mathbf{c}'=\frac{1}{2}\mathbf{c}$) (90)

XX33

$R3$ C_3^4 3 Trigonal

No. 146 $R3$ Patterson symmetry $R\bar{3}$

HEXAGONAL AXES

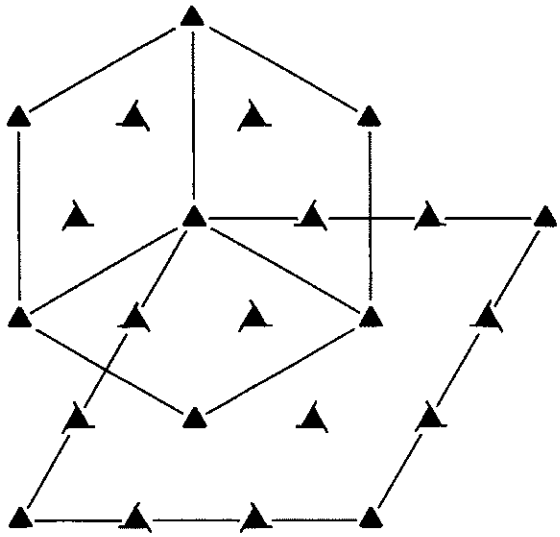

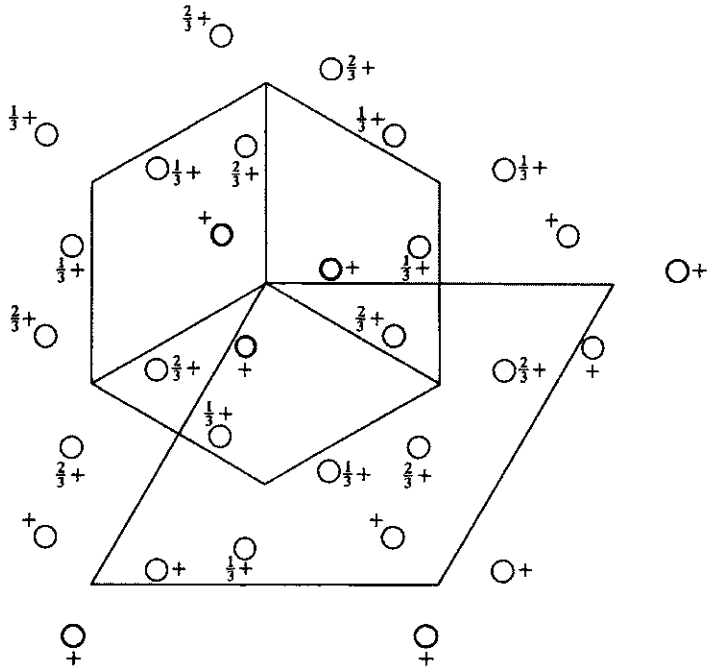

Origin on 3

Asymmetric unit $0 \le x \le \frac{2}{3}$; $0 \le y \le \frac{2}{3}$; $0 \le z \le \frac{1}{3}$; $x \le (1+y)/2$; $y \le \min(1-x,(1+x)/2)$

Vertices $0,0,0$ $\frac{1}{2},0,0$ $\frac{2}{3},\frac{1}{3},0$ $\frac{1}{3},\frac{2}{3},0$ $0,\frac{1}{2},0$
$0,0,\frac{1}{3}$ $\frac{1}{2},0,\frac{1}{3}$ $\frac{2}{3},\frac{1}{3},\frac{1}{3}$ $\frac{1}{3},\frac{2}{3},\frac{1}{3}$ $0,\frac{1}{2},\frac{1}{3}$

Symmetry operations

For $(0,0,0)+$ set

(1) 1 (2) 3^+ $0,0,z$ (3) 3^- $0,0,z$

For $(\frac{2}{3},\frac{1}{3},\frac{1}{3})+$ set

(1) $t(\frac{2}{3},\frac{1}{3},\frac{1}{3})$ (2) $3^+(0,0,\frac{1}{3})$ $\frac{1}{3},\frac{1}{3},z$ (3) $3^-(0,0,\frac{1}{3})$ $\frac{1}{3},0,z$

For $(\frac{1}{3},\frac{2}{3},\frac{2}{3})+$ set

(1) $t(\frac{1}{3},\frac{2}{3},\frac{2}{3})$ (2) $3^+(0,0,\frac{2}{3})$ $0,\frac{1}{3},z$ (3) $3^-(0,0,\frac{2}{3})$ $\frac{1}{3},\frac{1}{3},z$

XX34

Generators selected (1); $t(1,0,0)$; $t(0,1,0)$; $t(0,0,1)$; $t(\frac{2}{3},\frac{1}{3},\frac{1}{3})$; (2)

Positions

Multiplicity, Wyckoff letter, Site symmetry	Coordinates			Reflection conditions
	$(0,0,0)+$	$(\frac{2}{3},\frac{1}{3},\frac{1}{3})+$	$(\frac{1}{3},\frac{2}{3},\frac{2}{3})+$	General:
9 b 1	(1) x,y,z	(2) $\bar{y},x-y,z$	(3) $\bar{x}+y,\bar{x},z$	$hkil$: $-h+k+l=3n$ $hki0$: $-h+k=3n$ $hh\bar{2}hl$: $l=3n$ $h\bar{h}0l$: $h+l=3n$ $000l$: $l=3n$ $h\bar{h}00$: $h=3n$
				Special: no extra conditions
3 a 3.	$0,0,z$			

Symmetry of special projections

Along [001] $p3$
$\mathbf{a}'=\frac{1}{3}(2\mathbf{a}+\mathbf{b})$ $\mathbf{b}'=\frac{1}{3}(-\mathbf{a}+\mathbf{b})$
Origin at $0,0,z$

Along [100] $p1$
$\mathbf{a}'=\frac{1}{2}(\mathbf{a}+2\mathbf{b})$ $\mathbf{b}'=\frac{1}{3}(-\mathbf{a}-2\mathbf{b}+\mathbf{c})$
Origin at $x,0,0$

Along [210] $p1$
$\mathbf{a}'=\frac{1}{2}\mathbf{b}$ $\mathbf{b}'=\frac{1}{3}\mathbf{c}$
Origin at $x,\frac{1}{2}x,0$

Maximal non-isomorphic subgroups

I [3] $R1$ ($P1$, 1) 1+

IIa [3] $P3_2$ (145) 1; $2+(\frac{1}{3},\frac{2}{3},\frac{3}{3})$; $3+(\frac{2}{3},\frac{1}{3},\frac{1}{3})$
[3] $P3_1$ (144) 1; $2+(\frac{2}{3},\frac{1}{3},\frac{1}{3})$; $3+(\frac{1}{3},\frac{2}{3},\frac{2}{3})$
[3] $P3$ (143) 1; 2; 3

IIb none

Maximal isomorphic subgroups of lowest index

IIc [2] $R3$ ($\mathbf{a}'=-\mathbf{a},\mathbf{b}'=-\mathbf{b},\mathbf{c}'=2\mathbf{c}$) (146); [4] $R3$ ($\mathbf{a}'=-2\mathbf{a},\mathbf{b}'=-2\mathbf{b}$) (146)

Minimal non-isomorphic supergroups

I [2] $R\bar{3}$ (148); [2] $R32$ (155); [2] $R3m$ (160); [2] $R3c$ (161); [4] $P23$ (195); [4] $F23$ (196); [4] $I23$ (197); [4] $P2_13$ (198); [4] $I2_13$ (199)

II [3] $P3$ ($\mathbf{a}'=\frac{1}{3}(2\mathbf{a}+\mathbf{b}),\mathbf{b}'=\frac{1}{3}(-\mathbf{a}+\mathbf{b}),\mathbf{c}'=\frac{1}{3}\mathbf{c}$) (143)

XX35

$R3$ C_3^4 3 Trigonal

No. 146 $R3$ Patterson symmetry $R\bar{3}$

RHOMBOHEDRAL AXES

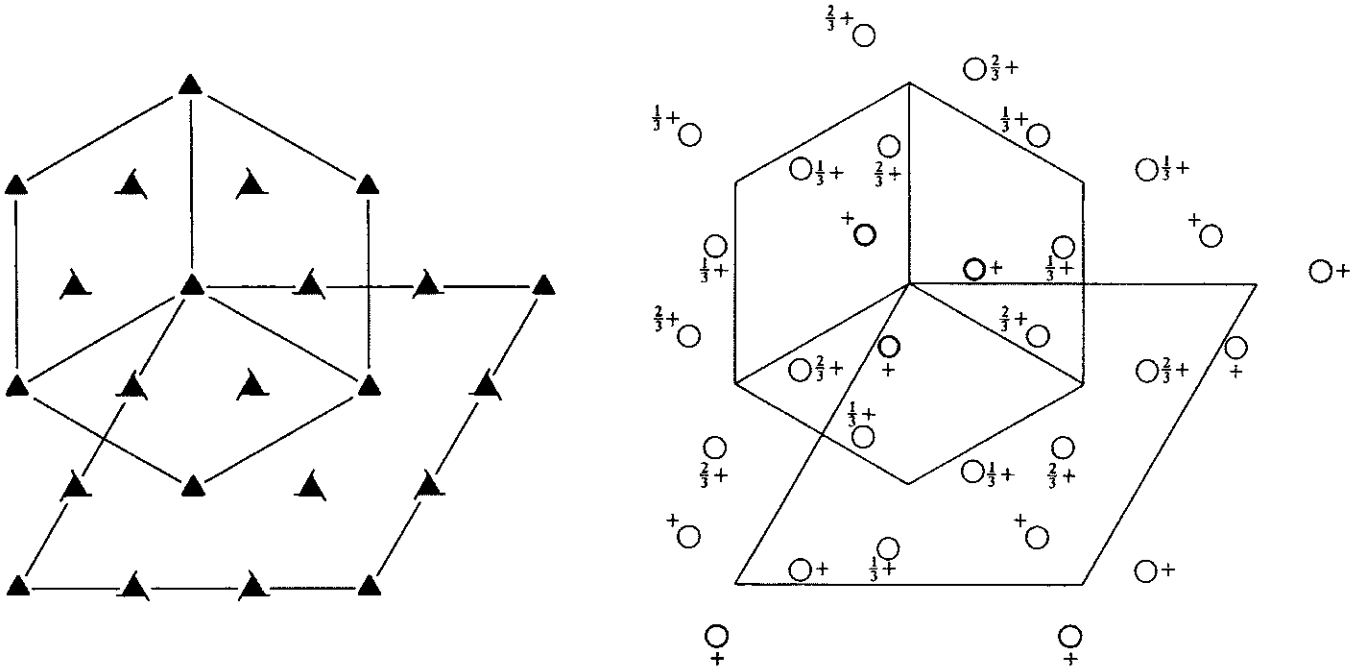

Heights refer to hexagonal axes

Origin on 3

Asymmetric unit $0 \le x \le 1;\quad 0 \le y \le 1;\quad 0 \le z \le 1;\quad z \le \min(x,y)$

Vertices 0,0,0 1,0,0 1,1,0 0,1,0 1,1,1

Symmetry operations

(1) 1 (2) 3^+ x,x,x (3) 3^- x,x,x

XX36

Generators selected (1); $t(1,0,0)$; $t(0,1,0)$; $t(0,0,1)$; (2)

Positions

Multiplicity, Wyckoff letter, Site symmetry	Coordinates			Reflection conditions
				General:
3 *b* 1	(1) x,y,z	(2) z,x,y	(3) y,z,x	no conditions
				Special: no extra conditions
1 *a* 3.	x,x,x			

Symmetry of special projections

Along [111] $p3$
$\mathbf{a}' = \frac{1}{3}(2\mathbf{a}-\mathbf{b}-\mathbf{c})$ $\mathbf{b}' = \frac{1}{3}(-\mathbf{a}+2\mathbf{b}-\mathbf{c})$
Origin at x,x,x

Along [1$\bar{1}$0] $p1$
$\mathbf{a}' = \frac{1}{3}(\mathbf{a}+\mathbf{b}-2\mathbf{c})$ $\mathbf{b}' = \mathbf{c}$
Origin at $x,\bar{x},0$

Along [2$\bar{1}\bar{1}$] $p1$
$\mathbf{a}' = \frac{1}{2}(\mathbf{b}-\mathbf{c})$ $\mathbf{b}' = \frac{1}{3}(\mathbf{a}+\mathbf{b}+\mathbf{c})$
Origin at $2x,\bar{x},\bar{x}$

Maximal non-isomorphic subgroups

I [3] $R1$ ($P1$, 1) 1

IIa none

IIb [3] $P3_2$ ($\mathbf{a}' = \mathbf{a}-\mathbf{b}, \mathbf{b}' = \mathbf{b}-\mathbf{c}, \mathbf{c}' = \mathbf{a}+\mathbf{b}+\mathbf{c}$) (145); [3] $P3_1$ ($\mathbf{a}' = \mathbf{a}-\mathbf{b}, \mathbf{b}' = \mathbf{b}-\mathbf{c}, \mathbf{c}' = \mathbf{a}+\mathbf{b}+\mathbf{c}$) (144); [3] $P3$ ($\mathbf{a}' = \mathbf{a}-\mathbf{b}, \mathbf{b}' = \mathbf{b}-\mathbf{c}, \mathbf{c}' = \mathbf{a}+\mathbf{b}+\mathbf{c}$) (143)

Maximal isomorphic subgroups of lowest index

IIc [2] $R3$ ($\mathbf{a}' = \mathbf{b}+\mathbf{c}, \mathbf{b}' = \mathbf{a}+\mathbf{c}, \mathbf{c}' = \mathbf{a}+\mathbf{b}$) (146); [4] $R3$ ($\mathbf{a}' = -\mathbf{a}+\mathbf{b}+\mathbf{c}, \mathbf{b}' = \mathbf{a}-\mathbf{b}+\mathbf{c}, \mathbf{c}' = \mathbf{a}+\mathbf{b}-\mathbf{c}$) (146)

Minimal non-isomorphic supergroups

I [2] $R\bar{3}$ (148); [2] $R32$ (155); [2] $R3m$ (160); [2] $R3c$ (161); [4] $P23$ (195); [4] $F23$ (196); [4] $I23$ (197); [4] $P2_13$ (198); [4] $I2_13$ (199)

II [3] $P3$ ($\mathbf{a}' = \frac{1}{3}(2\mathbf{a}-\mathbf{b}-\mathbf{c}), \mathbf{b}' = \frac{1}{3}(-\mathbf{a}+2\mathbf{b}-\mathbf{c}), \mathbf{c}' = \frac{1}{3}(\mathbf{a}+\mathbf{b}+\mathbf{c})$) (143)

XX37

$F\bar{4}3m$ T_d^2 $\bar{4}3m$ Cubic

No. 216 $F\bar{4}3m$ Patterson symmetry $Fm\bar{3}m$

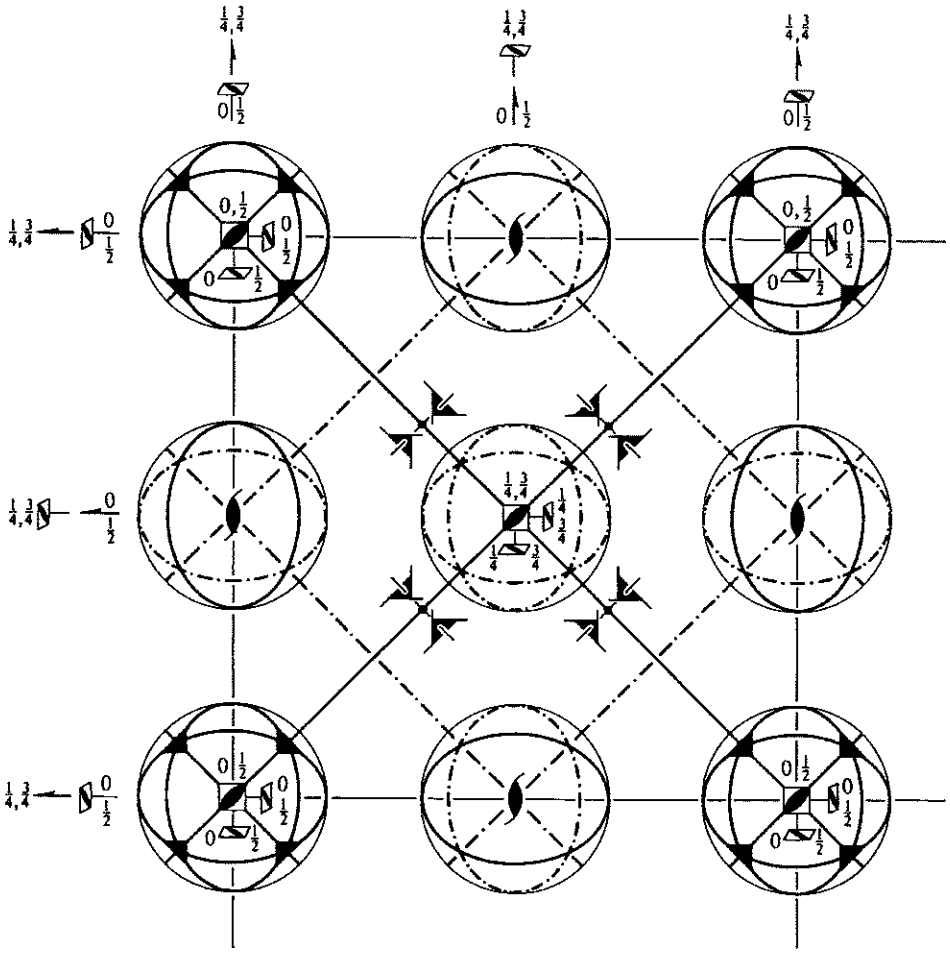

Upper left quadrant only

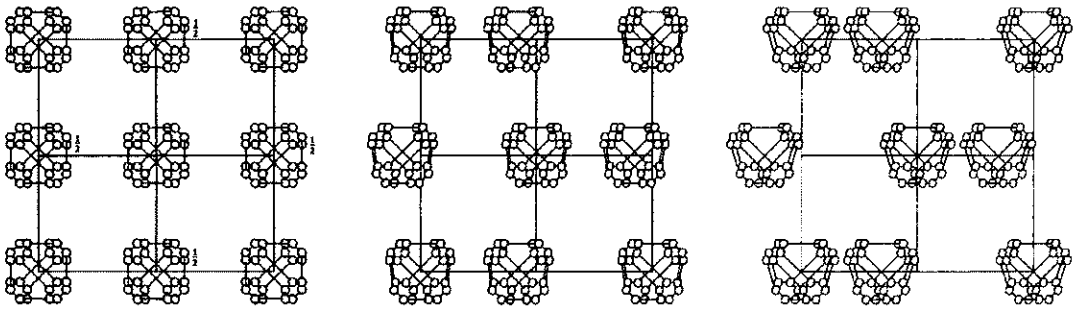

Origin at $\bar{4}3m$

Asymmetric unit $0 \le x \le \frac{1}{2}$; $0 \le y \le \frac{1}{4}$; $-\frac{1}{4} \le z \le \frac{1}{4}$; $y \le \min(x, \frac{1}{2}-x)$; $-y \le z \le y$

Vertices $0,0,0$ $\frac{1}{2},0,0$ $\frac{1}{4},\frac{1}{4},\frac{1}{4}$ $\frac{1}{4},\frac{1}{4},-\frac{1}{4}$

XX38

Symmetry operations

For (0,0,0)+ set

(1) 1	(2) 2 0,0,z	(3) 2 0,y,0	(4) 2 x,0,0
(5) 3^+ x,x,x	(6) 3^+ $\bar{x},x,\bar{x}$	(7) 3^+ $x,\bar{x},\bar{x}$	(8) 3^+ $\bar{x},\bar{x},x$
(9) 3^- x,x,x	(10) 3^- $x,\bar{x},\bar{x}$	(11) 3^- $\bar{x},\bar{x},x$	(12) 3^- $\bar{x},x,\bar{x}$
(13) m x,x,z	(14) m $x,\bar{x},z$	(15) $\bar{4}^+$ 0,0,z; 0,0,0	(16) $\bar{4}^-$ 0,0,z; 0,0,0
(17) m x,y,y	(18) $\bar{4}^+$ x,0,0; 0,0,0	(19) $\bar{4}^-$ x,0,0; 0,0,0	(20) m $x,y,\bar{y}$
(21) m x,y,x	(22) $\bar{4}^-$ 0,y,0; 0,0,0	(23) m $\bar{x},y,x$	(24) $\bar{4}^+$ 0,y,0; 0,0,0

For $(0,\frac{1}{2},\frac{1}{2})+$ set

(1) $t(0,\frac{1}{2},\frac{1}{2})$	(2) $2(0,0,\frac{1}{4})$ 0,0,$z+\frac{1}{4}$	(3) $2(0,\frac{1}{2},0)$ 0,y,$\frac{1}{4}$	(4) 2 $x,\frac{1}{4},\frac{1}{4}$
(5) $3^+(\frac{1}{3},\frac{1}{3},\frac{1}{3})$ $x-\frac{1}{3},x-\frac{1}{6},x$	(6) 3^+ $\bar{x},x+\frac{1}{2},\bar{x}$	(7) $3^+(-\frac{1}{3},\frac{1}{3},\frac{1}{3})$ $x+\frac{1}{3},\bar{x}-\frac{1}{6},\bar{x}$	(8) 3^+ $\bar{x},\bar{x}+\frac{1}{2},x$
(9) $3^-(\frac{1}{3},\frac{1}{3},\frac{1}{3})$ $x-\frac{1}{6},x+\frac{1}{6},x$	(10) $3^-(-\frac{1}{3},\frac{1}{3},\frac{1}{3})$ $x+\frac{1}{6},\bar{x}+\frac{1}{6},\bar{x}$	(11) 3^- $\bar{x}+\frac{1}{2},\bar{x}+\frac{1}{2},x$	(12) 3^- $\bar{x}-\frac{1}{2},x+\frac{1}{2},\bar{x}$
(13) $g(\frac{1}{4},\frac{1}{4},\frac{1}{2})$ $x-\frac{1}{4},x,z$	(14) $g(-\frac{1}{4},\frac{1}{4},\frac{1}{2})$ $x+\frac{1}{4},\bar{x},z$	(15) $\bar{4}^+$ $\frac{1}{4},\frac{1}{4},z$; $\frac{1}{4},\frac{1}{4},\frac{1}{4}$	(16) $\bar{4}^-$ $-\frac{1}{4},\frac{1}{4},z$; $-\frac{1}{4},\frac{1}{4},\frac{1}{4}$
(17) $g(0,\frac{1}{2},\frac{1}{2})$ x,y,y	(18) $\bar{4}^+$ $x,\frac{1}{2},0$; 0,$\frac{1}{2}$,0	(19) $\bar{4}^-$ x,0,$\frac{1}{2}$; 0,0,$\frac{1}{2}$	(20) m $x,y+\frac{1}{2},\bar{y}$
(21) $g(\frac{1}{4},\frac{1}{2},\frac{1}{4})$ $x-\frac{1}{4},y,x$	(22) $\bar{4}^-$ $\frac{1}{4},y,\frac{1}{4}$; $\frac{1}{4},\frac{1}{4},\frac{1}{4}$	(23) $g(-\frac{1}{4},\frac{1}{2},\frac{1}{4})$ $\bar{x}+\frac{1}{4},y,x$	(24) $\bar{4}^+$ $-\frac{1}{4},y,\frac{1}{4}$; $-\frac{1}{4},\frac{1}{4},\frac{1}{4}$

For $(\frac{1}{2},0,\frac{1}{2})+$ set

(1) $t(\frac{1}{2},0,\frac{1}{2})$	(2) $2(0,0,\frac{1}{2})$ $\frac{1}{4}$,0,z	(3) 2 $\frac{1}{4},y,\frac{1}{4}$	(4) $2(\frac{1}{2},0,0)$ x,0,$\frac{1}{4}$
(5) $3^+(\frac{1}{3},\frac{1}{3},\frac{1}{3})$ $x+\frac{1}{6},x-\frac{1}{6},x$	(6) $3^+(\frac{1}{3},-\frac{1}{3},\frac{1}{3})$ $\bar{x}+\frac{1}{6},x+\frac{1}{6},\bar{x}$	(7) 3^+ $x+\frac{1}{2},\bar{x}-\frac{1}{2},\bar{x}$	(8) 3^+ $\bar{x}+\frac{1}{2},\bar{x}+\frac{1}{2},x$
(9) $3^-(\frac{1}{3},\frac{1}{3},\frac{1}{3})$ $x-\frac{1}{6},x-\frac{1}{3},x$	(10) 3^- $x+\frac{1}{2},\bar{x},\bar{x}$	(11) 3^- $\bar{x}+\frac{1}{2},\bar{x},x$	(12) $3^-(\frac{1}{3},-\frac{1}{3},\frac{1}{3})$ $\bar{x}-\frac{1}{6},x+\frac{1}{3},\bar{x}$
(13) $g(\frac{1}{4},\frac{1}{4},\frac{1}{2})$ $x+\frac{1}{4},x,z$	(14) $g(\frac{1}{4},-\frac{1}{4},\frac{1}{2})$ $x+\frac{1}{4},\bar{x},z$	(15) $\bar{4}^+$ $\frac{1}{4},-\frac{1}{4},z$; $\frac{1}{4},-\frac{1}{4},\frac{1}{4}$	(16) $\bar{4}^-$ $\frac{1}{4},\frac{1}{4},z$; $\frac{1}{4},\frac{1}{4},\frac{1}{4}$
(17) $g(\frac{1}{2},\frac{1}{4},\frac{1}{4})$ $x,y-\frac{1}{4},y$	(18) $\bar{4}^+$ $x,\frac{1}{4},\frac{1}{4}$; $\frac{1}{4},\frac{1}{4},\frac{1}{4}$	(19) $\bar{4}^-$ $x,-\frac{1}{4},\frac{1}{4}$; $\frac{1}{4},-\frac{1}{4},\frac{1}{4}$	(20) $g(\frac{1}{2},-\frac{1}{4},\frac{1}{4})$ $x,y+\frac{1}{4},\bar{y}$
(21) $g(\frac{1}{2},0,\frac{1}{2})$ x,y,x	(22) $\bar{4}^-$ $\frac{1}{2},y,0$; $\frac{1}{2}$,0,0	(23) m $\bar{x}+\frac{1}{2},y,x$	(24) $\bar{4}^+$ 0,y,$\frac{1}{2}$; 0,0,$\frac{1}{2}$

For $(\frac{1}{2},\frac{1}{2},0)+$ set

(1) $t(\frac{1}{2},\frac{1}{2},0)$	(2) 2 $\frac{1}{4},\frac{1}{4},z$	(3) $2(0,\frac{1}{2},0)$ $\frac{1}{4},y$,0	(4) $2(\frac{1}{2},0,0)$ $x,\frac{1}{4}$,0
(5) $3^+(\frac{1}{3},\frac{1}{3},\frac{1}{3})$ $x+\frac{1}{6},x+\frac{1}{3},x$	(6) 3^+ $\bar{x}+\frac{1}{2},x,\bar{x}$	(7) 3^+ $x+\frac{1}{2},\bar{x},\bar{x}$	(8) $3^+(\frac{1}{3},\frac{1}{3},-\frac{1}{3})$ $\bar{x}+\frac{1}{6},\bar{x}+\frac{1}{3},x$
(9) $3^-(\frac{1}{3},\frac{1}{3},\frac{1}{3})$ $x+\frac{1}{3},x+\frac{1}{6},x$	(10) 3^- $x,\bar{x}+\frac{1}{2},\bar{x}$	(11) $3^-(\frac{1}{3},\frac{1}{3},-\frac{1}{3})$ $\bar{x}+\frac{1}{3},\bar{x}+\frac{1}{6},x$	(12) 3^- $\bar{x},x+\frac{1}{2},\bar{x}$
(13) $g(\frac{1}{2},\frac{1}{2},0)$ x,x,z	(14) m $x+\frac{1}{2},\bar{x},z$	(15) $\bar{4}^+$ $\frac{1}{2},0,z$; $\frac{1}{2},0,0$	(16) $\bar{4}^-$ 0,$\frac{1}{2}$,z; 0,$\frac{1}{2}$,0
(17) $g(\frac{1}{2},\frac{1}{4},\frac{1}{4})$ $x,y+\frac{1}{4},y$	(18) $\bar{4}^+$ $x,\frac{1}{4},-\frac{1}{4}$; $\frac{1}{4},\frac{1}{4},-\frac{1}{4}$	(19) $\bar{4}^-$ $x,\frac{1}{4},\frac{1}{4}$; $\frac{1}{4},\frac{1}{4},\frac{1}{4}$	(20) $g(\frac{1}{2},\frac{1}{4},-\frac{1}{4})$ $x,y+\frac{1}{4},\bar{y}$
(21) $g(\frac{1}{4},\frac{1}{2},\frac{1}{4})$ $x+\frac{1}{4},y,x$	(22) $\bar{4}^-$ $\frac{1}{4},y,-\frac{1}{4}$; $\frac{1}{4},\frac{1}{4},-\frac{1}{4}$	(23) $g(\frac{1}{4},\frac{1}{2},-\frac{1}{4})$ $\bar{x}+\frac{1}{4},y,x$	(24) $\bar{4}^+$ $\frac{1}{4},y,\frac{1}{4}$; $\frac{1}{4},\frac{1}{4},\frac{1}{4}$

Generators selected (1); $t(1,0,0)$; $t(0,1,0)$; $t(0,0,1)$; $t(0,\frac{1}{2},\frac{1}{2})$; $t(\frac{1}{2},0,\frac{1}{2})$; (2); (3); (5); (13)

Positions

Multiplicity, Wyckoff letter, Site symmetry			Coordinates (0,0,0)+	(0,½,½)+	(½,0,½)+	(½,½,0)+
96	i	1	(1) x,y,z	(2) $\bar{x},\bar{y},z$	(3) $\bar{x},y,\bar{z}$	(4) $x,\bar{y},\bar{z}$
			(5) z,x,y	(6) $z,\bar{x},\bar{y}$	(7) $\bar{z},\bar{x},y$	(8) $\bar{z},x,\bar{y}$
			(9) y,z,x	(10) $\bar{y},z,\bar{x}$	(11) $y,\bar{z},\bar{x}$	(12) $\bar{y},\bar{z},x$
			(13) y,x,z	(14) $\bar{y},\bar{x},z$	(15) $y,\bar{x},\bar{z}$	(16) $\bar{y},x,\bar{z}$
			(17) x,z,y	(18) $\bar{x},z,\bar{y}$	(19) $\bar{x},\bar{z},y$	(20) $x,\bar{z},\bar{y}$
			(21) z,y,x	(22) $z,\bar{y},\bar{x}$	(23) $\bar{z},y,\bar{x}$	(24) $\bar{z},\bar{y},x$
48	h	. . m	x,x,z $\bar{z},\bar{x},x$	$\bar{x},\bar{x},z$ $\bar{z},x,\bar{x}$	$\bar{x},x,\bar{z}$ x,z,x	$x,\bar{x},\bar{z}$ $\bar{x},z,\bar{x}$	z,x,x $x,\bar{z},\bar{x}$	$z,\bar{x},\bar{x}$ $\bar{x},\bar{z},x$
24	g	2 . mm	$x,\frac{1}{4},\frac{1}{4}$	$\bar{x},\frac{3}{4},\frac{1}{4}$	$\frac{1}{4},x,\frac{1}{4}$	$\frac{1}{4},\bar{x},\frac{3}{4}$	$\frac{1}{4},\frac{1}{4},x$	$\frac{3}{4},\frac{1}{4},\bar{x}$
24	f	2 . mm	$x,0,0$	$\bar{x},0,0$	$0,x,0$	$0,\bar{x},0$	$0,0,x$	$0,0,\bar{x}$
16	e	. 3 m	x,x,x	$\bar{x},\bar{x},x$	$\bar{x},x,\bar{x}$	$x,\bar{x},\bar{x}$		
4	d	$\bar{4}3m$	$\frac{3}{4},\frac{3}{4},\frac{3}{4}$					
4	c	$\bar{4}3m$	$\frac{1}{4},\frac{1}{4},\frac{1}{4}$					
4	b	$\bar{4}3m$	$\frac{1}{2},\frac{1}{2},\frac{1}{2}$					
4	a	$\bar{4}3m$	0,0,0					

Reflection conditions

h,k,l permutable

General:

hkl : $h+k,h+l,k+l=2n$
$0kl$: $k,l=2n$
hhl : $h+l=2n$
$h00$: $h=2n$

Special: no extra conditions

XX39

Symmetry of special projections

Along [001] $p4mm$
$\mathbf{a}' = \frac{1}{2}\mathbf{a}$ $\mathbf{b}' = \frac{1}{2}\mathbf{b}$
Origin at $0,0,z$

Along [111] $p31m$
$\mathbf{a}' = \frac{1}{6}(2\mathbf{a}-\mathbf{b}-\mathbf{c})$ $\mathbf{b}' = \frac{1}{6}(-\mathbf{a}+2\mathbf{b}-\mathbf{c})$
Origin at x,x,x

Along [110] $c1m1$
$\mathbf{a}' = \frac{1}{2}(-\mathbf{a}+\mathbf{b})$ $\mathbf{b}' = \mathbf{c}$
Origin at $x,x,0$

Maximal non-isomorphic subgroups

I

[2] $F231$ ($F23$, 196) (1; 2; 3; 4; 5; 6; 7; 8; 9; 10; 11; 12)+

[3] $F\bar{4}1m$ ($I\bar{4}m2$, 119) (1; 2; 3; 4; 13; 14; 15; 16)+

[3] $F\bar{4}1m$ ($I\bar{4}m2$, 119) (1; 2; 3; 4; 17; 18; 19; 20)+

[3] $F\bar{4}1m$ ($I\bar{4}m2$, 119) (1; 2; 3; 4; 21; 22; 23; 24)+

[4] $F13m$ ($R3m$, 160) (1; 5; 9; 13; 17; 21)+

[4] $F13m$ ($R3m$, 160) (1; 6; 12; 14; 20; 21)+

[4] $F13m$ ($R3m$, 160) (1; 7; 10; 14; 17; 23)+

[4] $F13m$ ($R3m$, 160) (1; 8; 11; 13; 20; 23)+

IIa

[4] $P\bar{4}3m$ (215) 1; 2; 3; 4; 5; 6; 7; 8; 9; 10; 11; 12; 13; 14; 15; 16; 17; 18; 19; 20; 21; 22; 23; 24

[4] $P\bar{4}3m$ (215) 1; 2; 3; 4; 13; 14; 15; 16; (9; 10; 11; 12; 17; 18; 19; 20) + $(0,\frac{1}{2},\frac{1}{2})$; (5; 6; 7; 8; 21; 22; 23; 24) + $(\frac{1}{2},0,\frac{1}{2})$

[4] $P\bar{4}3m$ (215) 1; 2; 3; 4; 17; 18; 19; 20; (9; 10; 11; 12; 21; 22; 23; 24) + $(\frac{1}{2},0,\frac{1}{2})$; (5; 6; 7; 8; 13; 14; 15; 16) + $(\frac{1}{2},\frac{1}{2},0)$

[4] $P\bar{4}3m$ (215) 1; 2; 3; 4; 21; 22; 23; 24; (5; 6; 7; 8; 17; 18; 19; 20) + $(0,\frac{1}{2},\frac{1}{2})$; (9; 10; 11; 12; 13; 14; 15; 16) + $(\frac{1}{2},\frac{1}{2},0)$

[4] $P\bar{4}3m$ (215) 1; 5; 9; 13; 17; 21; (4; 6; 11; 15; 20; 22) + $(0,\frac{1}{2},\frac{1}{2})$; (3; 8; 10; 16; 18; 23) + $(\frac{1}{2},0,\frac{1}{2})$; (2; 7; 12; 14; 19; 24) + $(\frac{1}{2},\frac{1}{2},0)$

[4] $P\bar{4}3m$ (215) 1; 6; 12; 14; 20; 21; (4; 5; 10; 16; 17; 22) + $(0,\frac{1}{2},\frac{1}{2})$; (3; 7; 11; 15; 19; 23) + $(\frac{1}{2},0,\frac{1}{2})$; (2; 8; 9; 13; 18; 24) + $(\frac{1}{2},\frac{1}{2},0)$

[4] $P\bar{4}3m$ (215) 1; 7; 10; 14; 17; 23; (4; 8; 12; 16; 20; 24) + $(0,\frac{1}{2},\frac{1}{2})$; (3; 6; 9; 15; 18; 21) + $(\frac{1}{2},0,\frac{1}{2})$; (2; 5; 11; 13; 19; 22) + $(\frac{1}{2},\frac{1}{2},0)$

[4] $P\bar{4}3m$ (215) 1; 8; 11; 13; 20; 23; (4; 7; 9; 15; 17; 24) + $(0,\frac{1}{2},\frac{1}{2})$; (3; 5; 12; 16; 19; 21) + $(\frac{1}{2},0,\frac{1}{2})$; (2; 6; 10; 14; 18; 22) + $(\frac{1}{2},\frac{1}{2},0)$

IIb none

Maximal isomorphic subgroups of lowest index

IIc [27] $F\bar{4}3m$ ($\mathbf{a}' = 3\mathbf{a}, \mathbf{b}' = 3\mathbf{b}, \mathbf{c}' = 3\mathbf{c}$) (216)

Minimal non-isomorphic supergroups

I [2] $Fm\bar{3}m$ (225); [2] $Fd\bar{3}m$ (227)

II [2] $P\bar{4}3m$ ($\mathbf{a}' = \frac{1}{2}\mathbf{a}, \mathbf{b}' = \frac{1}{2}\mathbf{b}, \mathbf{c}' = \frac{1}{2}\mathbf{c}$) (215)

XX40

$Fd\bar{3}m$ O_h^7 $m\bar{3}m$ Cubic

No. 227 $F\ 4_1/d\ \bar{3}\ 2/m$ Patterson symmetry $Fm\bar{3}m$

ORIGIN CHOICE 1

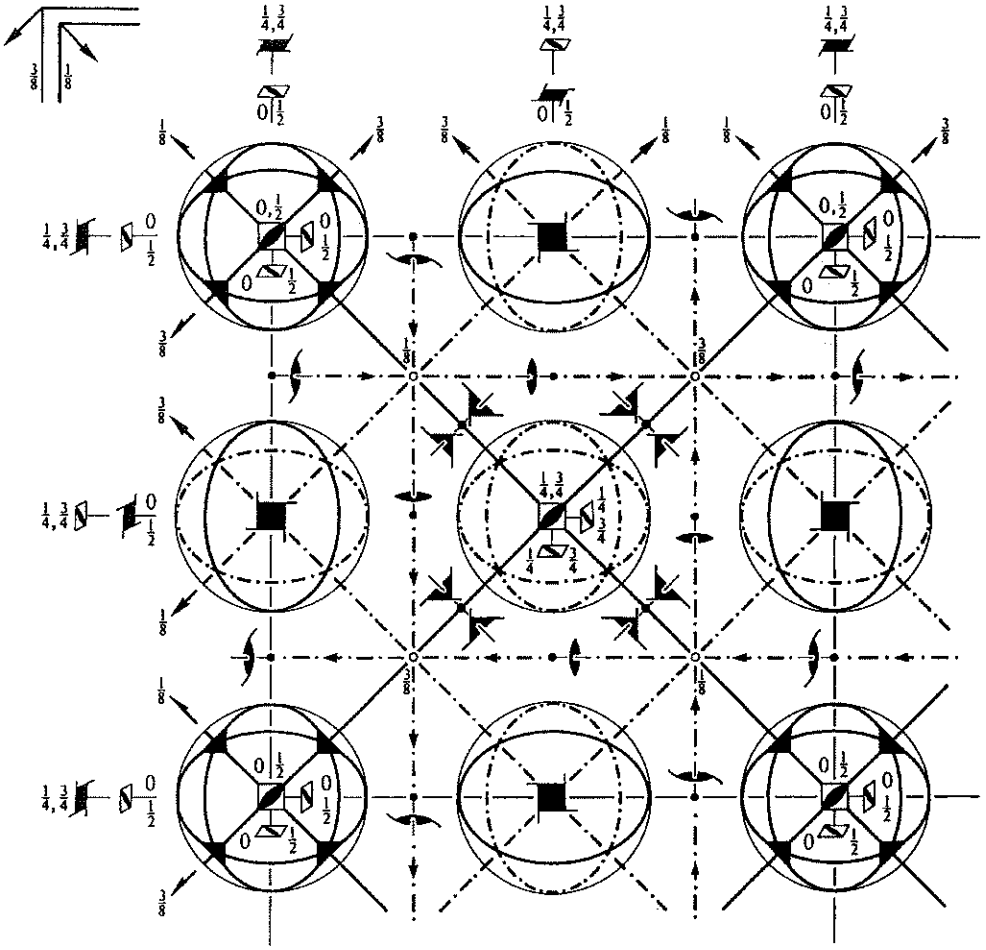

Upper left quadrant only

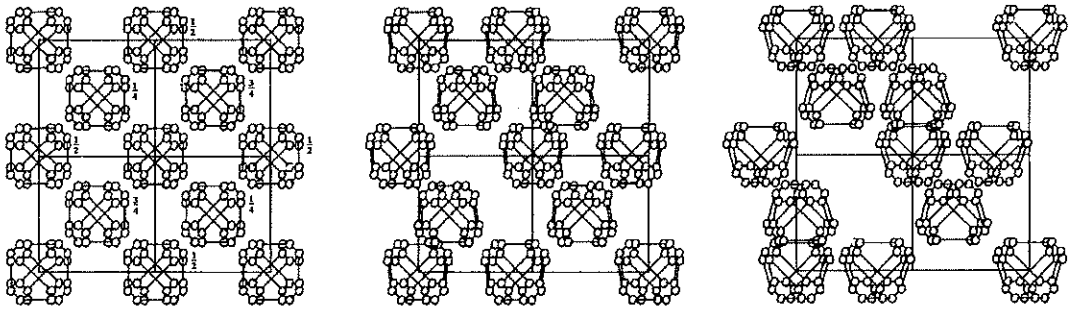

Origin at $\bar{4}3m$, at $-\frac{1}{8},-\frac{1}{8},-\frac{1}{8}$ from centre $(\bar{3}m)$

Asymmetric unit $0 \le x \le \frac{1}{2}$; $0 \le y \le \frac{1}{8}$; $-\frac{1}{8} \le z \le \frac{1}{8}$; $y \le \min(\frac{1}{2}-x, x)$; $-y \le z \le y$

Vertices $0,0,0$ $\frac{1}{2},0,0$ $\frac{3}{8},\frac{1}{8},\frac{1}{8}$ $\frac{1}{8},\frac{1}{8},\frac{1}{8}$ $\frac{3}{8},\frac{1}{8},-\frac{1}{8}$ $\frac{1}{8},\frac{1}{8},-\frac{1}{8}$

Symmetry operations

(*given on page* 699)

XX41

Generators selected (1); $t(1,0,0)$; $t(0,1,0)$; $t(0,0,1)$; $t(0,\frac{1}{2},\frac{1}{2})$; $t(\frac{1}{2},0,\frac{1}{2})$; (2); (3); (5); (13); (25)

Positions

Multiplicity, Wyckoff letter, Site symmetry			Coordinates (0,0,0)+	(0,½,½)+	(½,0,½)+	(½,½,0)+	Reflection conditions
							h,k,l permutable
							General:
192	i	1	(1) x,y,z	(2) $\bar{x},\bar{y}+\frac{1}{2},z+\frac{1}{2}$	(3) $\bar{x}+\frac{1}{2},y+\frac{1}{2},\bar{z}$	(4) $x+\frac{1}{2},\bar{y},\bar{z}+\frac{1}{2}$	hkl : $h+k=2n$ and $h+l,k+l=2n$
			(5) z,x,y	(6) $z+\frac{1}{2},\bar{x},\bar{y}+\frac{1}{2}$	(7) $\bar{z},\bar{x}+\frac{1}{2},y+\frac{1}{2}$	(8) $\bar{z}+\frac{1}{2},x+\frac{1}{2},\bar{y}$	
			(9) y,z,x	(10) $\bar{y}+\frac{1}{2},z+\frac{1}{2},\bar{x}$	(11) $y+\frac{1}{2},\bar{z},\bar{x}+\frac{1}{2}$	(12) $\bar{y},\bar{z}+\frac{1}{2},x+\frac{1}{2}$	$0kl$: $k+l=4n$ and $k,l=2n$
			(13) $y+\frac{3}{4},x+\frac{1}{4},\bar{z}+\frac{3}{4}$	(14) $\bar{y}+\frac{1}{4},\bar{x}+\frac{1}{4},\bar{z}+\frac{1}{4}$	(15) $y+\frac{1}{4},\bar{x}+\frac{3}{4},z+\frac{3}{4}$	(16) $\bar{y}+\frac{3}{4},x+\frac{3}{4},z+\frac{1}{4}$	hhl : $h+l=2n$
			(17) $x+\frac{3}{4},z+\frac{1}{4},\bar{y}+\frac{3}{4}$	(18) $\bar{x}+\frac{3}{4},z+\frac{3}{4},y+\frac{1}{4}$	(19) $\bar{x}+\frac{1}{4},\bar{z}+\frac{1}{4},\bar{y}+\frac{1}{4}$	(20) $x+\frac{1}{4},\bar{z}+\frac{3}{4},y+\frac{3}{4}$	$h00$: $h=4n$
			(21) $z+\frac{3}{4},y+\frac{1}{4},\bar{x}+\frac{3}{4}$	(22) $z+\frac{1}{4},\bar{y}+\frac{3}{4},x+\frac{3}{4}$	(23) $\bar{z}+\frac{3}{4},y+\frac{3}{4},x+\frac{1}{4}$	(24) $\bar{z}+\frac{1}{4},\bar{y}+\frac{1}{4},\bar{x}+\frac{1}{4}$	
			(25) $\bar{x}+\frac{1}{4},\bar{y}+\frac{1}{4},\bar{z}+\frac{1}{4}$	(26) $x+\frac{1}{4},y+\frac{3}{4},\bar{z}+\frac{3}{4}$	(27) $x+\frac{3}{4},\bar{y}+\frac{3}{4},z+\frac{1}{4}$	(28) $\bar{x}+\frac{3}{4},y+\frac{1}{4},z+\frac{3}{4}$	
			(29) $\bar{z}+\frac{1}{4},\bar{x}+\frac{1}{4},\bar{y}+\frac{1}{4}$	(30) $\bar{z}+\frac{3}{4},x+\frac{1}{4},y+\frac{3}{4}$	(31) $z+\frac{1}{4},x+\frac{3}{4},\bar{y}+\frac{3}{4}$	(32) $z+\frac{3}{4},\bar{x}+\frac{3}{4},y+\frac{1}{4}$	
			(33) $\bar{y}+\frac{1}{4},\bar{z}+\frac{1}{4},\bar{x}+\frac{1}{4}$	(34) $y+\frac{3}{4},\bar{z}+\frac{3}{4},x+\frac{1}{4}$	(35) $\bar{y}+\frac{3}{4},z+\frac{1}{4},x+\frac{3}{4}$	(36) $y+\frac{1}{4},z+\frac{3}{4},\bar{x}+\frac{3}{4}$	
			(37) $\bar{y}+\frac{1}{2},\bar{x},z+\frac{1}{2}$	(38) y,x,z	(39) $\bar{y},x+\frac{1}{2},\bar{z}+\frac{1}{2}$	(40) $y+\frac{1}{2},\bar{x}+\frac{1}{2},\bar{z}$	
			(41) $\bar{x}+\frac{1}{2},\bar{z},y+\frac{1}{2}$	(42) $x+\frac{1}{2},\bar{z}+\frac{1}{2},\bar{y}$	(43) x,z,y	(44) $\bar{x},z+\frac{1}{2},\bar{y}+\frac{1}{2}$	
			(45) $\bar{z}+\frac{1}{2},\bar{y},x+\frac{1}{2}$	(46) $\bar{z},y+\frac{1}{2},\bar{x}+\frac{1}{2}$	(47) $z+\frac{1}{2},\bar{y}+\frac{1}{2},\bar{x}$	(48) z,y,x	
							Special: as above, plus
96	h	..2	$\frac{1}{8},y,\bar{y}+\frac{1}{4}$	$\frac{7}{8},\bar{y}+\frac{1}{2},\bar{y}+\frac{3}{4}$	$\frac{3}{8},y+\frac{1}{2},y+\frac{3}{4}$	$\frac{5}{8},\bar{y},y+\frac{1}{4}$	no extra conditions
			$\bar{y}+\frac{1}{4},\frac{1}{8},y$	$\bar{y}+\frac{3}{4},\frac{7}{8},\bar{y}+\frac{1}{2}$	$y+\frac{3}{4},\frac{3}{8},y+\frac{1}{2}$	$y+\frac{1}{4},\frac{5}{8},\bar{y}$	
			$y,\bar{y}+\frac{1}{4},\frac{1}{8}$	$\bar{y}+\frac{1}{2},\bar{y}+\frac{3}{4},\frac{7}{8}$	$y+\frac{1}{2},y+\frac{3}{4},\frac{3}{8}$	$\bar{y},y+\frac{1}{4},\frac{5}{8}$	
			$\frac{1}{8},\bar{y}+\frac{1}{4},y$	$\frac{3}{8},y+\frac{3}{4},y+\frac{1}{2}$	$\frac{7}{8},\bar{y}+\frac{3}{4},\bar{y}+\frac{1}{2}$	$\frac{5}{8},y+\frac{1}{4},\bar{y}$	
			$y,\frac{1}{8},\bar{y}+\frac{1}{4}$	$y+\frac{1}{2},\frac{3}{8},y+\frac{3}{4}$	$\bar{y}+\frac{1}{2},\frac{7}{8},\bar{y}+\frac{3}{4}$	$\bar{y},\frac{5}{8},y+\frac{1}{4}$	
			$\bar{y}+\frac{1}{4},y,\frac{1}{8}$	$y+\frac{3}{4},y+\frac{1}{2},\frac{3}{8}$	$\bar{y}+\frac{3}{4},\bar{y}+\frac{1}{2},\frac{7}{8}$	$y+\frac{1}{4},\bar{y},\frac{5}{8}$	
96	g	..m	x,x,z	$\bar{x},\bar{x}+\frac{1}{2},z+\frac{1}{2}$	$\bar{x}+\frac{1}{2},x+\frac{1}{2},\bar{z}$	$x+\frac{1}{2},\bar{x},\bar{z}+\frac{1}{2}$	no extra conditions
			z,x,x	$z+\frac{1}{2},\bar{x},\bar{x}+\frac{1}{2}$	$\bar{z},\bar{x}+\frac{1}{2},x+\frac{1}{2}$	$\bar{z}+\frac{1}{2},x+\frac{1}{2},\bar{x}$	
			x,z,x	$\bar{x}+\frac{1}{2},z+\frac{1}{2},\bar{x}$	$x+\frac{1}{2},\bar{z},\bar{x}+\frac{1}{2}$	$\bar{x},\bar{z}+\frac{1}{2},x+\frac{1}{2}$	
			$x+\frac{3}{4},x+\frac{1}{4},\bar{z}+\frac{3}{4}$	$\bar{x}+\frac{1}{4},\bar{x}+\frac{1}{4},\bar{z}+\frac{1}{4}$	$x+\frac{1}{4},\bar{x}+\frac{3}{4},z+\frac{3}{4}$	$\bar{x}+\frac{3}{4},x+\frac{3}{4},z+\frac{1}{4}$	
			$x+\frac{3}{4},z+\frac{1}{4},\bar{x}+\frac{3}{4}$	$\bar{x}+\frac{3}{4},z+\frac{3}{4},x+\frac{1}{4}$	$\bar{x}+\frac{1}{4},\bar{z}+\frac{1}{4},\bar{x}+\frac{1}{4}$	$x+\frac{1}{4},\bar{z}+\frac{3}{4},x+\frac{3}{4}$	
			$z+\frac{3}{4},x+\frac{1}{4},\bar{x}+\frac{3}{4}$	$z+\frac{1}{4},\bar{x}+\frac{3}{4},x+\frac{3}{4}$	$\bar{z}+\frac{3}{4},x+\frac{3}{4},x+\frac{1}{4}$	$\bar{z}+\frac{1}{4},\bar{x}+\frac{1}{4},\bar{x}+\frac{1}{4}$	
48	f	2.mm	$x,0,0$	$\bar{x},\frac{1}{2},\frac{1}{2}$	$0,x,0$	$\frac{1}{2},\bar{x},\frac{1}{2}$	$0,0,x$	$\frac{1}{2},\frac{1}{2},\bar{x}$	hkl : $h=2n+1$ or $h+k+l=4n$
			$\frac{3}{4},x+\frac{1}{4},\frac{3}{4}$	$\frac{1}{4},\bar{x}+\frac{1}{4},\frac{1}{4}$	$x+\frac{3}{4},\frac{3}{4},\frac{1}{4}$	$\bar{x}+\frac{3}{4},\frac{3}{4},\frac{1}{4}$	$\frac{3}{4},\frac{1}{4},\bar{x}+\frac{3}{4}$	$\frac{1}{4},\frac{3}{4},x+\frac{3}{4}$	
32	e	.3m	x,x,x	$\bar{x},\bar{x}+\frac{1}{2},x+\frac{1}{2}$			no extra conditions
			$\bar{x}+\frac{1}{2},x+\frac{1}{2},\bar{x}$	$x+\frac{1}{2},\bar{x},\bar{x}+\frac{1}{2}$			
			$x+\frac{3}{4},x+\frac{1}{4},\bar{x}+\frac{3}{4}$	$\bar{x}+\frac{1}{4},\bar{x}+\frac{1}{4},\bar{x}+\frac{1}{4}$			
			$x+\frac{1}{4},\bar{x}+\frac{3}{4},x+\frac{3}{4}$	$\bar{x}+\frac{3}{4},x+\frac{3}{4},x+\frac{1}{4}$			
16	d	.$\bar{3}$$m$	$\frac{5}{8},\frac{5}{8},\frac{5}{8}$	$\frac{3}{8},\frac{7}{8},\frac{1}{8}$	$\frac{7}{8},\frac{1}{8},\frac{3}{8}$	$\frac{1}{8},\frac{3}{8},\frac{7}{8}$	hkl : $h=2n+1$ or $h,k,l=4n+2$ or $h,k,l=4n$
16	c	.$\bar{3}$$m$	$\frac{1}{8},\frac{1}{8},\frac{1}{8}$	$\frac{7}{8},\frac{3}{8},\frac{5}{8}$	$\frac{3}{8},\frac{5}{8},\frac{7}{8}$	$\frac{5}{8},\frac{7}{8},\frac{3}{8}$	
8	b	$\bar{4}3m$	$\frac{1}{2},\frac{1}{2},\frac{1}{2}$	$\frac{1}{4},\frac{3}{4},\frac{1}{4}$			hkl : $h=2n+1$ or $h+k+l=4n$
8	a	$\bar{4}3m$	$0,0,0$	$\frac{3}{4},\frac{1}{4},\frac{3}{4}$			

Symmetry of special projections

Along [001] $p4mm$
$\mathbf{a}' = \frac{1}{4}(\mathbf{a}-\mathbf{b})$ $\mathbf{b}' = \frac{1}{4}(\mathbf{a}+\mathbf{b})$
Origin at $0,0,z$

Along [111] $p6mm$
$\mathbf{a}' = \frac{1}{6}(2\mathbf{a}-\mathbf{b}-\mathbf{c})$ $\mathbf{b}' = \frac{1}{6}(-\mathbf{a}+2\mathbf{b}-\mathbf{c})$
Origin at x,x,x

Along [110] $c2mm$
$\mathbf{a}' = \frac{1}{2}(-\mathbf{a}+\mathbf{b})$ $\mathbf{b}' = \mathbf{c}$
Origin at $x,x,\frac{1}{8}$

XX42

ORIGIN CHOICE 1

Maximal non-isomorphic subgroups

I
- [2] $F\bar{4}3m$ (216) (1; 2; 3; 4; 5; 6; 7; 8; 9; 10; 11; 12; 37; 38; 39; 40; 41; 42; 43; 44; 45; 46; 47; 48)+
- [2] $F4_132$ (210) (1; 2; 3; 4; 5; 6; 7; 8; 9; 10; 11; 12; 13; 14; 15; 16; 17; 18; 19; 20; 21; 22; 23; 24)+
- [2] $Fd\bar{3}1$ ($Fd\bar{3}$, 203) (1; 2; 3; 4; 5; 6; 7; 8; 9; 10; 11; 12; 25; 26; 27; 28; 29; 30; 31; 32; 33; 34; 35; 36)+
- [3] $F4_1/d12/m$ ($I4_1/amd$, 141) (1; 2; 3; 4; 13; 14; 15; 16; 25; 26; 27; 28; 37; 38; 39; 40)+
- [3] $F4_1/d12/m$ ($I4_1/amd$, 141) (1; 2; 3; 4; 17; 18; 19; 20; 25; 26; 27; 28; 41; 42; 43; 44)+
- [3] $F4_1/d12/m$ ($I4_1/amd$, 141) (1; 2; 3; 4; 21; 22; 23; 24; 25; 26; 27; 28; 45; 46; 47; 48)+
- [4] $F1\bar{3}2/m$ ($R\bar{3}m$, 166) (1; 5; 9; 14; 19; 24; 25; 29; 33; 38; 43; 48)+
- [4] $F1\bar{3}2/m$ ($R\bar{3}m$, 166) (1; 6; 12; 13; 18; 24; 25; 30; 36; 37; 42; 48)+
- [4] $F1\bar{3}2/m$ ($R\bar{3}m$, 166) (1; 7; 10; 13; 19; 22; 25; 31; 34; 37; 43; 46)+
- [4] $F1\bar{3}2/m$ ($R\bar{3}m$, 166) (1; 8; 11; 14; 18; 22; 25; 32; 35; 38; 42; 46)+

IIa none

IIb none

Maximal isomorphic subgroups of lowest index

IIc [27] $Fd\bar{3}m$ ($\mathbf{a}' = 3\mathbf{a}, \mathbf{b}' = 3\mathbf{b}, \mathbf{c}' = 3\mathbf{c}$) (227)

Minimal non-isomorphic supergroups

I none

II [2] $Pn\bar{3}m$ ($\mathbf{a}' = \frac{1}{2}\mathbf{a}, \mathbf{b}' = \frac{1}{2}\mathbf{b}, \mathbf{c}' = \frac{1}{2}\mathbf{c}$) (224)

XX43

Symmetry operations

For (0,0,0)+ set

(1) 1
(2) $2(0,0,\frac{1}{2})$ $0,\frac{1}{4},z$
(3) $2(0,\frac{1}{2},0)$ $\frac{1}{4},y,0$
(4) $2(\frac{1}{2},0,0)$ $x,0,\frac{1}{4}$
(5) 3^+ x,x,x
(6) $3^+(\frac{1}{3},-\frac{1}{3},\frac{1}{3})$ $\bar{x}+\frac{1}{6},x+\frac{1}{6},\bar{x}$
(7) $3^+(-\frac{1}{3},\frac{1}{3},\frac{1}{3})$ $x+\frac{1}{3},\bar{x}-\frac{1}{6},\bar{x}$
(8) $3^+(\frac{1}{3},\frac{1}{3},-\frac{1}{3})$ $\bar{x}+\frac{1}{6},\bar{x}+\frac{1}{3},x$
(9) 3^- x,x,x
(10) 3^- $x,\bar{x}+\frac{1}{2},\bar{x}$
(11) 3^- $\bar{x}+\frac{1}{2},\bar{x},x$
(12) 3^- $\bar{x}-\frac{1}{2},x+\frac{1}{2},\bar{x}$
(13) $2(\frac{1}{2},\frac{1}{2},0)$ $x,x-\frac{1}{4},\frac{3}{8}$
(14) 2 $x,\bar{x}+\frac{1}{4},\frac{1}{8}$
(15) $4^-(0,0,\frac{3}{4})$ $\frac{1}{2},\frac{1}{4},z$
(16) $4^+(0,0,\frac{1}{4})$ $0,\frac{3}{4},z$
(17) $4^-(\frac{3}{4},0,0)$ $x,\frac{1}{2},\frac{1}{4}$
(18) $2(0,\frac{1}{2},\frac{1}{2})$ $\frac{3}{8},y+\frac{1}{4},y$
(19) 2 $\frac{1}{8},y+\frac{1}{4},\bar{y}$
(20) $4^+(\frac{1}{4},0,0)$ $x,0,\frac{3}{4}$
(21) $4^+(0,\frac{1}{4},0)$ $\frac{3}{4},y,0$
(22) $2(\frac{1}{2},0,\frac{1}{2})$ $x-\frac{1}{4},\frac{3}{8},x$
(23) $4^-(0,\frac{3}{4},0)$ $\frac{1}{4},y,\frac{1}{2}$
(24) 2 $\bar{x}+\frac{1}{4},\frac{1}{8},x$
(25) $\bar{1}$ $\frac{1}{8},\frac{1}{8},\frac{1}{8}$
(26) $d(\frac{1}{4},\frac{3}{4},0)$ $x,y,\frac{3}{8}$
(27) $d(\frac{3}{4},0,\frac{1}{4})$ $x,\frac{3}{8},z$
(28) $d(0,\frac{1}{4},\frac{3}{4})$ $\frac{3}{8},y,z$
(29) $\bar{3}^+$ $x,x,x;$ $\frac{1}{8},\frac{1}{8},\frac{1}{8}$
(30) $\bar{3}^+$ $\bar{x}-1,x+1,\bar{x};$ $-\frac{1}{8},\frac{1}{8},\frac{7}{8}$
(31) $\bar{3}^+$ $x,\bar{x}+1,\bar{x};$ $\frac{1}{8},\frac{7}{8},-\frac{1}{8}$
(32) $\bar{3}^+$ $\bar{x}+1,\bar{x},x;$ $\frac{7}{8},-\frac{1}{8},\frac{1}{8}$
(33) $\bar{3}^-$ $x,x,x;$ $\frac{1}{8},\frac{1}{8},\frac{1}{8}$
(34) $\bar{3}^-$ $x+\frac{3}{2},\bar{x}-1,\bar{x};$ $\frac{5}{8},-\frac{1}{8},\frac{7}{8}$
(35) $\bar{3}^-$ $\bar{x}+\frac{1}{2},\bar{x}+\frac{3}{2},x;$ $-\frac{1}{8},\frac{7}{8},\frac{5}{8}$
(36) $\bar{3}^-$ $\bar{x}+1,x+\frac{1}{2},\bar{x};$ $\frac{7}{8},\frac{5}{8},-\frac{1}{8}$
(37) $g(\frac{1}{4},-\frac{1}{4},\frac{1}{2})$ $x+\frac{1}{4},\bar{x},z$
(38) m x,x,z
(39) $\bar{4}^-$ $-\frac{1}{4},\frac{1}{4},z;$ $-\frac{1}{4},\frac{1}{4},\frac{1}{4}$
(40) $\bar{4}^+$ $\frac{1}{2},0,z;$ $\frac{1}{2},0,0$
(41) $\bar{4}^-$ $x,-\frac{1}{4},\frac{1}{4};$ $\frac{1}{4},-\frac{1}{4},\frac{1}{4}$
(42) $g(\frac{1}{2},\frac{1}{4},-\frac{1}{4})$ $x,y+\frac{1}{4},\bar{y}$
(43) m x,y,y
(44) $\bar{4}^+$ $x,\frac{1}{2},0;$ $0,\frac{1}{2},0$
(45) $\bar{4}^+$ $0,y,\frac{1}{2};$ $0,0,\frac{1}{2}$
(46) $g(-\frac{1}{4},\frac{1}{2},\frac{1}{4})$ $\bar{x}+\frac{1}{4},y,x$
(47) $\bar{4}^-$ $\frac{1}{4},y,-\frac{1}{4};$ $\frac{1}{4},\frac{1}{4},-\frac{1}{4}$
(48) m x,y,x

For $(0,\frac{1}{2},\frac{1}{2})$+ set

(1) $t(0,\frac{1}{2},\frac{1}{2})$
(2) 2 $0,0,z$
(3) 2 $\frac{1}{4},y,\frac{1}{4}$
(4) $2(\frac{1}{2},0,0)$ $x,\frac{1}{4},0$
(5) $3^+(\frac{1}{3},\frac{1}{3},\frac{1}{3})$ $x-\frac{1}{3},x-\frac{1}{6},x$
(6) 3^+ $\bar{x}+\frac{1}{2},x,\bar{x}$
(7) 3^+ $x,\bar{x},\bar{x}$
(8) 3^+ $\bar{x}+\frac{1}{2},\bar{x}+\frac{1}{2},x$
(9) $3^-(\frac{1}{3},\frac{1}{3},\frac{1}{3})$ $x-\frac{1}{6},x+\frac{1}{6},x$
(10) 3^- $x+\frac{1}{2},\bar{x},\bar{x}$
(11) $3^-(\frac{1}{3},\frac{1}{3},-\frac{1}{3})$ $\bar{x}+\frac{1}{3},\bar{x}+\frac{1}{6},x$
(12) 3^- $\bar{x},x,\bar{x}$
(13) $2(\frac{3}{4},\frac{3}{4},0)$ $x,x,\frac{1}{8}$
(14) $2(-\frac{1}{4},\frac{1}{4},0)$ $x,\bar{x}+\frac{1}{2},\frac{3}{8}$
(15) $4^-(0,0,\frac{1}{4})$ $\frac{1}{4},0,z$
(16) $4^+(0,0,\frac{3}{4})$ $\frac{1}{4},\frac{1}{2},z$
(17) $4^-(\frac{3}{4},0,0)$ $x,\frac{1}{2},-\frac{1}{4}$
(18) $2(0,\frac{1}{2},\frac{1}{2})$ $\frac{3}{8},y-\frac{1}{4},y$
(19) 2 $\frac{1}{8},y+\frac{3}{4},\bar{y}$
(20) $4^+(\frac{1}{4},0,0)$ $x,0,\frac{1}{4}$
(21) $4^+(0,\frac{3}{4},0)$ $\frac{1}{2},y,-\frac{1}{4}$
(22) $2(\frac{1}{4},0,\frac{1}{4})$ $x,\frac{1}{8},x$
(23) $4^-(0,\frac{1}{4},0)$ $0,y,\frac{3}{4}$
(24) $2(-\frac{1}{4},0,\frac{1}{4})$ $\bar{x}+\frac{1}{2},\frac{3}{8},x$
(25) $\bar{1}$ $\frac{1}{8},\frac{3}{8},\frac{3}{8}$
(26) $d(\frac{1}{4},\frac{1}{4},0)$ $x,y,\frac{1}{8}$
(27) $d(\frac{3}{4},0,\frac{3}{4})$ $x,\frac{1}{8},z$
(28) $d(0,\frac{3}{4},\frac{1}{4})$ $\frac{3}{8},y,z$
(29) $\bar{3}^+$ $x,x+\frac{1}{2},x;$ $\frac{1}{8},\frac{5}{8},\frac{1}{8}$
(30) $\bar{3}^+$ $\bar{x}-1,x+\frac{3}{2},\bar{x};$ $-\frac{1}{8},\frac{5}{8},\frac{7}{8}$
(31) $\bar{3}^+$ $x,\bar{x}+\frac{1}{2},\bar{x};$ $\frac{1}{8},\frac{3}{8},-\frac{1}{8}$
(32) $\bar{3}^+$ $\bar{x}+1,\bar{x}-\frac{1}{2},x;$ $\frac{7}{8},-\frac{5}{8},\frac{1}{8}$
(33) $\bar{3}^-$ $x-\frac{1}{2},x-\frac{1}{2},x;$ $\frac{1}{8},\frac{1}{8},\frac{5}{8}$
(34) $\bar{3}^-$ $x+1,\bar{x}-\frac{3}{2},\bar{x};$ $\frac{1}{8},-\frac{5}{8},\frac{7}{8}$
(35) $\bar{3}^-$ $\bar{x},\bar{x}+1,x;$ $-\frac{1}{8},\frac{7}{8},\frac{1}{8}$
(36) $\bar{3}^-$ $\bar{x}+\frac{1}{2},x,\bar{x};$ $\frac{3}{8},\frac{1}{8},-\frac{1}{8}$
(37) m $x+\frac{1}{2},\bar{x},z$
(38) $g(\frac{1}{4},\frac{1}{4},\frac{1}{2})$ $x-\frac{1}{4},x,z$
(39) $\bar{4}^-$ $0,0,z;$ $0,0,0$
(40) $\bar{4}^+$ $\frac{1}{4},-\frac{1}{4},z;$ $\frac{1}{4},-\frac{1}{4},\frac{1}{4}$
(41) $\bar{4}^-$ $x,\frac{1}{4},\frac{1}{4};$ $\frac{1}{4},\frac{1}{4},\frac{1}{4}$
(42) $g(\frac{1}{2},-\frac{1}{4},\frac{1}{4})$ $x,y+\frac{1}{4},\bar{y}$
(43) $g(0,\frac{1}{2},\frac{1}{2})$ x,y,y
(44) $\bar{4}^+$ $x,0,0;$ $0,0,0$
(45) $\bar{4}^+$ $\frac{1}{4},y,\frac{1}{4};$ $\frac{1}{4},\frac{1}{4},\frac{1}{4}$
(46) m $\bar{x},y,x$
(47) $\bar{4}^-$ $\frac{1}{2},y,0;$ $\frac{1}{2},0,0$
(48) $g(\frac{1}{4},\frac{1}{2},\frac{1}{4})$ $x-\frac{1}{4},y,x$

For $(\frac{1}{2},0,\frac{1}{2})$+ set

(1) $t(\frac{1}{2},0,\frac{1}{2})$
(2) 2 $\frac{1}{4},\frac{1}{4},z$
(3) $2(0,\frac{1}{2},0)$ $0,y,\frac{1}{4}$
(4) 2 $x,0,0$
(5) $3^+(\frac{1}{3},\frac{1}{3},\frac{1}{3})$ $x+\frac{1}{6},x-\frac{1}{6},x$
(6) 3^+ $\bar{x},x,\bar{x}$
(7) 3^+ $x+\frac{1}{2},\bar{x},\bar{x}$
(8) 3^+ $\bar{x},\bar{x}+\frac{1}{2},x$
(9) $3^-(\frac{1}{3},\frac{1}{3},\frac{1}{3})$ $x-\frac{1}{6},x-\frac{1}{3},x$
(10) $3^-(-\frac{1}{3},\frac{1}{3},\frac{1}{3})$ $x+\frac{1}{6},\bar{x}+\frac{1}{6},\bar{x}$
(11) 3^- $\bar{x},\bar{x},x$
(12) 3^- $\bar{x},x+\frac{1}{2},\bar{x}$
(13) $2(\frac{1}{4},\frac{1}{4},0)$ $x,x,\frac{1}{8}$
(14) $2(\frac{1}{4},-\frac{1}{4},0)$ $x,\bar{x}+\frac{1}{2},\frac{3}{8}$
(15) $4^-(0,0,\frac{1}{4})$ $\frac{3}{4},0,z$
(16) $4^+(0,0,\frac{3}{4})$ $-\frac{1}{4},\frac{1}{2},z$
(17) $4^-(\frac{1}{4},0,0)$ $x,\frac{1}{4},0$
(18) $2(0,\frac{3}{4},\frac{3}{4})$ $\frac{1}{8},y,y$
(19) $2(0,-\frac{1}{4},\frac{1}{4})$ $\frac{3}{8},y+\frac{1}{2},\bar{y}$
(20) $4^+(\frac{3}{4},0,0)$ $x,\frac{1}{4},\frac{1}{2}$
(21) $4^+(0,\frac{1}{4},0)$ $\frac{1}{4},y,0$
(22) $2(\frac{1}{2},0,\frac{1}{2})$ $x+\frac{1}{4},\frac{3}{8},x$
(23) $4^-(0,\frac{3}{4},0)$ $-\frac{1}{4},y,\frac{1}{2}$
(24) 2 $\bar{x}+\frac{3}{4},\frac{1}{8},x$
(25) $\bar{1}$ $\frac{3}{8},\frac{1}{8},\frac{3}{8}$
(26) $d(\frac{3}{4},\frac{3}{4},0)$ $x,y,\frac{1}{8}$
(27) $d(\frac{1}{4},0,\frac{3}{4})$ $x,\frac{3}{8},z$
(28) $d(0,\frac{1}{4},\frac{1}{4})$ $\frac{1}{8},y,z$
(29) $\bar{3}^+$ $x-\frac{1}{2},x-\frac{1}{2},x;$ $\frac{1}{8},\frac{1}{8},\frac{5}{8}$
(30) $\bar{3}^+$ $\bar{x}-\frac{1}{2},x+\frac{1}{2},\bar{x};$ $-\frac{1}{8},\frac{1}{8},\frac{3}{8}$
(31) $\bar{3}^+$ $x-\frac{1}{2},\bar{x}+\frac{3}{2},\bar{x};$ $\frac{1}{8},\frac{7}{8},-\frac{5}{8}$
(32) $\bar{3}^+$ $\bar{x}+\frac{3}{2},\bar{x}+\frac{1}{2},x;$ $\frac{7}{8},-\frac{1}{8},\frac{5}{8}$
(33) $\bar{3}^-$ $x+\frac{1}{2},x,x;$ $\frac{5}{8},\frac{1}{8},\frac{1}{8}$
(34) $\bar{3}^-$ $x+1,\bar{x}-1,\bar{x};$ $\frac{1}{8},-\frac{1}{8},\frac{7}{8}$
(35) $\bar{3}^-$ $\bar{x},\bar{x}+\frac{1}{2},x;$ $-\frac{1}{8},\frac{3}{8},\frac{1}{8}$
(36) $\bar{3}^-$ $\bar{x}+\frac{3}{2},x-\frac{1}{2},\bar{x};$ $\frac{7}{8},\frac{1}{8},-\frac{5}{8}$
(37) m $x,\bar{x},z$
(38) $g(\frac{1}{4},\frac{1}{4},\frac{1}{2})$ $x+\frac{1}{4},x,z$
(39) $\bar{4}^-$ $0,\frac{1}{2},z;$ $0,\frac{1}{2},0$
(40) $\bar{4}^+$ $\frac{1}{4},\frac{1}{4},z;$ $\frac{1}{4},\frac{1}{4},\frac{1}{4}$
(41) $\bar{4}^-$ $x,0,0;$ $0,0,0$
(42) m $x,y,y+\frac{1}{2},\bar{y}$
(43) $g(\frac{1}{2},\frac{1}{4},\frac{1}{4})$ $x,y-\frac{1}{4},y$
(44) $\bar{4}^+$ $x,\frac{1}{2},-\frac{1}{4};$ $\frac{1}{4},\frac{1}{4},-\frac{1}{4}$
(45) $\bar{4}^+$ $0,y,0;$ $0,0,0$
(46) $g(\frac{1}{4},\frac{1}{2},-\frac{1}{4})$ $\bar{x}+\frac{1}{4},y,x$
(47) $\bar{4}^-$ $\frac{1}{4},y,\frac{1}{4};$ $\frac{1}{4},\frac{1}{4},\frac{1}{4}$
(48) $g(\frac{1}{2},0,\frac{1}{2})$ x,y,x

For $(\frac{1}{2},\frac{1}{2},0)$+ set

(1) $t(\frac{1}{2},\frac{1}{2},0)$
(2) $2(0,0,\frac{1}{2})$ $\frac{1}{4},0,z$
(3) 2 $0,y,0$
(4) 2 $x,\frac{1}{4},\frac{1}{4}$
(5) $3^+(\frac{1}{3},\frac{1}{3},\frac{1}{3})$ $x+\frac{1}{6},x+\frac{1}{3},x$
(6) 3^+ $\bar{x},x+\frac{1}{2},\bar{x}$
(7) 3^+ $x+\frac{1}{2},\bar{x}-\frac{1}{2},\bar{x}$
(8) 3^+ $\bar{x},\bar{x},x$
(9) $3^-(\frac{1}{3},\frac{1}{3},\frac{1}{3})$ $x+\frac{1}{3},x+\frac{1}{6},x$
(10) 3^- $x,\bar{x},\bar{x}$
(11) 3^- $\bar{x}+\frac{1}{2},\bar{x}+\frac{1}{2},x$
(12) $3^-(\frac{1}{3},-\frac{1}{3},\frac{1}{3})$ $\bar{x}-\frac{1}{6},x+\frac{1}{3},\bar{x}$
(13) $2(\frac{1}{2},\frac{1}{2},0)$ $x,x+\frac{1}{4},\frac{3}{8}$
(14) 2 $x,\bar{x}+\frac{3}{4},\frac{1}{8}$
(15) $4^-(0,0,\frac{3}{4})$ $\frac{1}{2},-\frac{1}{4},z$
(16) $4^+(0,0,\frac{1}{4})$ $0,\frac{1}{4},z$
(17) $4^-(\frac{1}{4},0,0)$ $x,\frac{3}{4},0$
(18) $2(0,\frac{1}{4},\frac{1}{4})$ $\frac{1}{8},y,y$
(19) $2(0,\frac{1}{4},-\frac{1}{4})$ $\frac{3}{8},y+\frac{1}{2},\bar{y}$
(20) $4^+(\frac{3}{4},0,0)$ $x,-\frac{1}{4},\frac{1}{2}$
(21) $4^+(0,\frac{3}{4},0)$ $\frac{1}{2},y,\frac{1}{4}$
(22) $2(\frac{3}{4},0,\frac{3}{4})$ $x,\frac{1}{8},x$
(23) $4^-(0,\frac{1}{4},0)$ $0,y,\frac{1}{4}$
(24) $2(\frac{1}{2},0,-\frac{1}{4})$ $\bar{x}+\frac{1}{2},\frac{3}{8},x$
(25) $\bar{1}$ $\frac{3}{8},\frac{3}{8},\frac{1}{8}$
(26) $d(\frac{3}{4},\frac{1}{4},0)$ $x,y,\frac{3}{8}$
(27) $d(\frac{1}{4},0,\frac{1}{4})$ $x,\frac{1}{8},z$
(28) $d(0,\frac{3}{4},\frac{3}{4})$ $\frac{1}{8},y,z$
(29) $\bar{3}^+$ $x+\frac{1}{2},x,x;$ $\frac{5}{8},\frac{1}{8},\frac{1}{8}$
(30) $\bar{3}^+$ $\bar{x}-\frac{3}{2},x+1,\bar{x};$ $-\frac{5}{8},\frac{1}{8},\frac{7}{8}$
(31) $\bar{3}^+$ $x+\frac{1}{2},\bar{x}+1,\bar{x};$ $\frac{5}{8},\frac{7}{8},-\frac{1}{8}$
(32) $\bar{3}^+$ $\bar{x}+\frac{1}{2},\bar{x},x;$ $\frac{3}{8},-\frac{1}{8},\frac{1}{8}$
(33) $\bar{3}^-$ $x,x+\frac{1}{2},x;$ $\frac{1}{8},\frac{5}{8},\frac{1}{8}$
(34) $\bar{3}^-$ $x+\frac{1}{2},\bar{x}-\frac{1}{2},\bar{x};$ $\frac{1}{8},-\frac{1}{8},\frac{3}{8}$
(35) $\bar{3}^-$ $\bar{x}-\frac{1}{2},\bar{x}+1,x;$ $-\frac{5}{8},\frac{7}{8},\frac{1}{8}$
(36) $\bar{3}^-$ $\bar{x}+1,x,\bar{x};$ $\frac{7}{8},\frac{1}{8},-\frac{1}{8}$
(37) $g(-\frac{1}{4},\frac{1}{4},\frac{1}{2})$ $x+\frac{1}{4},\bar{x},z$
(38) $g(\frac{1}{2},\frac{1}{2},0)$ x,x,z
(39) $\bar{4}^-$ $\frac{1}{4},\frac{1}{4},z;$ $\frac{1}{4},\frac{1}{4},\frac{1}{4}$
(40) $\bar{4}^+$ $0,0,z;$ $0,0,0$
(41) $\bar{4}^-$ $x,0,\frac{1}{2};$ $0,0,\frac{1}{2}$
(42) m $x,y,\bar{y}$
(43) $g(\frac{1}{2},\frac{1}{4},\frac{1}{4})$ $x,y+\frac{1}{4},y$
(44) $\bar{4}^+$ $x,\frac{1}{4},\frac{1}{4};$ $\frac{1}{4},\frac{1}{4},\frac{1}{4}$
(45) $\bar{4}^+$ $-\frac{1}{4},y,\frac{1}{4};$ $-\frac{1}{4},\frac{1}{4},\frac{1}{4}$
(46) m $\bar{x}+\frac{1}{2},y,x$
(47) $\bar{4}^-$ $0,y,0;$ $0,0,0$
(48) $g(\frac{1}{4},\frac{1}{2},\frac{1}{4})$ $x+\frac{1}{4},y,x$

XX44

$F\,d\,\bar{3}\,m$ O_h^7 $m\bar{3}m$ Cubic

No. 227 $F\ 4_1/d\ \bar{3}\ 2/m$ Patterson symmetry $F\,m\,\bar{3}\,m$

ORIGIN CHOICE 2

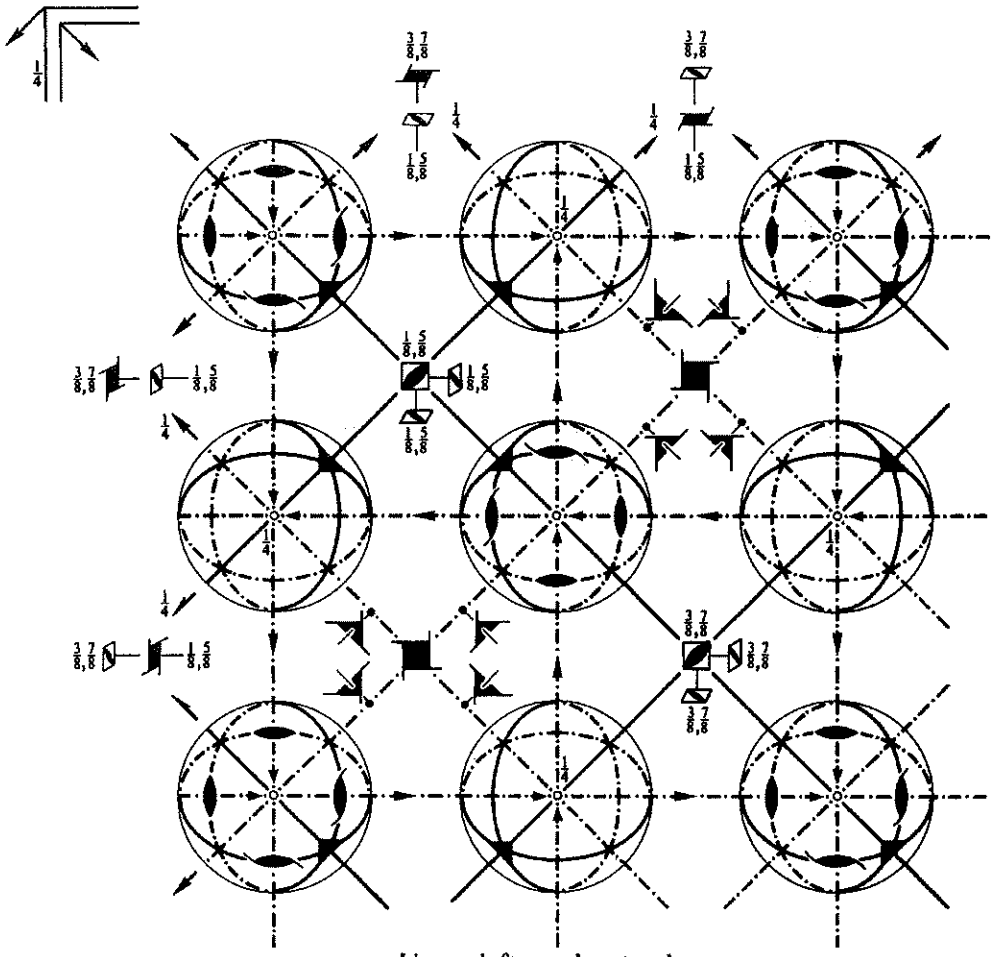

Upper left quadrant only

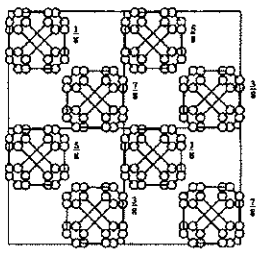

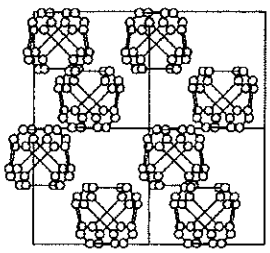

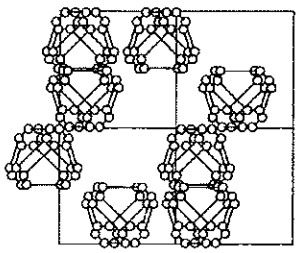

Origin at centre $(\bar{3}\,m)$, at $\frac{1}{8},\frac{1}{8},\frac{1}{8}$ from $\bar{4}\,3\,m$

Asymmetric unit $-\frac{1}{8}\le x\le\frac{3}{8};\quad -\frac{1}{8}\le y\le 0;\quad -\frac{1}{4}\le z\le 0;\quad y\le\min(\frac{1}{4}-x,x);\quad -y-\frac{1}{4}\le z\le y$

Vertices $-\frac{1}{8},-\frac{1}{8},-\frac{1}{8}\quad \frac{3}{8},-\frac{1}{8},-\frac{1}{8}\quad \frac{1}{4},0,0\quad 0,0,0\quad \frac{1}{4},0,-\frac{1}{4}\quad 0,0,-\frac{1}{4}$

Symmetry operations

(*given on page* 703)

XX45

Generators selected (1); $t(1,0,0)$; $t(0,1,0)$; $t(0,0,1)$; $t(0,\frac{1}{2},\frac{1}{2})$; $t(\frac{1}{2},0,\frac{1}{2})$; (2); (3); (5); (13); (25)

Positions

Multiplicity, Wyckoff letter, Site symmetry			Coordinates				Reflection conditions
			$(0,0,0)+$	$(0,\frac{1}{2},\frac{1}{2})+$	$(\frac{1}{2},0,\frac{1}{2})+$	$(\frac{1}{2},\frac{1}{2},0)+$	h,k,l permutable
							General:
192	i	1	(1) x,y,z	(2) $\bar{x}+\frac{3}{4},\bar{y}+\frac{1}{4},z+\frac{1}{2}$	(3) $\bar{x}+\frac{1}{4},y+\frac{1}{2},\bar{z}+\frac{3}{4}$	(4) $x+\frac{1}{2},\bar{y}+\frac{3}{4},\bar{z}+\frac{1}{4}$	hkl : $h+k=2n$ and $h+l,k+l=2n$
			(5) z,x,y	(6) $z+\frac{1}{2},\bar{x}+\frac{3}{4},\bar{y}+\frac{1}{4}$	(7) $\bar{z}+\frac{3}{4},\bar{x}+\frac{1}{4},y+\frac{1}{2}$	(8) $\bar{z}+\frac{1}{4},x+\frac{1}{2},\bar{y}+\frac{3}{4}$	
			(9) y,z,x	(10) $\bar{y}+\frac{1}{4},z+\frac{1}{2},\bar{x}+\frac{3}{4}$	(11) $y+\frac{1}{2},\bar{z}+\frac{3}{4},\bar{x}+\frac{1}{4}$	(12) $\bar{y}+\frac{3}{4},\bar{z}+\frac{1}{4},x+\frac{1}{2}$	$0kl$: $k+l=4n$ and $k,l=2n$
			(13) $y+\frac{3}{4},x+\frac{1}{4},\bar{z}+\frac{1}{2}$	(14) $\bar{y},\bar{x},\bar{z}$	(15) $y+\frac{1}{4},\bar{x}+\frac{1}{2},z+\frac{3}{4}$	(16) $\bar{y}+\frac{1}{2},x+\frac{3}{4},z+\frac{1}{4}$	
			(17) $x+\frac{3}{4},z+\frac{1}{4},\bar{y}+\frac{1}{2}$	(18) $\bar{x}+\frac{1}{2},z+\frac{3}{4},y+\frac{1}{4}$	(19) $\bar{x},\bar{z},\bar{y}$	(20) $x+\frac{1}{4},\bar{z}+\frac{1}{2},y+\frac{3}{4}$	hhl : $h+l=2n$
			(21) $z+\frac{3}{4},y+\frac{1}{4},\bar{x}+\frac{1}{2}$	(22) $z+\frac{1}{4},\bar{y}+\frac{1}{2},x+\frac{3}{4}$	(23) $\bar{z}+\frac{1}{2},y+\frac{3}{4},x+\frac{1}{4}$	(24) $\bar{z},\bar{y},\bar{x}$	$h00$: $h=4n$
			(25) $\bar{x},\bar{y},\bar{z}$	(26) $x+\frac{1}{4},y+\frac{3}{4},\bar{z}+\frac{1}{2}$	(27) $x+\frac{3}{4},\bar{y}+\frac{1}{2},z+\frac{1}{4}$	(28) $\bar{x}+\frac{1}{2},y+\frac{1}{4},z+\frac{3}{4}$	
			(29) $\bar{z},\bar{x},\bar{y}$	(30) $\bar{z}+\frac{1}{2},x+\frac{1}{4},y+\frac{3}{4}$	(31) $z+\frac{1}{4},x+\frac{3}{4},\bar{y}+\frac{1}{2}$	(32) $z+\frac{3}{4},\bar{x}+\frac{1}{2},y+\frac{1}{4}$	
			(33) $\bar{y},\bar{z},\bar{x}$	(34) $y+\frac{3}{4},\bar{z}+\frac{1}{2},x+\frac{1}{4}$	(35) $\bar{y}+\frac{1}{2},z+\frac{1}{4},x+\frac{3}{4}$	(36) $y+\frac{1}{4},z+\frac{3}{4},\bar{x}+\frac{1}{2}$	
			(37) $\bar{y}+\frac{1}{4},\bar{x}+\frac{3}{4},z+\frac{1}{2}$	(38) y,x,z	(39) $\bar{y}+\frac{3}{4},x+\frac{1}{2},\bar{z}+\frac{1}{4}$	(40) $y+\frac{1}{2},\bar{x}+\frac{1}{4},\bar{z}+\frac{3}{4}$	
			(41) $\bar{x}+\frac{1}{4},\bar{z}+\frac{3}{4},y+\frac{1}{2}$	(42) $x+\frac{1}{2},\bar{z}+\frac{1}{4},\bar{y}+\frac{3}{4}$	(43) x,z,y	(44) $\bar{x}+\frac{3}{4},z+\frac{1}{2},\bar{y}+\frac{1}{4}$	
			(45) $\bar{z}+\frac{1}{4},\bar{y}+\frac{3}{4},x+\frac{1}{2}$	(46) $\bar{z}+\frac{3}{4},y+\frac{1}{2},\bar{x}+\frac{1}{4}$	(47) $z+\frac{1}{2},\bar{y}+\frac{1}{4},\bar{x}+\frac{3}{4}$	(48) z,y,x	
							Special: as above, plus
96	h	. . 2	$0,y,\bar{y}$	$\frac{3}{4},\bar{y}+\frac{1}{4},\bar{y}+\frac{1}{2}$	$\frac{1}{4},y+\frac{1}{2},y+\frac{3}{4}$	$\frac{1}{2},\bar{y}+\frac{3}{4},y+\frac{1}{4}$	no extra conditions
			$\bar{y},0,y$	$\bar{y}+\frac{1}{2},\frac{3}{4},\bar{y}+\frac{1}{4}$	$y+\frac{3}{4},\frac{1}{4},y+\frac{1}{2}$	$y+\frac{1}{4},\frac{1}{2},\bar{y}+\frac{3}{4}$	
			$y,\bar{y},0$	$\bar{y}+\frac{1}{4},\bar{y}+\frac{1}{2},\frac{3}{4}$	$y+\frac{1}{2},y+\frac{3}{4},\frac{1}{4}$	$\bar{y}+\frac{3}{4},y+\frac{1}{4},\frac{1}{2}$	
			$0,\bar{y},y$	$\frac{1}{4},y+\frac{3}{4},y+\frac{1}{2}$	$\frac{3}{4},\bar{y}+\frac{1}{2},\bar{y}+\frac{1}{4}$	$\frac{1}{2},y+\frac{1}{4},\bar{y}+\frac{3}{4}$	
			$y,0,\bar{y}$	$y+\frac{1}{2},\frac{1}{4},y+\frac{3}{4}$	$\bar{y}+\frac{1}{4},\frac{3}{4},\bar{y}+\frac{1}{2}$	$\bar{y}+\frac{3}{4},\frac{1}{2},y+\frac{1}{4}$	
			$\bar{y},y,0$	$y+\frac{3}{4},y+\frac{1}{2},\frac{1}{4}$	$\bar{y}+\frac{1}{2},\bar{y}+\frac{1}{4},\frac{3}{4}$	$y+\frac{1}{4},\bar{y}+\frac{3}{4},\frac{1}{2}$	
96	g	. . m	x,x,z	$\bar{x}+\frac{3}{4},\bar{x}+\frac{1}{4},z+\frac{1}{2}$	$\bar{x}+\frac{1}{4},x+\frac{1}{2},\bar{z}+\frac{3}{4}$	$x+\frac{1}{2},\bar{x}+\frac{3}{4},\bar{z}+\frac{1}{4}$	no extra conditions
			z,x,x	$z+\frac{1}{2},\bar{x}+\frac{3}{4},\bar{x}+\frac{1}{4}$	$\bar{z}+\frac{3}{4},\bar{x}+\frac{1}{4},x+\frac{1}{2}$	$\bar{z}+\frac{1}{4},x+\frac{1}{2},\bar{x}+\frac{3}{4}$	
			x,z,x	$\bar{x}+\frac{1}{4},z+\frac{1}{2},\bar{x}+\frac{3}{4}$	$x+\frac{1}{2},\bar{z}+\frac{3}{4},\bar{x}+\frac{1}{4}$	$\bar{x}+\frac{3}{4},\bar{z}+\frac{1}{4},x+\frac{1}{2}$	
			$x+\frac{3}{4},x+\frac{1}{4},\bar{z}+\frac{1}{2}$	$\bar{x},\bar{x},\bar{z}$	$x+\frac{1}{4},\bar{x}+\frac{1}{2},z+\frac{3}{4}$	$\bar{x}+\frac{1}{2},x+\frac{3}{4},z+\frac{1}{4}$	
			$x+\frac{3}{4},z+\frac{1}{4},\bar{x}+\frac{1}{2}$	$\bar{x}+\frac{1}{2},z+\frac{3}{4},x+\frac{1}{4}$	$\bar{x},\bar{z},\bar{x}$	$x+\frac{1}{4},\bar{z}+\frac{1}{2},x+\frac{3}{4}$	
			$z+\frac{3}{4},x+\frac{1}{4},\bar{x}+\frac{1}{2}$	$z+\frac{1}{4},\bar{x}+\frac{1}{2},x+\frac{3}{4}$	$\bar{z}+\frac{1}{2},x+\frac{3}{4},x+\frac{1}{4}$	$\bar{z},\bar{x},\bar{x}$	
48	f	2 . mm	$x,\frac{1}{8},\frac{1}{8}$	$\bar{x}+\frac{3}{4},\frac{1}{8},\frac{5}{8}$	$\frac{1}{8},x,\frac{1}{8}$	$\frac{5}{8},\bar{x}+\frac{3}{4},\frac{1}{8}$	$\frac{1}{8},\frac{1}{8},x$	$\frac{1}{8},\frac{5}{8},\bar{x}+\frac{3}{4}$	hkl : $h=2n+1$ or $h+k+l=4n$
			$\frac{7}{8},x+\frac{1}{4},\frac{3}{8}$	$\frac{7}{8},\bar{x},\frac{7}{8}$	$x+\frac{3}{4},\frac{3}{8},\frac{3}{8}$	$\bar{x}+\frac{1}{2},\frac{7}{8},\frac{3}{8}$	$\frac{7}{8},\frac{3}{8},\bar{x}+\frac{1}{2}$	$\frac{3}{8},\frac{3}{8},x+\frac{3}{4}$	
32	e	. 3 m	x,x,x	$\bar{x}+\frac{3}{4},\bar{x}+\frac{1}{4},x+\frac{1}{2}$					no extra conditions
			$\bar{x}+\frac{3}{4},x+\frac{1}{2},\bar{x}+\frac{3}{4}$	$x+\frac{1}{2},\bar{x}+\frac{3}{4},\bar{x}+\frac{1}{4}$					
			$x+\frac{3}{4},x+\frac{1}{4},\bar{x}+\frac{1}{2}$	$\bar{x},\bar{x},\bar{x}$					
			$x+\frac{1}{4},\bar{x}+\frac{1}{2},x+\frac{3}{4}$	$\bar{x}+\frac{1}{2},x+\frac{3}{4},x+\frac{1}{4}$					
16	d	. $\bar{3}$ m	$\frac{1}{2},\frac{1}{2},\frac{1}{2}$	$\frac{1}{4},\frac{3}{4},0$	$\frac{3}{4},0,\frac{1}{4}$	$0,\frac{1}{4},\frac{3}{4}$			hkl : $h=2n+1$ or $h,k,l=4n+2$ or $h,k,l=4n$
16	c	. $\bar{3}$ m	$0,0,0$	$\frac{3}{4},\frac{1}{4},\frac{1}{2}$	$\frac{1}{4},\frac{1}{2},\frac{3}{4}$	$\frac{1}{2},\frac{3}{4},\frac{1}{4}$			
8	b	$\bar{4}$ 3 m	$\frac{3}{8},\frac{3}{8},\frac{3}{8}$	$\frac{1}{8},\frac{5}{8},\frac{1}{8}$					hkl : $h=2n+1$ or $h+k+l=4n$
8	a	$\bar{4}$ 3 m	$\frac{1}{8},\frac{1}{8},\frac{1}{8}$	$\frac{7}{8},\frac{3}{8},\frac{3}{8}$					

Symmetry of special projections

Along [001] $p4mm$
$\mathbf{a}' = \frac{1}{4}(\mathbf{a}-\mathbf{b})$ $\mathbf{b}' = \frac{1}{4}(\mathbf{a}+\mathbf{b})$
Origin at $\frac{1}{8},\frac{3}{8},z$

Along [111] $p6mm$
$\mathbf{a}' = \frac{1}{6}(2\mathbf{a}-\mathbf{b}-\mathbf{c})$ $\mathbf{b}' = \frac{1}{6}(-\mathbf{a}+2\mathbf{b}-\mathbf{c})$
Origin at x,x,x

Along [110] $c2mm$
$\mathbf{a}' = \frac{1}{2}(-\mathbf{a}+\mathbf{b})$ $\mathbf{b}' = \mathbf{c}$
Origin at $x,x,0$

XX46

ORIGIN CHOICE 2

Maximal non-isomorphic subgroups

I [2] $F\bar{4}3m$ (216) (1; 2; 3; 4; 5; 6; 7; 8; 9; 10; 11; 12; 37; 38; 39; 40; 41; 42; 43; 44; 45; 46; 47; 48)+
[2] $F4_132$ (210) (1; 2; 3; 4; 5; 6; 7; 8; 9; 10; 11; 12; 13; 14; 15; 16; 17; 18; 19; 20; 21; 22; 23; 24)+
[2] $Fd\bar{3}1$ ($Fd\bar{3}$, 203) (1; 2; 3; 4; 5; 6; 7; 8; 9; 10; 11; 12; 25; 26; 27; 28; 29; 30; 31; 32; 33; 34; 35; 36)+
[3] $F4_1/d12/m$ ($I4_1/amd$, 141) (1; 2; 3; 4; 13; 14; 15; 16; 25; 26; 27; 28; 37; 38; 39; 40)+
[3] $F4_1/d12/m$ ($I4_1/amd$, 141) (1; 2; 3; 4; 17; 18; 19; 20; 25; 26; 27; 28; 41; 42; 43; 44)+
[3] $F4_1/d12/m$ ($I4_1/amd$, 141) (1; 2; 3; 4; 21; 22; 23; 24; 25; 26; 27; 28; 45; 46; 47; 48)+
[4] $F1\bar{3}2/m$ ($R\bar{3}m$, 166) (1; 5; 9; 14; 19; 24; 25; 29; 33; 38; 43; 48)+
[4] $F1\bar{3}2/m$ ($R\bar{3}m$, 166) (1; 6; 12; 13; 18; 24; 25; 30; 36; 37; 42; 48)+
[4] $F1\bar{3}2/m$ ($R\bar{3}m$, 166) (1; 7; 10; 13; 19; 22; 25; 31; 34; 37; 43; 46)+
[4] $F1\bar{3}2/m$ ($R\bar{3}m$, 166) (1; 8; 11; 14; 18; 22; 25; 32; 35; 38; 42; 46)+

IIa none

IIb none

Maximal isomorphic subgroups of lowest index

IIc [27] $Fd\bar{3}m$ ($\mathbf{a}' = 3\mathbf{a}, \mathbf{b}' = 3\mathbf{b}, \mathbf{c}' = 3\mathbf{c}$) (227)

Minimal non-isomorphic supergroups

I none

II [2] $Pn\bar{3}m$ ($\mathbf{a}' = \frac{1}{2}\mathbf{a}, \mathbf{b}' = \frac{1}{2}\mathbf{b}, \mathbf{c}' = \frac{1}{2}\mathbf{c}$) (224)

XX47

Symmetry operations

For (0,0,0)+ set

(1) 1
(2) $2(0,0,\frac{1}{2})$ $\frac{3}{8},\frac{1}{8},z$
(3) $2(0,\frac{1}{2},0)$ $\frac{1}{8},y,\frac{3}{8}$
(4) $2(\frac{1}{2},0,0)$ $x,\frac{3}{8},\frac{1}{8}$
(5) 3^+ x,x,x
(6) 3^+ $\bar{x}+\frac{1}{2},x+\frac{1}{4},\bar{x}$
(7) 3^+ $x+\frac{3}{4},\bar{x}-\frac{1}{2},\bar{x}$
(8) 3^+ $\bar{x}+\frac{1}{4},\bar{x}+\frac{3}{4},x$
(9) 3^- x,x,x
(10) $3^-(-\frac{1}{3},\frac{1}{3},\frac{1}{3})$ $x+\frac{5}{12},\bar{x}+\frac{1}{6},\bar{x}$
(11) $3^-(\frac{1}{3},\frac{1}{3},-\frac{1}{3})$ $\bar{x}+\frac{7}{12},\bar{x}+\frac{5}{12},x$
(12) $3^-(\frac{1}{3},-\frac{1}{3},\frac{1}{3})$ $\bar{x}-\frac{1}{6},x+\frac{7}{12},\bar{x}$
(13) $2(\frac{1}{2},\frac{1}{2},0)$ $x,x-\frac{1}{4},\frac{1}{4}$
(14) 2 $x,\bar{x},0$
(15) $4^-(0,0,\frac{3}{4})$ $\frac{3}{8},\frac{1}{8},z$
(16) $4^+(0,0,\frac{1}{4})$ $-\frac{1}{8},\frac{5}{8},z$
(17) $4^-(\frac{3}{4},0,0)$ $x,\frac{3}{8},\frac{1}{8}$
(18) $2(0,\frac{1}{2},\frac{1}{2})$ $\frac{1}{4},y+\frac{1}{4},y$
(19) 2 $0,y,\bar{y}$
(20) $4^+(\frac{1}{4},0,0)$ $x,-\frac{1}{8},\frac{5}{8}$
(21) $4^+(0,\frac{1}{4},0)$ $\frac{5}{8},y,-\frac{1}{8}$
(22) $2(\frac{1}{2},0,\frac{1}{2})$ $x-\frac{1}{4},\frac{1}{4},x$
(23) $4^-(0,\frac{3}{4},0)$ $\frac{1}{8},y,\frac{3}{8}$
(24) 2 $\bar{x},0,x$
(25) $\bar{1}$ 0,0,0
(26) $d(\frac{1}{4},\frac{3}{4},0)$ $x,y,\frac{1}{4}$
(27) $d(\frac{3}{4},0,\frac{1}{4})$ $x,\frac{1}{4},z$
(28) $d(0,\frac{1}{4},\frac{3}{4})$ $\frac{1}{4},y,z$
(29) $\bar{3}^+$ $x,x,x;$ 0,0,0
(30) $\bar{3}^+$ $\bar{x}-1,x+\frac{3}{4},\bar{x};$ $-\frac{1}{4},0,\frac{3}{4}$
(31) $\bar{3}^+$ $x-\frac{1}{4},\bar{x}+1,\bar{x};$ $0,\frac{3}{4},-\frac{1}{4}$
(32) $\bar{3}^+$ $\bar{x}+\frac{3}{4},\bar{x}-\frac{1}{4},x;$ $\frac{3}{4},-\frac{1}{4},0$
(33) $\bar{3}^-$ $x,x,x;$ 0,0,0
(34) $\bar{3}^-$ $x+\frac{5}{4},\bar{x}-1,\bar{x};$ $\frac{1}{2},-\frac{1}{4},\frac{3}{4}$
(35) $\bar{3}^-$ $\bar{x}+\frac{1}{4},\bar{x}+\frac{5}{4},x;$ $-\frac{1}{4},\frac{3}{4},\frac{1}{2}$
(36) $\bar{3}^-$ $\bar{x}+1,x+\frac{1}{4},\bar{x};$ $\frac{3}{4},\frac{1}{2},-\frac{1}{4}$
(37) $g(-\frac{1}{4},\frac{1}{4},\frac{1}{2})$ $x+\frac{1}{2},\bar{x},z$
(38) m x,x,z
(39) $\bar{4}^-$ $\frac{1}{8},\frac{5}{8},z;$ $\frac{1}{8},\frac{5}{8},\frac{1}{8}$
(40) $\bar{4}^+$ $\frac{3}{8},-\frac{1}{8},z;$ $\frac{3}{8},-\frac{1}{8},\frac{3}{8}$
(41) $\bar{4}^-$ $x,\frac{1}{8},\frac{5}{8};$ $\frac{1}{8},\frac{1}{8},\frac{5}{8}$
(42) $g(\frac{1}{2},-\frac{1}{4},\frac{1}{4})$ $x,y+\frac{1}{2},\bar{y}$
(43) m x,y,y
(44) $\bar{4}^+$ $x,\frac{3}{8},-\frac{1}{8};$ $\frac{3}{8},\frac{3}{8},-\frac{1}{8}$
(45) $\bar{4}^+$ $-\frac{1}{8},y,\frac{3}{8};$ $-\frac{1}{8},\frac{3}{8},\frac{3}{8}$
(46) $g(\frac{1}{4},\frac{1}{2},-\frac{1}{4})$ $\bar{x}+\frac{1}{2},y,x$
(47) $\bar{4}^-$ $\frac{5}{8},y,\frac{1}{8};$ $\frac{5}{8},\frac{1}{8},\frac{1}{8}$
(48) m x,y,x

For $(0,\frac{1}{2},\frac{1}{2})+$ set

(1) $t(0,\frac{1}{2},\frac{1}{2})$
(2) 2 $\frac{3}{8},\frac{3}{8},z$
(3) 2 $\frac{1}{8},y,\frac{1}{8}$
(4) $2(\frac{1}{2},0,0)$ $x,\frac{1}{8},\frac{3}{8}$
(5) $3^+(\frac{1}{3},\frac{1}{3},\frac{1}{3})$ $x-\frac{1}{3},x-\frac{1}{6},x$
(6) $3^+(\frac{1}{3},-\frac{1}{3},\frac{1}{3})$ $\bar{x}+\frac{1}{6},x+\frac{5}{12},\bar{x}$
(7) 3^+ $x+\frac{3}{4},\bar{x},\bar{x}$
(8) 3^+ $\bar{x}+\frac{1}{4},\bar{x}+\frac{1}{4},x$
(9) $3^-(\frac{1}{3},\frac{1}{3},\frac{1}{3})$ $x-\frac{1}{6},x+\frac{1}{6},x$
(10) 3^- $x+\frac{1}{4},\bar{x},\bar{x}$
(11) 3^- $\bar{x}+\frac{3}{4},\bar{x}+\frac{1}{4},x$
(12) 3^- $\bar{x},x+\frac{3}{4},\bar{x}$
(13) $2(\frac{3}{4},\frac{3}{4},0)$ $x,x,0$
(14) $2(-\frac{1}{4},\frac{1}{4},0)$ $x,\bar{x}+\frac{1}{4},\frac{1}{4}$
(15) $4^-(0,0,\frac{1}{4})$ $\frac{1}{8},-\frac{1}{8},z$
(16) $4^+(0,0,\frac{3}{4})$ $\frac{1}{8},\frac{3}{8},z$
(17) $4^-(\frac{3}{4},0,0)$ $x,\frac{3}{8},-\frac{3}{8}$
(18) $2(0,\frac{1}{2},\frac{1}{2})$ $\frac{1}{4},y-\frac{1}{4},y$
(19) 2 $0,y+\frac{1}{2},\bar{y}$
(20) $4^+(\frac{1}{4},0,0)$ $x,-\frac{1}{8},\frac{1}{8}$
(21) $4^+(0,\frac{3}{4},0)$ $\frac{3}{8},y,-\frac{3}{8}$
(22) $2(\frac{1}{4},0,\frac{1}{4})$ $x,0,x$
(23) $4^-(0,\frac{1}{4},0)$ $-\frac{1}{8},y,\frac{5}{8}$
(24) $2(-\frac{1}{4},0,\frac{1}{4})$ $\bar{x}+\frac{1}{4},\frac{1}{4},x$
(25) $\bar{1}$ $0,\frac{1}{4},\frac{1}{4}$
(26) $d(\frac{1}{4},\frac{1}{4},0)$ $x,y,0$
(27) $d(\frac{3}{4},0,\frac{3}{4})$ $x,0,z$
(28) $d(0,\frac{3}{4},\frac{1}{4})$ $\frac{1}{4},y,z$
(29) $\bar{3}^+$ $x,x+\frac{1}{2},x;$ $0,\frac{1}{2},0$
(30) $\bar{3}^+$ $\bar{x}-1,x+\frac{5}{4},\bar{x};$ $-\frac{1}{4},\frac{1}{2},\frac{3}{4}$
(31) $\bar{3}^+$ $x-\frac{1}{4},\bar{x}+\frac{1}{2},\bar{x};$ $0,\frac{1}{4},-\frac{1}{4}$
(32) $\bar{3}^+$ $\bar{x}+\frac{3}{4},\bar{x}-\frac{3}{4},x;$ $\frac{3}{4},-\frac{3}{4},0$
(33) $\bar{3}^-$ $x-\frac{1}{2},x-\frac{1}{2},x;$ $0,0,\frac{1}{2}$
(34) $\bar{3}^-$ $x+\frac{3}{4},\bar{x}-\frac{3}{2},\bar{x};$ $0,-\frac{3}{4},\frac{3}{4}$
(35) $\bar{3}^-$ $\bar{x}-\frac{1}{4},\bar{x}+\frac{3}{4},x;$ $-\frac{1}{4},\frac{3}{4},0$
(36) $\bar{3}^-$ $\bar{x}+\frac{1}{2},x-\frac{1}{4},\bar{x};$ $\frac{1}{4},0,-\frac{1}{4}$
(37) m $x+\frac{1}{4},\bar{x},z$
(38) $g(\frac{1}{4},\frac{1}{4},\frac{1}{2})$ $x-\frac{1}{4},x,z$
(39) $\bar{4}^-$ $\frac{3}{8},\frac{3}{8},z;$ $\frac{3}{8},\frac{3}{8},\frac{3}{8}$
(40) $\bar{4}^+$ $\frac{5}{8},\frac{1}{8},z;$ $\frac{5}{8},\frac{1}{8},\frac{1}{8}$
(41) $\bar{4}^-$ $x,\frac{1}{8},\frac{1}{8};$ $\frac{1}{8},\frac{1}{8},\frac{1}{8}$
(42) $g(\frac{1}{2},\frac{1}{4},-\frac{1}{4})$ $x,y+\frac{1}{2},\bar{y}$
(43) $g(0,\frac{1}{2},\frac{1}{2})$ x,y,y
(44) $\bar{4}^+$ $x,\frac{3}{8},\frac{3}{8};$ $\frac{3}{8},\frac{3}{8},\frac{3}{8}$
(45) $\bar{4}^+$ $\frac{1}{8},y,\frac{1}{8};$ $\frac{1}{8},\frac{1}{8},\frac{1}{8}$
(46) m $\bar{x}+\frac{3}{4},y,x$
(47) $\bar{4}^-$ $\frac{3}{8},y,-\frac{1}{8};$ $\frac{3}{8},\frac{3}{8},-\frac{1}{8}$
(48) $g(\frac{1}{4},\frac{1}{2},\frac{1}{4})$ $x-\frac{1}{4},y,x$

For $(\frac{1}{2},0,\frac{1}{2})+$ set

(1) $t(\frac{1}{2},0,\frac{1}{2})$
(2) 2 $\frac{1}{8},\frac{1}{8},z$
(3) $2(0,\frac{1}{2},0)$ $\frac{3}{8},y,\frac{1}{8}$
(4) 2 $x,\frac{3}{8},\frac{3}{8}$
(5) $3^+(\frac{1}{3},\frac{1}{3},\frac{1}{3})$ $x+\frac{1}{6},x-\frac{1}{6},x$
(6) 3^+ $\bar{x},x+\frac{3}{4},\bar{x}$
(7) 3^+ $x+\frac{1}{4},\bar{x},\bar{x}$
(8) $3^+(\frac{1}{3},\frac{1}{3},-\frac{1}{3})$ $\bar{x}+\frac{5}{12},\bar{x}+\frac{7}{12},x$
(9) $3^-(\frac{1}{3},\frac{1}{3},\frac{1}{3})$ $x-\frac{1}{6},x-\frac{1}{3},x$
(10) 3^- $x+\frac{1}{4},\bar{x}+\frac{1}{2},\bar{x}$
(11) 3^- $\bar{x}+\frac{3}{4},\bar{x}+\frac{3}{4},x$
(12) 3^- $\bar{x},x+\frac{1}{4},\bar{x}$
(13) $2(\frac{1}{4},\frac{1}{4},0)$ $x,x,0$
(14) $2(\frac{1}{4},-\frac{1}{4},0)$ $x,\bar{x}+\frac{1}{4},\frac{1}{4}$
(15) $4^-(0,0,\frac{1}{4})$ $\frac{5}{8},-\frac{1}{8},z$
(16) $4^+(0,0,\frac{3}{4})$ $-\frac{3}{8},\frac{3}{8},z$
(17) $4^-(\frac{1}{4},0,0)$ $x,\frac{1}{8},-\frac{1}{8}$
(18) $2(0,\frac{3}{4},\frac{3}{4})$ $0,y,y$
(19) $2(0,-\frac{1}{4},\frac{1}{4})$ $\frac{1}{4},y+\frac{1}{4},\bar{y}$
(20) $4^+(\frac{3}{4},0,0)$ $x,\frac{1}{8},\frac{3}{8}$
(21) $4^+(0,\frac{1}{4},0)$ $\frac{1}{8},y,\frac{1}{8}$
(22) $2(\frac{1}{2},0,\frac{1}{2})$ $x+\frac{1}{4},\frac{1}{4},x$
(23) $4^-(0,\frac{3}{4},0)$ $-\frac{3}{8},y,\frac{3}{8}$
(24) 2 $\bar{x}+\frac{1}{2},0,x$
(25) $\bar{1}$ $\frac{1}{4},0,\frac{1}{4}$
(26) $d(\frac{3}{4},\frac{3}{4},0)$ $x,y,0$
(27) $d(\frac{1}{4},0,\frac{3}{4})$ $x,\frac{1}{4},z$
(28) $d(0,\frac{1}{4},\frac{1}{4})$ $0,y,z$
(29) $\bar{3}^+$ $x-\frac{1}{2},x-\frac{1}{2},x;$ $0,0,\frac{1}{2}$
(30) $\bar{3}^+$ $\bar{x}-\frac{1}{2},x+\frac{1}{4},\bar{x};$ $-\frac{1}{4},0,\frac{1}{4}$
(31) $\bar{3}^+$ $x-\frac{3}{4},\bar{x}+\frac{3}{2},\bar{x};$ $0,\frac{3}{4},-\frac{3}{4}$
(32) $\bar{3}^+$ $\bar{x}+\frac{5}{4},\bar{x}+\frac{1}{4},x;$ $\frac{3}{4},-\frac{1}{4},\frac{1}{2}$
(33) $\bar{3}^-$ $x+\frac{1}{2},x,x;$ $\frac{1}{2},0,0$
(34) $\bar{3}^-$ $x+\frac{3}{4},\bar{x}-1,\bar{x};$ $0,-\frac{1}{4},\frac{3}{4}$
(35) $\bar{3}^-$ $\bar{x}-\frac{1}{4},\bar{x}+\frac{1}{4},x;$ $-\frac{1}{4},\frac{1}{4},0$
(36) $\bar{3}^-$ $\bar{x}+\frac{3}{2},x-\frac{3}{4},\bar{x};$ $\frac{3}{4},0,-\frac{3}{4}$
(37) m $x+\frac{3}{4},\bar{x},z$
(38) $g(\frac{1}{4},\frac{1}{4},\frac{1}{2})$ $x+\frac{1}{4},x,z$
(39) $\bar{4}^-$ $-\frac{1}{8},\frac{3}{8},z;$ $-\frac{1}{8},\frac{3}{8},\frac{3}{8}$
(40) $\bar{4}^+$ $\frac{1}{8},\frac{1}{8},z;$ $\frac{1}{8},\frac{1}{8},\frac{1}{8}$
(41) $\bar{4}^-$ $x,\frac{3}{8},\frac{3}{8};$ $\frac{3}{8},\frac{3}{8},\frac{3}{8}$
(42) m $x,y+\frac{1}{4},\bar{y}$
(43) $g(\frac{1}{2},\frac{1}{4},\frac{1}{4})$ $x,y-\frac{1}{4},y$
(44) $\bar{4}^+$ $x,\frac{5}{8},\frac{1}{8};$ $\frac{1}{8},\frac{5}{8},\frac{1}{8}$
(45) $\bar{4}^+$ $\frac{3}{8},y,\frac{3}{8};$ $\frac{3}{8},\frac{3}{8},\frac{3}{8}$
(46) $g(-\frac{1}{4},\frac{1}{2},\frac{1}{4})$ $\bar{x}+\frac{1}{2},y,x$
(47) $\bar{4}^-$ $\frac{1}{8},y,\frac{1}{8};$ $\frac{1}{8},\frac{1}{8},\frac{1}{8}$
(48) $g(\frac{1}{2},0,\frac{1}{2})$ x,y,x

For $(\frac{1}{2},\frac{1}{2},0)+$ set

(1) $t(\frac{1}{2},\frac{1}{2},0)$
(2) $2(0,0,\frac{1}{2})$ $\frac{1}{8},\frac{3}{8},z$
(3) 2 $\frac{3}{8},y,\frac{3}{8}$
(4) 2 $x,\frac{1}{8},\frac{1}{8}$
(5) $3^+(\frac{1}{3},\frac{1}{3},\frac{1}{3})$ $x+\frac{1}{6},x+\frac{1}{3},x$
(6) 3^+ $\bar{x},x+\frac{1}{4},\bar{x}$
(7) $3^+(-\frac{1}{3},\frac{1}{3},\frac{1}{3})$ $x+\frac{7}{12},\bar{x}-\frac{1}{6},\bar{x}$
(8) 3^+ $\bar{x}+\frac{3}{4},\bar{x}+\frac{3}{4},x$
(9) $3^-(\frac{1}{3},\frac{1}{3},\frac{1}{3})$ $x+\frac{1}{3},x+\frac{1}{6},x$
(10) 3^- $x+\frac{3}{4},\bar{x},\bar{x}$
(11) 3^- $\bar{x}+\frac{1}{4},\bar{x}+\frac{1}{4},x$
(12) 3^- $\bar{x}-\frac{1}{2},x+\frac{3}{4},\bar{x}$
(13) $2(\frac{1}{2},\frac{1}{2},0)$ $x,x+\frac{1}{4},\frac{1}{4}$
(14) 2 $x,\bar{x}+\frac{1}{2},0$
(15) $4^-(0,0,\frac{3}{4})$ $\frac{3}{8},-\frac{3}{8},z$
(16) $4^+(0,0,\frac{1}{4})$ $-\frac{1}{8},\frac{1}{8},z$
(17) $4^-(\frac{1}{4},0,0)$ $x,\frac{5}{8},-\frac{1}{8}$
(18) $2(0,\frac{1}{4},\frac{1}{4})$ $0,y,y$
(19) $2(0,\frac{1}{4},-\frac{1}{4})$ $\frac{1}{4},y+\frac{1}{4},\bar{y}$
(20) $4^+(\frac{3}{4},0,0)$ $x,-\frac{3}{8},\frac{3}{8}$
(21) $4^+(0,\frac{3}{4},0)$ $\frac{3}{8},y,\frac{1}{8}$
(22) $2(\frac{3}{4},0,\frac{3}{4})$ $x,0,x$
(23) $4^-(0,\frac{1}{4},0)$ $-\frac{1}{8},y,\frac{1}{8}$
(24) $2(\frac{1}{4},0,-\frac{1}{4})$ $\bar{x}+\frac{1}{4},\frac{1}{4},x$
(25) $\bar{1}$ $\frac{1}{4},\frac{1}{4},0$
(26) $d(\frac{3}{4},\frac{1}{4},0)$ $x,y,\frac{1}{4}$
(27) $d(\frac{1}{4},0,\frac{1}{4})$ $x,0,z$
(28) $d(0,\frac{3}{4},\frac{3}{4})$ $0,y,z$
(29) $\bar{3}^+$ $x+\frac{1}{2},x,x;$ $\frac{1}{2},0,0$
(30) $\bar{3}^+$ $\bar{x}-\frac{3}{2},x+\frac{3}{4},\bar{x};$ $-\frac{3}{4},0,\frac{3}{4}$
(31) $\bar{3}^+$ $x+\frac{1}{4},\bar{x}+1,\bar{x};$ $\frac{1}{2},\frac{3}{4},-\frac{1}{4}$
(32) $\bar{3}^+$ $\bar{x}+\frac{1}{4},\bar{x}-\frac{1}{4},x;$ $\frac{1}{4},-\frac{1}{4},0$
(33) $\bar{3}^-$ $x,x+\frac{1}{2},x;$ $0,\frac{1}{2},0$
(34) $\bar{3}^-$ $x+\frac{1}{4},\bar{x}-\frac{1}{2},\bar{x};$ $0,-\frac{1}{4},\frac{1}{4}$
(35) $\bar{3}^-$ $\bar{x}-\frac{3}{4},\bar{x}+\frac{3}{4},x;$ $-\frac{3}{4},\frac{3}{4},0$
(36) $\bar{3}^-$ $\bar{x}+1,x-\frac{1}{4},\bar{x};$ $\frac{3}{4},0,-\frac{1}{4}$
(37) $g(\frac{1}{4},-\frac{1}{4},\frac{1}{2})$ $x+\frac{1}{2},\bar{x},z$
(38) $g(\frac{1}{2},\frac{1}{2},0)$ x,x,z
(39) $\bar{4}^-$ $\frac{1}{8},\frac{1}{8},z;$ $\frac{1}{8},\frac{1}{8},\frac{1}{8}$
(40) $\bar{4}^+$ $\frac{3}{8},\frac{3}{8},z;$ $\frac{3}{8},\frac{3}{8},\frac{3}{8}$
(41) $\bar{4}^-$ $x,-\frac{1}{8},\frac{3}{8};$ $\frac{3}{8},-\frac{1}{8},\frac{3}{8}$
(42) m $x,y+\frac{3}{4},\bar{y}$
(43) $g(\frac{1}{2},\frac{1}{4},\frac{1}{4})$ $x,y+\frac{1}{4},y$
(44) $\bar{4}^+$ $x,\frac{1}{8},\frac{1}{8};$ $\frac{1}{8},\frac{1}{8},\frac{1}{8}$
(45) $\bar{4}^+$ $\frac{1}{8},y,\frac{5}{8};$ $\frac{1}{8},\frac{1}{8},\frac{5}{8}$
(46) m $\bar{x}+\frac{1}{4},y,x$
(47) $\bar{4}^-$ $\frac{3}{8},y,\frac{3}{8};$ $\frac{3}{8},\frac{3}{8},\frac{3}{8}$
(48) $g(\frac{1}{4},\frac{1}{2},\frac{1}{4})$ $x+\frac{1}{4},y,x$

XX48

Table 8.3.5.1. *Sequence of generators for the crystal classes*

The *space-group* generators differ from those listed here by their glide or screw components. The generator 1 is omitted, except for crystal class 1. The subscript of a symbol denotes the characteristic direction of that operation, where necessary. The subscripts z, y, 110, $1\bar{1}0$, $10\bar{1}$ and 111 refer to the directions [001], [010], [110], [1$\bar{1}$0], [10$\bar{1}$] and [111], respectively. For mirror reflections m, the 'direction of m' refers to the normal to the mirror plane. The subscripts may be likewise interpreted as Miller indices of that plane.

Hermann–Mauguin symbol of crystal class	Generators G_i (sequence left to right)
1	1
$\bar{1}$	$\bar{1}$
2	2_z
m	m_z
$2/m$	$2_z, \bar{1}$
222	$2_z, 2_y$
$mm2$	$2_z, m_y$
mmm	$2_z, 2_y, \bar{1}$
4	$2_z, 4$
$\bar{4}$	$2_z, \bar{4}$
$4/m$	$2_z, 4, \bar{1}$
422	$2_z, 4, 2_y$
$4mm$	$2_z, 4, m_y$
$\bar{4}2m$	$2_z, \bar{4}, 2_y$
$\bar{4}m2$	$2_z, \bar{4}, m_y$
$4/mmm$	$2_z, 4, 2_y, \bar{1}$
3	3
$\bar{3}$	$3, \bar{1}$
321	$3, 2_{110}$
(rhombohedral coordinates	$3_{111}, 2_{10\bar{1}}$)
312	$3, 2_{1\bar{1}0}$
$3m1$	$3, m_{110}$
(rhombohedral coordinates	$3_{111}, m_{10\bar{1}}$)
$31m$	$3, m_{1\bar{1}0}$
$\bar{3}m1$	$3, 2_{110}, \bar{1}$
(rhombohedral coordinates	$3_{111}, 2_{10\bar{1}}, \bar{1}$)
$\bar{3}1m$	$3, 2_{1\bar{1}0}, \bar{1}$
6	$3, 2_z$
$\bar{6}$	$3, m_z$
$6/m$	$3, 2_z, \bar{1}$
622	$3, 2_z, 2_{110}$
$6mm$	$3, 2_z, m_{110}$
$\bar{6}m2$	$3, m_z, m_{110}$
$\bar{6}2m$	$3, m_z, 2_{110}$
$6/mmm$	$3, 2_z, 2_{110}, \bar{1}$
23	$2_z, 2_y, 3_{111}$
$m\bar{3}$	$2_z, 2_y, 3_{111}, \bar{1}$
432	$2_z, 2_y, 3_{111}, 2_{110}$
$\bar{4}3m$	$2_z, 2_y, 3_{111}, m_{1\bar{1}0}$
$m\bar{3}m$	$2_z, 2_y, 3_{111}, 2_{110}, \bar{1}$

group $m\bar{3}m$ can be described by two generators. Different choices of generators are possible. For the present *Tables*, generators and generating procedures have been chosen such as to make the entries in the blocks *General position* (*cf.* Section 2.2.11) and *Symmetry operations* (*cf.* Section 2.2.9) as transparent as possible. Space groups of the same crystal class are generated in the same way (for sequence chosen, see Table 8.3.5.1), and the aim has been to accentuate important subgroups of space groups as much as possible. Accordingly, a process of generation in the form of a 'composition series' has been adopted, see Ledermann (1976). The generator G_1 is defined as the identity operation, represented by (1) x, y, z. G_2, G_3 and G_4 are the translations with translation vectors **a**, **b** and **c**, respectively. Thus, the coefficients k_2, k_3 and k_4 may have any integral value. If centring translations exist, they are generated by translations G_5 (and G_6 in the case of an F lattice) with translation vectors **d** (and **e**). For a C lattice, for example, **d** is given by $\mathbf{d} = \frac{1}{2}(\mathbf{a} + \mathbf{b})$. The exponents k_5 (and k_6) are restricted to the following values:

Lattice letter A, B, C, I: $k_5 = 0$ or 1.
Lattice letter R (hexagonal axes): $k_5 = 0$, 1 or 2.
Lattice letter F: $k_5 = 0$ or 1; $k_6 = 0$ or 1.

As a consequence, any translation T of $\mathcal{G}$ with translation vector

$$\mathbf{t} = k_2\mathbf{a} + k_3\mathbf{b} + k_4\mathbf{c}(+k_5\mathbf{d} + k_6\mathbf{e})$$

can be obtained as a product

$$\mathsf{T} = (\mathsf{G}_6)^{k_6} * (\mathsf{G}_5)^{k_5} * \mathsf{G}_4^{k_4} * \mathsf{G}_3^{k_3} * \mathsf{G}_2^{k_2} * \mathsf{G}_1,$$

where $k_2, \ldots, k_6$ are integers determined by T. G_6 and G_5 are enclosed between parentheses because they are effective only in centred lattices.

The remaining generators generate those symmetry operations that are not translations. They are chosen in such a way that only terms G_j or G_j^2 occur. For further specific rules, see below.

The process of generating the entries of the space-group tables may be demonstrated by the example of Table 8.3.5.2, where $\mathcal{G}_j$ denotes the group generated by $G_1, G_2, \ldots, G_j$. For $j \geq 5$, the next generator G_{j+1} has always been taken as soon as $G_j^{k_j} \in \mathcal{G}_{j-1}$, because in this case no new symmetry operation would be generated by $G_j^{k_j}$. The generating process is terminated when there is no further generator. In the present example, G_7 completes the generation: $\mathcal{G}_7 \equiv P6_122$.

8.3.5.1. *Selected order for non-translational generators*

For the non-translational generators, the following sequence has been adopted:

(*a*) In all centrosymmetric space groups, an inversion (if possible at the origin O) has been selected as the last generator.

(*b*) Rotations precede symmetry operations of the second kind. In crystal classes $\bar{4}2m$–$\bar{4}m2$ and $\bar{6}2m$–$\bar{6}m2$, as an exception, $\bar{4}$ and $\bar{6}$ are generated first in order to take into account the conventional choice of origin in the fixed points of $\bar{4}$ and $\bar{6}$.

(*c*) The non-translational generators of space groups with C, A, B, F, I or R symbols are those of the corresponding space group with a P symbol, if possible. For instance, the generators of $I2_12_12_1$ are those of $P2_12_12_1$ and the generators of *Ibca* are those of *Pbca*, apart from the centring translations.

Exceptions: *I4cm* and *I4/mcm* are generated *via* *P4cc* and *P4/mcc*, because *P4cm* and *P4/mcm* do not exist. In space groups with d glides (except $I\bar{4}2d$) and also in $I4_1/a$, the corresponding rotation subgroup has been generated first. The generators of this subgroup are the same as those of the corresponding space group with a lattice symbol P.

Example
$F4_1/d\bar{3}2/m : P4_132 \rightarrow F4_132 \rightarrow F4_1/d\bar{3}2/m$.

(*d*) In some cases, rule (*c*) could not be followed without breaking rule (*a*), *e.g.* in *Cmme*. In such cases, the generators are chosen to correspond to the Hermann–Mauguin symbol as far as possible. For instance, the generators (apart from centring) of *Cmme* and *Imma* are

XX49

ing duplicate Wyckoff designations within a structure, provided atomic coordinates do not overlap. For instance, the Wyckoff site with letter c in space group 62 has flexibility in the x and z coordinates, so that both the calcium and oxygen atoms in the $CaTiO_3$ (*Pnma*) perovskite structure (AB3C_oP20_62_c_cd_a) have the same letter designation. In general, structures with identical sets of Wyckoff positions can be distinct with different choices of Wyckoff variables, resulting in entries in the library that have duplicate AFLOW labels despite being unique prototypes. With the countless potential structures left to explore, the library is constantly growing and collecting more structural prototypes.

This article presents the continued work and second installment of the AFLOW Library of Crystallographic Prototypes. In Part 2, the crystallographic library is extended by 302 structure prototypes, including **i.** structures from the remaining 138 space groups not represented in Part 1, **ii.** structures with a *Strukturbericht* designation not listed in Part 1, and **iii.** structures of interest to the community and/or the authors (*e.g.*, metallic phases of hydrogen sulfide [33] and the quaternary Heusler [34, 35]). The online version of the library contains all of the prototypes from Part 1 and Part 2.

The outline of this article is as follows: Section 2 highlights the enantiomorphic space groups. Section 3 discusses the Wigner-Seitz cell and showcases the Jmol functionality. Section 4 introduces the two-dimensional plane groups (or "wallpaper" groups). Section 5 describes the different space group symbols, including the Hermann-Mauguin, Hall, International, and Schönflies notations, along with the origin/setting choices used throughout the library. Section 6 summarizes the descriptions of each entry in the library and introduces new web features, including the Jmol applet and online prototype generator.

2. Enantiomorphic Space Groups

In affine space — *i.e.*, no defined origin — there are only 219 space groups (referred to as the affine space groups). The eleven remaining space groups are mirror images (left-handed versus right-handed structures) of one of the other 219 space groups and are equivalent in the affine space. These pairs of space groups are the enantiomorphic pairs, in which two prototypes can be formed as mirror images of a single structure. The eleven pairs of enantiomorphic space groups [36, 37] are:

- $P4_1$ (#76) and $P4_3$ (#78),
- $P4_122$ (#91) and $P4_322$ (#95),
- $P4_12_12$ (#92) and $P4_32_12$ (#96),
- $P3_1$ (#144) and $P3_2$ (#145),
- $P3_112$ (#151) and $P3_212$ (#153),
- $P3_121$ (#152) and $P3_221$ (#154),
- $P6_1$ (#169) and $P6_5$ (#170),
- $P6_2$ (#171) and $P6_4$ (#172),
- $P6_122$ (#178) and $P6_522$ (#179),
- $P6_222$ (#180) and $P6_422$ (#181), and
- $P4_132$ (#213) and $P4_332$ (#212).

The relationship between the enantiomorphic pairs is exploited in Part 2 to generate prototypes for otherwise unrepresented space groups.

If we look at space group $P4_1$ (#76), we see that it has one Wyckoff position (4a), with operations [38]

$$(x, y, z)\ \left(-x, -y, z+\frac{1}{2}\right)\ \left(-y, x, z+\frac{1}{4}\right)\ \left(y, -x, z+\frac{3}{4}\right).$$

If we then look at space group $P4_3$ (#78), we find it also has one (4a) Wyckoff position, with operations

$$(x, y, z)\ \left(-x, -y, z+\frac{1}{2}\right)\ \left(-y, x, z+\frac{3}{4}\right)\ \left(y, -x, z+\frac{1}{4}\right),$$

where the only difference is that the 1/4 and 3/4 fractions have swapped positions. We can easily show that space group #78 is a mirror reflection of #76 in the $z = 0$ plane.

To see this more clearly, consider the Cs_3P_7 structure (A3B7_tP40_76_3a_7a[1]). This structure was found in space group #76, but if we reflect all of the coordinates through the $z = 0$ plane, it transforms into a structure in space group #78, as shown in the Jmol [39] rendering in Figure 1.

The distance between any pair of atoms is the same in the $P4_3$ structure as it is in the $P4_1$ structure, and the angle between any three atoms is the same in both structures. It

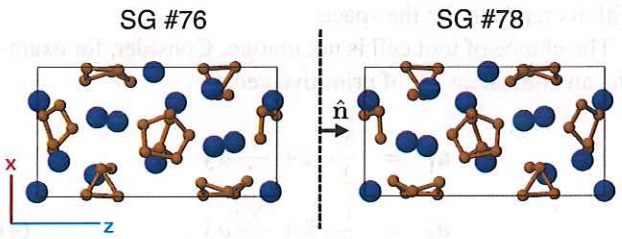

Figure 1: **Illustration of enantiomorphic structures.** Cs_3P_7 in space group $P4_1$ (#76) (left), and reflected through the $z = 0$ plane into space group $P4_3$ (#78) (right). The positive z direction is to the right in both figures, with the mirror plane perpendicular to the page. The figures were produced by Jmol [39].

[1]This structure can be found in the Library of Crystallographic Prototypes at http://aflow.org/CrystalDatabase/A3B7_tP40_76_3a_7a.html.

XX50

follows that the structures are degenerate, there is no difference in energy between them, and they should be equally likely to form.

Any structure in space group $P4_1$ can be transformed into $P4_3$ by this method. Pairs of space groups which allow these transformations are said to be enantiomorphic [36, 37], or chiral.[2]

In addition, forty-three other space groups allow chiral crystal structures. The complete set of sixty-five space groups are known as the Sohncke groups [36].

3. The Wigner-Seitz Primitive Cell

Given a lattice described by a set of primitive lattice vectors, $\mathbf{a}_1$, $\mathbf{a}_2$, and $\mathbf{a}_3$, we can define a *unit cell* as a volume which, when translated through every vector of the form $N_1\,\mathbf{a}_1 + N_2\,\mathbf{a}_2 + N_3\,\mathbf{a}_3$, completely fills space without overlap. Even if we require that this cell have the minimum volume,

$$V = \mathbf{a}_1 \cdot (\mathbf{a}_2 \times \mathbf{a}_3), \tag{1}$$

this is not a unique definition, and in fact there are an infinite number of choices for the primitive vectors.

As an example, consider the two-dimensional hexagonal lattice with primitive vectors

$$\begin{aligned} \mathbf{a}_1 &= \frac{1}{2}\,a\,\hat{\mathbf{x}} - \frac{\sqrt{3}}{2}\,a\,\hat{\mathbf{y}} \\ \mathbf{a}_2 &= \frac{1}{2}\,a\,\hat{\mathbf{x}} + \frac{\sqrt{3}}{2}\,a\,\hat{\mathbf{y}}\,. \end{aligned} \tag{2}$$

We show this lattice in Figure 2, along with a two-site basis (the gray squares). Perhaps the simplest unit cell we can construct here is a parallelogram, as seen in Figure 2. This is a unit cell, as it has the area of the primitive cell,

$$A = \frac{\sqrt{3}}{2}\,a^2, \tag{3}$$

each of its replicas contains two basis points, and the cell with its replicas tile the space.

The choice of unit cell is not unique. Consider, for example, an equivalent set of primitive vectors,

$$\begin{aligned} \mathbf{a}'_1 &= \frac{3}{2}\,a\,\hat{\mathbf{x}} + \frac{\sqrt{3}}{2}\,a\,\hat{\mathbf{y}} \\ \mathbf{a}'_2 &= \frac{1}{2}\,a\,\hat{\mathbf{x}} + \frac{\sqrt{3}}{2}\,a\,\hat{\mathbf{y}}\,, \end{aligned} \tag{4}$$

and the accompanying unit cell shown in Figure 3. This choice of unit cell has the proper area given by Equation (3), contains both basis points, and tiles the space. Both Figures 2 and 3 describe the same lattice plus basis, and so are both unit cells for the lattice.

[2]Formally, any object has *chirality* if it is not superposable on its mirror image [36]. Chirality is a fundamental aspect of life on Earth. All amino acids found in living organisms are left-handed [40].

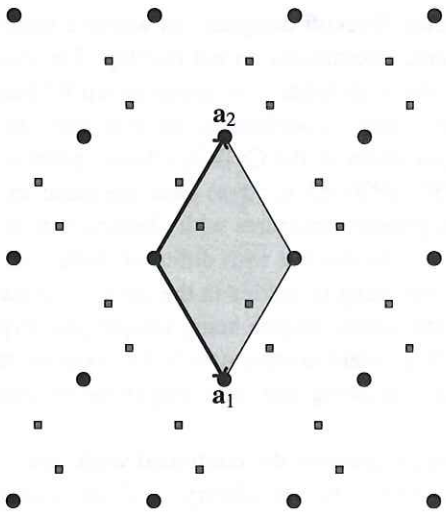

Figure 2: **A two-dimensional hexagonal lattice with basis.** The black circles show the positions of the lattice vectors, $N_1\,\mathbf{a}_1 + N_2\,\mathbf{a}_2$, where N_1 and N_2 are integers and $\mathbf{a}_1$ and $\mathbf{a}_2$ are given by Equation (2). The gray squares are a two-site basis for this lattice.

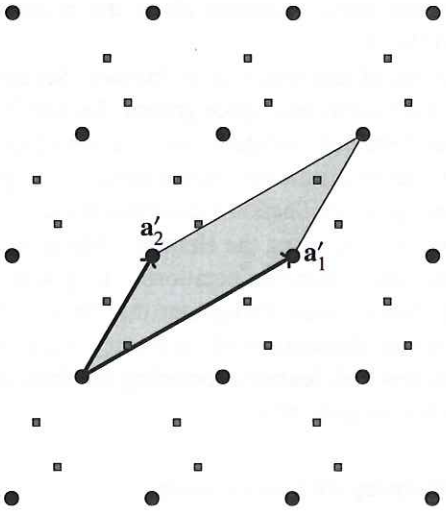

Figure 3: **A two-dimensional hexagonal lattice with non-standard primitive vectors.** This is the same hexagonal lattice from Figure 2 with primitive vectors given by Equation (4). Each unit cell still contains images of the two sites in the basis.

Though not required, it is frequently useful to have a primitive cell that is uniquely defined. Some lattice reduction techniques transform a cell into a standard representation — such as Minkowski, Niggli, and other standards — which are often unique up to a rotation [41, 42, 43]. However, an alternative distinct primitive representation exists, known as the Wigner-Seitz cell [44], which exhibits the symmetry of the lattice. The Wigner-Seitz cell is defined as the locus of all points closer to a given lattice point than to any other lattice point. We have constructed the Wigner-Seitz cell for our two-dimensional hexagonal lattice

Table 1: **A list of the various space group notations.** The space group number, orientation, Hermann-Mauguin symbol, Hall symbol, International symbol, and Schönflies symbol are listed.

Number	Orientation	Hermann-Mauguin	Hall	International	Schönflies
1		P 1	P 1	$P1$	C_1^1
2		P -1	-P 1	$P\bar{1}$	C_i^1
3	b	P 1 2 1	P 2y	$P2$	C_2^1
4	b	P 1 21 1	P 2yb	$P2_1$	C_2^2
5	b1	C 1 2 1	C 2y	$C2$	C_2^3
6	b	P 1 m 1	P -2y	Pm	C_s^1
7	b1	P 1 c 1	P -2yc	Pc	C_s^2
8	b1	C 1 m 1	C -2y	Cm	C_s^3
9	b1	C 1 c 1	C -2yc	Cc	C_s^4
10	b	P 1 2/m 1	-P 2y	$P2/m$	C_{2h}^1
11	b	P 1 21/m 1	-P 2yb	$P2_1/m$	C_{2h}^2
12	b1	C 1 2/m 1	-C 2y	$C2/m$	C_{2h}^3
13	b1	P 1 2/c 1	-P 2yc	$P2/c$	C_{2h}^4
14	b1	P 1 21/c 1	-P 2ybc	$P2_1/c$	C_{2h}^5
15	b1	C 1 2/c 1	-C 2yc	$C2/c$	C_{2h}^6
16		P 2 2 2	P 2 2	$P222$	D_2^1
17		P 2 2 21	P 2c 2	$P222_1$	D_2^2
18		P 21 21 2	P 2 2ab	$P2_12_12$	D_2^3
19		P 21 21 21	P 2ac 2ab	$P2_12_12_1$	D_2^4
20		C 2 2 21	C 2c 2	$C222_1$	D_2^5
21		C 2 2 2	C 2 2	$C222$	D_2^6
22		F 2 2 2	F 2 2	$F222$	D_2^7
23		I 2 2 2	I 2 2	$I222$	D_2^8
24		I 21 21 21	I 2b 2c	$I2_12_12_1$	D_2^9
25		P m m 2	P 2 -2	$Pmm2$	C_{2v}^1
26		P m c 21	P 2c -2	$Pmc2_1$	C_{2v}^2
27		P c c 2	P 2 -2c	$Pcc2$	C_{2v}^3
28		P m a 2	P 2 -2a	$Pma2$	C_{2v}^4
29		P c a 21	P 2c -2ac	$Pca2_1$	C_{2v}^5
30		P n c 2	P 2 -2bc	$Pnc2$	C_{2v}^6
31		P m n 21	P 2ac -2	$Pmn2_1$	C_{2v}^7
32		P b a 2	P 2 -2ab	$Pba2$	C_{2v}^8
33		P n a 21	P 2c -2n	$Pna2_1$	C_{2v}^9
34		P n n 2	P 2 -2n	$Pnn2$	C_{2v}^{10}
35		C m m 2	C 2 -2	$Cmm2$	C_{2v}^{11}
36		C m c 21	C 2c -2	$Cmc2_1$	C_{2v}^{12}
37		C c c 2	C 2 -2c	$Ccc2$	C_{2v}^{13}
38		A m m 2	A 2 -2	$Amm2$	C_{2v}^{14}
39		A b m 2	A 2 -2c	$Aem2$	C_{2v}^{15}
40		A m a 2	A 2 -2a	$Ama2$	C_{2v}^{16}
41		A b a 2	A 2 -2ac	$Aea2$	C_{2v}^{17}
42		F m m 2	F 2 -2	$Fmm2$	C_{2v}^{18}
43		F d d 2	F 2 -2d	$Fdd2$	C_{2v}^{19}
44		I m m 2	I 2 -2	$Imm2$	C_{2v}^{20}
45		I b a 2	I 2 -2c	$Iba2$	C_{2v}^{21}
46		I m a 2	I 2 -2a	$Ima2$	C_{2v}^{22}

XXS2

Table 1 (continued): **A list of the various space group notations.** The space group number, orientation, Hermann-Mauguin symbol, Hall symbol, International symbol, and Schönflies symbol are listed.

Number	Orientation	Hermann-Mauguin	Hall	International	Schönflies
47		P 2/m 2/m 2/m	-P 2 2	*Pmmm*	D_{2h}^{1}
48	2	P 2/n 2/n 2/n:2	-P 2ab 2bc	*Pnnn*	D_{2h}^{2}
49		P 2/c 2/c 2/m	-P 2 2c	*Pccm*	D_{2h}^{3}
50	2	P 2/b 2/a 2/n:2	-P 2ab 2b	*Pban*	D_{2h}^{4}
51		P 21/m 2/m 2/a	-P 2a 2a	*Pmma*	D_{2h}^{5}
52		P 2/n 21/n 2/a	-P 2a 2bc	*Pnna*	D_{2h}^{6}
53		P 2/m 2/n 21/a	-P 2ac 2	*Pmna*	D_{2h}^{7}
54		P 21/c 2/c 2/a	-P 2a 2ac	*Pcca*	D_{2h}^{8}
55		P 21/b 21/a 2/m	-P 2 2ab	*Pbam*	D_{2h}^{9}
56		P 21/c 21/c 2/n	-P 2ab 2ac	*Pccn*	D_{2h}^{10}
57		P 2/b 21/c 21/m	-P 2c 2b	*Pbcm*	D_{2h}^{11}
58		P 21/n 21/n 2/m	-P 2 2n	*Pnnm*	D_{2h}^{12}
59	2	P 21/m 21/m 2/n:2	-P 2ab 2a	*Pmmn*	D_{2h}^{13}
60		P 21/b 2/c 21/n	-P 2n 2ab	*Pbcn*	D_{2h}^{14}
61		P 21/b 21/c 21/a	-P 2ac 2ab	*Pbca*	D_{2h}^{15}
62		P 21/n 21/m 21/a	-P 2ac 2n	*Pnma*	D_{2h}^{16}
63		C 2/m 2/c 21/m	-C 2c 2	*Cmcm*	D_{2h}^{17}
64		C 2/m 2/c 21/a	-C 2bc 2	*Cmca*	D_{2h}^{18}
65		C 2/m 2/m 2/m	-C 2 2	*Cmmm*	D_{2h}^{19}
66		C 2/c 2/c 2/m	-C 2 2c	*Cccm*	D_{2h}^{20}
67		C 2/m 2/m 2/a	-C 2b 2	*Cmma*	D_{2h}^{21}
68	2	C 2/c 2/c 2/a:2	-C 2b 2bc	*Ccca*	D_{2h}^{22}
69		F 2/m 2/m 2/m	-F 2 2	*Fmmm*	D_{2h}^{23}
70	2	F 2/d 2/d 2/d:2	-F 2uv 2vw	*Fddd*	D_{2h}^{24}
71		I 2/m 2/m 2/m	-I 2 2	*Immm*	D_{2h}^{25}
72		I 2/b 2/a 2/m	-I 2 2c	*Ibam*	D_{2h}^{26}
73		I 2/b 2/c 2/a	-I 2b 2c	*Ibca*	D_{2h}^{27}
74		I 2/m 2/m 2/a	-I 2b 2	*Imma*	D_{2h}^{28}
75		P 4	P 4	*P*4	C_{4}^{1}
76		P 41	P 4w	$P4_1$	C_{4}^{2}
77		P 42	P 4c	$P4_2$	C_{4}^{3}
78		P 43	P 4cw	$P4_3$	C_{4}^{4}
79		I 4	I 4	*I*4	C_{4}^{5}
80		I 41	I 4bw	$I4_1$	C_{4}^{6}
81		P -4	P -4	$P\bar{4}$	S_{4}^{1}
82		I -4	I -4	$I\bar{4}$	S_{4}^{2}
83		P 4/m	-P 4	*P*4/*m*	C_{4h}^{1}
84		P 42/m	-P 4c	$P4_2/m$	C_{4h}^{2}
85	2	P 4/n:2	-P 4a	*P*4/*n*	C_{4h}^{3}
86	2	P 42/n:2	-P 4bc	$P4_2/n$	C_{4h}^{4}
87		I 4/m	-I 4	*I*4/*m*	C_{4h}^{5}
88	2	I 41/a:2	-I 4ad	$I4_1/a$	C_{4h}^{6}
89		P 4 2 2	P 4 2	*P*422	D_{4}^{1}
90		P 4 21 2	P 4ab 2ab	$P42_12$	D_{4}^{2}
91		P 41 2 2	P 4w 2c	$P4_122$	D_{4}^{3}
92		P 41 21 2	P 4abw 2nw	$P4_12_12$	D_{4}^{4}

XXS3

Table 1 (continued): **A list of the various space group notations.** The space group number, orientation, Hermann-Mauguin symbol, Hall symbol, International symbol, and Schönflies symbol are listed.

Number	Orientation	Hermann-Mauguin	Hall	International	Schönflies
93		P 42 2 2	P 4c 2	$P4_222$	D_4^5
94		P 42 21 2	P 4n 2n	$P4_22_12$	D_4^6
95		P 43 2 2	P 4cw 2c	$P4_322$	D_4^7
96		P 43 21 2	P 4nw 2abw	$P4_32_12$	D_4^8
97		I 4 2 2	I 4 2	$I422$	D_4^9
98		I 41 2 2	I 4bw 2bw	$I4_122$	D_4^{10}
99		P 4 m m	P 4 -2	$P4mm$	C_{4v}^1
100		P 4 b m	P 4 -2ab	$P4bm$	C_{4v}^2
101		P 42 c m	P 4c -2c	$P4_2cm$	C_{4v}^3
102		P 42 n m	P 4n -2n	$P4_2nm$	C_{4v}^4
103		P 4 c c	P 4 -2c	$P4cc$	C_{4v}^5
104		P 4 n c	P 4 -2n	$P4nc$	C_{4v}^6
105		P 42 m c	P 4c -2	$P4_2mc$	C_{4v}^7
106		P 42 b c	P 4c -2ab	P_2bc	C_{4v}^8
107		I 4 m m	I 4 -2	$I4mm$	C_{4v}^9
108		I 4 c m	I 4 -2c	$I4cm$	C_{4v}^{10}
109		I 41 m d	I 4bw -2	$I4_1md$	C_{4v}^{11}
110		I 41 c d	I 4bw -2c	$I4_1cd$	C_{4v}^{12}
111		P -4 2 m	P -4 2	$P\bar{4}2m$	D_{2d}^1
112		P -4 2 c	P -4 2c	$P\bar{4}2c$	D_{2d}^2
113		P -4 21 m	P -4 2ab	$P\bar{4}2_1m$	D_{2d}^3
114		P -4 21 c	P -4 2n	$P\bar{4}2_1c$	D_{2d}^4
115		P -4 m 2	P -4 -2	$P\bar{4}m2$	D_{2d}^5
116		P -4 c 2	P -4 -2c	$P\bar{4}c2$	D_{2d}^6
117		P -4 b 2	P -4 -2ab	$P\bar{4}b2$	D_{2d}^7
118		P -4 n 2	P -4 -2n	$P\bar{4}n2$	D_{2d}^8
119		I -4 m 2	I -4 -2	$I\bar{4}m2$	D_{2d}^9
120		I -4 c 2	I -4 -2c	$I\bar{4}c2$	D_{2d}^{10}
121		I -4 2 m	I -4 2	$I\bar{4}2m$	D_{2d}^{11}
122		I -4 2 d	I -4 2bw	$I\bar{4}2d$	D_{2d}^{12}
123		P 4/m 2/m 2/m	-P 4 2	$P4/mmm$	D_{4h}^1
124		P 4/m 2/c 2/c	-P 4 2c	$P4/mcc$	D_{4h}^2
125	2	P 4/n 2/b 2/m:2	-P 4a 2b	$P4/nbm$	D_{4h}^3
126	2	P 4/n 2/n 2/c:2	-P 4a 2bc	$P4/nnc$	D_{4h}^4
127		P 4/m 21/b 2/m	-P 4 2ab	$P4/mbm$	D_{4h}^5
128		P 4/m 21/n 2/c	-P 4 2n	$P4/mnc$	D_{4h}^6
129	2	P 4/n 21/m 2/m:2	-P 4a 2a	$P4/nmm$	D_{4h}^7
130	2	P 4/n 21/c 2/c:2	-P 4a 2ac	$P4/ncc$	D_{4h}^8
131		P 42/m 2/m 2/c	-P 4c 2	$P4_2/mmc$	D_{4h}^9
132		P 42/m 2/c 2/m	-P 4c 2c	$P4_2/mcm$	D_{4h}^{10}
133	2	P 42/n 2/b 2/c:2	-P 4ac 2b	$P4_2/nbc$	D_{4h}^{11}
134	2	P 42/n 2/n 2/m:2	-P 4ac 2bc	$P4_2/nnm$	D_{4h}^{12}
135		P 42/m 21/b 2/c	-P 4c 2ab	$P4_2/mbc$	D_{4h}^{13}
136		P 42/m 21/n 2/m	-P 4n 2n	$P4_2/mnm$	D_{4h}^{14}
137	2	P 42/n 21/m 2/c:2	-P 4ac 2a	$P4_2/nmc$	D_{4h}^{15}
138	2	P 42/n 21/c 2/m:2	-P 4ac 2ac	$P4_2/ncm$	D_{4h}^{16}

XX54

Table 1 (continued): **A list of the various space group notations.** The space group number, orientation, Hermann-Mauguin symbol, Hall symbol, International symbol, and Schönflies symbol are listed.

Number	Orientation	Hermann-Mauguin	Hall	International	Schönflies
139		I 4/m 2/m 2/m	-I 4 2	$I4/mmm$	D_{4h}^{17}
140		I 4/m 2/c 2/m	-I 4 2c	$I4/mcm$	D_{4h}^{18}
141	2	I 41/a 2/m 2/d:2	-I 4bd 2	$I4_1/amd$	D_{4h}^{19}
142	2	I 41/a 2/c 2/d:2	-I 4bd 2c	$I4_1/acd$	D_{4h}^{20}
143		P 3	P 3	$P3$	C_3^1
144		P 31	P 31	$P3_1$	C_3^2
145		P 32	P 32	$P3_2$	C_3^3
146	H	R 3:H	R 3	$R3$	C_3^4
147		P -3	-P 3	$P\bar{3}$	C_{3i}^1
148	H	R -3:H	-R 3	$R\bar{3}$	C_{3i}^2
149		P 3 1 2	P 3 2	$P312$	D_3^1
150		P 3 2 1	P 3 2"	$P321$	D_3^2
151		P 31 1 2	P 31 2c (0 0 1)	$P3_112$	D_3^3
152		P 31 2 1	P 31 2"	$P3_121$	D_3^4
153		P 32 1 2	P 32 2c (0 0 -1)	$P3_212$	D_3^5
154		P 32 2 1	P 32 2"	$P3_221$	D_3^6
155	H	R 32:H	R 3 2"	$R32$	D_3^7
156		P 3 m 1	P 3 -2"	$P3m1$	C_{3v}^1
157		P 3 1 m	P 3 -2	$P31m$	C_{3v}^2
158		P 3 c 1	P 3 -2"c	$P3c1$	C_{3v}^3
159		P 3 1 c	P 3 -2c	$P31c$	C_{3v}^4
160	H	R 3 m:H	R 3 -2"	$R3m$	C_{3v}^5
161	H	R 3 c:H	R 3 -2"c	$R3c$	C_{3v}^6
162		P -3 1 2/m	-P 3 2	$P\bar{3}1m$	D_{3d}^1
163		P -3 1 2/c	-P 3 2c	$P\bar{3}1c$	D_{3d}^2
164		P -3 2/m 1	-P 3 2"	$P\bar{3}m1$	D_{3d}^3
165		P -3 2/c 1	-P 3 2"c	$P\bar{3}c1$	D_{3d}^4
166	H	R -3 2/m:H	-R 3 2"	$R\bar{3}m$	D_{3d}^5
167	H	R -3 2/c:H	-R 3 2"c	$R\bar{3}c$	D_{3d}^6
168		P 6	P 6	$P6$	C_6^1
169		P 61	P 61	$P6_1$	C_6^2
170		P 65	P 65	$P6_5$	C_6^3
171		P 62	P 62	$P6_2$	C_6^4
172		P 64	P 64	$P6_4$	C_6^5
173		P 63	P 6c	$P6_3$	C_6^6
174		P -6	P -6	$P\bar{6}$	C_{3h}^1
175		P 6/m	-P 6	$P6/m$	C_{6h}^1
176		P 63/m	-P 6c	$P6_3/m$	C_{6h}^2
177		P 6 2 2	P 6 2	$P622$	D_6^1
178		P 61 2 2	P 61 2 (0 0 -1)	$P6_122$	D_6^2
179		P 65 2 2	P 65 2 (0 0 1)	$P6_522$	D_6^3
180		P 62 2 2	P 62 2c (0 0 1)	$P6_222$	D_6^4
181		P 64 2 2	P 64 2c (0 0 -1)	$P6_422$	D_6^5
182		P 63 2 2	P 6c 2c	$P6_322$	D_6^6
183		P 6 m m	P 6 -2	$P6mm$	C_{6v}^1
184		P 6 c c	P 6 -2c	$P6cc$	C_{6v}^2

XX55

Table 1 (continued): **A list of the various space group notations.** The space group number, orientation, Hermann-Mauguin symbol, Hall symbol, International symbol, and Schönflies symbol are listed.

Number	Orientation	Hermann-Mauguin	Hall	International	Schönflies
185		P 63 c m	P 6c -2	$P6_3cm$	C_{6v}^3
186		P 63 m c	P 6c -2c	$P6_3mc$	C_{6v}^4
187		P -6 m 2	P -6 2	$P\bar{6}m2$	D_{3h}^1
188		P -6 c 2	P -6c 2	$P\bar{6}c2$	D_{3h}^2
189		P -6 2 m	P -6 -2	$P\bar{6}2m$	D_{3h}^3
190		P -6 2 c	P -6c -2c	$P\bar{6}2c$	D_{3h}^4
191		P 6/m 2/m 2/m	-P 6 2	$P6/mmm$	D_{6h}^1
192		P 6/m 2/c 2/c	-P 6 2c	$P6/mcc$	D_{6h}^2
193		P 63/m 2/c 2/m	-P 6c 2	$P6_3/mcm$	D_{6h}^3
194		P 63/m 2/m 2/c	-P 6c 2c	$P6_3/mmc$	D_{6h}^4
195		P 2 3	P 2 2 3	$P23$	T^1
196		F 2 3	F 2 2 3	$F23$	T^2
197		I 2 3	I 2 2 3	$I23$	T^3
198		P 21 3	P 2ac 2ab 3	$P2_13$	T^4
199		I 21 3	I 2b 2c 3	$I2_13$	T^5
200		P 2/m -3	-P 2 2 3	$Pm\bar{3}$	T_h^1
201	2	P 2/n -3:2	-P 2ab 2bc 3	$Pn\bar{3}$	T_h^2
202		F 2/m -3	-F 2 2 3	$Fm\bar{3}$	T_h^3
203	2	F 2/d -3:2	-F 2uv 2vw 3	$Fd\bar{3}$	T_h^4
204		I 2/m -3	-I 2 2 3	$Im\bar{3}$	T_h^5
205		P 21/a -3	-P 2ac 2ab 3	$Pa\bar{3}$	T_h^6
206		I 21/a -3	-I 2b 2c 3	$Ia\bar{3}$	T_h^7
207		P 4 3 2	P 4 2 3	$P432$	O^1
208		P 42 3 2	P 4n 2 3	$P4_232$	O^2
209		F 4 3 2	F 4 2 3	$F432$	O^3
210		F 41 3 2	F 4d 2 3	$F4_132$	O^4
211		I 4 3 2	I 4 2 3	$I432$	O^5
212		P 43 3 2	P 4acd 2ab 3	$P4_332$	O^6
213		P 41 3 2	P 4bd 2ab 3	$P4_132$	O^7
214		I 41 3 2	I 4bd 2c 3	$I4_132$	O^8
215		P -4 3 m	P -4 2 3	$P\bar{4}3m$	T_d^1
216		F -4 3 m	F -4 2 3	$F\bar{4}3m$	T_d^2
217		I -4 3 m	I -4 2 3	$I\bar{4}3m$	T_d^3
218		P -4 3 n	P -4n 2 3	$P\bar{4}3n$	T_d^4
219		F -4 3 c	F -4c 2 3	$F\bar{4}3c$	T_d^5
220		I -4 3 d	I -4bd 2c 3	$I\bar{4}3d$	T_d^6
221		P 4/m -3 2/m	-P 4 2 3	$Pm\bar{3}m$	O_h^1
222	2	P 4/n -3 2/n:2	-P 4a 2bc 3	$Pn\bar{3}n$	O_h^2
223		P 42/m -3 2/n	-P 4n 2 3	$Pm\bar{3}n$	O_h^3
224	2	P 42/n -3 2/m:2	-P 4bc 2bc 3	$Pn\bar{3}m$	O_h^4
225		F 4/m -3 2/m	-F 4 2 3	$Fm\bar{3}m$	O_h^5
226		F 4/m -3 2/c	-F 4c 2 3	$Fm\bar{3}c$	O_h^6
227	2	F 41/d -3 2/m:2	-F 4vw 2vw 3	$Fd\bar{3}m$	O_h^7
228	2	F 41/d -3 2/c:2	-F 4cvw 2vw 3	$Fd\bar{3}c$	O_h^8
229		I 4/m -3 2/m	-I 4 2 3	$Im\bar{3}m$	O_h^9
230		I 41/a -3 2/d	-I 4bd 2c 3	$Ia\bar{3}d$	O_h^{10}

XX56

FOUNDATIONS
ADVANCES

ISSN: 2053-2733
journals.iucr.org/a

AFLOW-SYM: platform for the complete, automatic and self-consistent symmetry analysis of crystals

David Hicks, Corey Oses, Eric Gossett, Geena Gomez, Richard H. Taylor, Cormac Toher, Michael J. Mehl, Ohad Levy and Stefano Curtarolo

Acta Cryst. (2018). A**74**, 184–203

XX57

FOUNDATIONS ADVANCES

ISSN 2053-2733

AFLOW-SYM: platform for the complete, automatic and self-consistent symmetry analysis of crystals

David Hicks,[a,b] Corey Oses,[a,b] Eric Gossett,[a,b] Geena Gomez,[a,b] Richard H. Taylor,[a,b,c] Cormac Toher,[a,b] Michael J. Mehl,[d] Ohad Levy[a,b,e] and Stefano Curtarolo[a,b,f]*

[a]Department of Mechanical Engineering and Materials Science, Duke University, Durham, North Carolina 27708, USA, [b]Center for Materials Genomics, Duke University, Durham, North Carolina 27708, USA, [c]Department of Materials Science and Engineering, Massachusetts Institute of Technology, Massachusetts 02139, USA, [d]United States Naval Academy, Annapolis, Maryland 21402, USA, [e]Department of Physics, NRCN, PO Box 9001, Beer-Sheva 84190, Israel, and [f]Fritz-Haber-Institut der Max-Planck-Gesellschaft, 14195 Berlin-Dahlem, Germany. *Correspondence e-mail: stefano@duke.edu

Received 8 December 2017
Accepted 22 February 2018

Edited by A. Altomare, Institute of Crystallography - CNR, Bari, Italy

Keywords: crystal structure analysis; automation; materials genomics; *AFLOW-SYM*.

Supporting information: this article has supporting information at journals.iucr.org/a

Determination of the symmetry profile of structures is a persistent challenge in materials science. Results often vary amongst standard packages, hindering autonomous materials development by requiring continuous user attention and educated guesses. This article presents a robust procedure for evaluating the complete suite of symmetry properties, featuring various representations for the point, factor and space groups, site symmetries and Wyckoff positions. The protocol determines a system-specific mapping tolerance that yields symmetry operations entirely commensurate with fundamental crystallographic principles. The self-consistent tolerance characterizes the effective spatial resolution of the reported atomic positions. The approach is compared with the most used programs and is successfully validated against the space-group information provided for over 54 000 entries in the Inorganic Crystal Structure Database (ICSD). Subsequently, a complete symmetry analysis is applied to all 1.7+ million entries of the *AFLOW* data repository. The *AFLOW-SYM* package has been implemented in, and made available for, public use through the automated *ab initio* framework *AFLOW*.

1. Introduction

Symmetry fundamentally characterizes all crystals, establishing a tractable connection between observed phenomena and the underlying physical/chemical interactions. Beyond crystal periodicity, symmetry within the unit cell guides materials classification (Mehl *et al.*, 2017), optimizes materials-properties calculations and instructs structure-enumeration methods (Buerger, 1947; Hart & Forcade, 2008). Careful exploitation of crystal symmetry has made possible the characterization of electronic (Setyawan & Curtarolo, 2010), mechanical (Toher *et al.*, 2014, 2017) and thermal properties (Nath *et al.*, 2016, 2017; Plata *et al.*, 2017) in high-throughput fashion (Curtarolo *et al.*, 2013), giving rise to large materials-properties databases such as *AFLOW* (Curtarolo *et al.*, 2012; Yang *et al.*, 2016; Carrete *et al.*, 2014; Levy *et al.*, 2011; Setyawan & Curtarolo, 2010; Levy, Hart & Curtarolo, 2010*a*; Levy, Chepulskii *et al.*, 2010; Levy Hart & Curtarolo, 2010*b*; Hart *et al.*, 2013; Mehl *et al.*, 2017; Supka *et al.*, 2017), *NoMaD* (Scheffler & Draxl, 2014), *Materials Project* (Jain *et al.*, 2011) and *OQMD* (Saal *et al.*, 2013). As these databases incorporate more properties and grow increasingly integrated, access to rapid and consistent symmetry characterizations becomes of paramount importance.

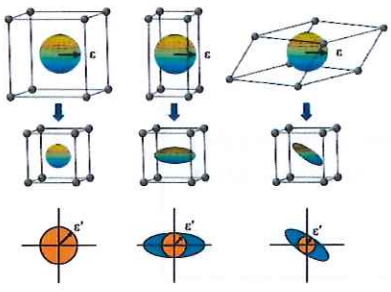

Central to each symmetry analysis is the identification of spatial and angular tolerances, quantifying the threshold at which two points or angles are considered equivalent. These tolerances must account for numerical instabilities and, more importantly, for atypical data stemming from finite temperature measurements or deviations in experimentally measured values (Le Page, 1987). Existing symmetry platforms, such as *FINDSYM* (Stokes & Hatch, 2005; Stokes, 1995), *PLATON* (Spek, 2003) and *Spglib* (Togo, 2017*a*), all cater to different symmetry objectives, and thus address tolerance issues in unique ways. The authors of *FINDSYM*, which is designed for ease of use, acknowledge that its algorithms cannot handle noisy data, and it applies no treatments for ill-conditioned data (Stokes & Hatch, 2005). The *PLATON* geometry package, containing the subroutine *ADDSYM*, allows a small percentage of candidate atomic mappings to fail and attempts to capture missing higher-symmetry descriptions (Spek, 2003). Lower-symmetry descriptions in atomic coordinates can originate from (i) extraction issues with X-ray diffraction data (*e.g.* incorrectly identified crystal system, altered Laue class within a crystal system and neglected inversion) and (ii) *ab initio* relaxations (*e.g.* lost internal translations) (Baur & Tillmanns, 1986; Herbstein & Marsh, 1982; Marsh & Herbstein, 1983). The *Spglib* package applies independent tolerance scans within subroutines, *e.g.* in its methods for finding the primitive cell (`get_primitive`) and Wyckoff positions (`ssm_get_exact_positions`), if certain crystallographic conventions are violated, potentially yielding globally inconsistent symmetry descriptions (Togo, 2017*a*). These packages present suggested default tolerance values that are largely arbitrary and often justified *a posteriori* on a limited test set. In the general case, or in the event where these global defaults fail, the packages fall back on user-defined tolerances. Unfortunately, it is difficult to compare results across packages outside of these default values because tolerances are defined differently. *FINDSYM* and *Spglib* both offer a tunable atomic mapping tolerance, along with a lattice tolerance (*FINDSYM*) and an angular tolerance (*Spglib*), whereas *PLATON* has four separate input tolerances, each specific to a particular operation type. Ultimately, these inconsistencies are symptomatic of an underlying inability to appropriately address tolerances in symmetry analyses.

Managing input/output formats for these packages also presents a challenge. *FINDSYM* and *PLATON* both read CIF and SPF files, which are particularly useful for structures deriving from larger crystal-structure databases, such as the Inorganic Crystal Structure Database (ICSD) (Bergerhoff *et al.*, 1983; Belsky *et al.*, 2002) and Cambridge Structural Database (CSD) (Groom *et al.*, 2016). *PLATON* also supports a few other useful input formats, while *Spglib* has its own input format. Package-specific formats are useful for the developers, but create an unnecessary hurdle for the user, who may need to implement structure-file converters. This is particularly problematic when package developers change the formats of these inputs with new version updates, forcing the user to continuously adapt workflows/frameworks. Additionally, all output formats are package specific, with a medley of symmetry descriptions and representations provided among the three. The assortment of outputs presents yet another hurdle for users trying to build custom solutions for framework integration. Furthermore, it forces users to become locked-in to these packages.

These issues require extensive maintenance on the side of the user, with little guarantee of the validity of the resulting symmetry descriptions. In the case of large materials-properties databases, providing such individual attention to each compound's symmetry description becomes entirely impractical. Herein, we present a robust symmetry package implemented in the automated *ab initio* computational framework *AFLOW*, known as *AFLOW-SYM*. The module delivers a complete symmetry analysis of the crystal, including the symmetry operations for the lattice point group, reciprocal-space lattice point group, factor group, crystal point group, dual of the crystal point group, symmetry-equivalent atoms, site symmetry and space group (see Appendix *A* for an overview of symmetry groups). Moreover, it provides general crystallographic descriptions including the space-group number and label(s), Pearson symbol, Bravais lattice type and variations, Wyckoff positions, and standard representations of the crystal. The routine employs an adaptive structure-specific tolerance scheme capable of handling even the most skewed unit cells. By default, two independent symmetry procedures are applied, enabling corroboration of the characterization. The scheme has been tested on 54 000 compounds from the ICSD in the http://www.aflow.org/ repository, showing substantial improvement in characterizing space groups and lattice types compared with other packages. Along with a standardized text output, *AFLOW-SYM* presents the results in JavaScript Object Notation (JSON) for easy integration into different workflows. The software is completely written in C++ and it can be compiled in UNIX, Linux and MacOSX environments using the gcc/g++ suite of compilers. The package is open source and is available under the GNU-GPL license. An *AFLOW-SYM* Python module is also available to facilitate integration with other workflow packages, *e.g.* *AFLOWπ* (Supka *et al.*, 2017; Agapito *et al.*, 2015) and *NoMaD* (Scheffler & Draxl, 2014). Thus, *AFLOW-SYM* serves as a robust one-stop symmetry shop for the materials-science community.

2. Methods

2.1. Periodic boundary conditions in skewed cells

Analyzing the symmetry of materials involves determining the full set of their isometries. Algorithmically, candidate symmetry operators are applied to a set of atoms and validated if (i) distances between atoms and their transformed counterparts are within a mapping tolerance ε, and (ii) the mappings are isomorphic (one-to-one). For convenience, ε is defined in units of a Euclidean space – ångströms in this case. An explicit mapping function is defined, indicating whether atom mappings are successful:

XX59

$$\text{map}_{\text{atom}}(\mathbf{d}_c) = \begin{cases} \text{true} & \text{if } \|\mathbf{d}_c\| < \varepsilon \\ \text{false} & \text{otherwise} \end{cases}, \quad (1)$$

where $\mathbf{d}_c$ is the Cartesian distance vector between an atom and a transformed atom. Symmetries of the crystal are discovered when successful isomorphic mappings – given by equation (1) – exist between all of the original and transformed atoms. Under periodic boundary conditions, the minimum distance for the mapping function is identified by considering equivalent atoms of nearby cells [so-called method of images (Hloucha & Deiters, 1998)]:

$$\mathbf{d}_c^{\min} = \min_{n_a,n_b,n_c} (\mathbf{d}_c + n_a\mathbf{a} + n_b\mathbf{b} + n_c\mathbf{c}), \quad (2)$$

where $\mathbf{a}$, $\mathbf{b}$, $\mathbf{c}$ are the lattice vectors; n_a, n_b, n_c are the indices of neighboring cells; and $\mathbf{d}_c^{\min}$ is the globally optimal Cartesian distance vector. In the simplest case of a purely orthorhombic cell, the approach requires exploration of the 26 surrounding unit cells ($-1 \leq n_a, n_b, n_c \leq 1$). However, additional neighboring cells should be considered with increased skewness of the lattice vectors (see §2.7), making it prohibitively expensive. Instead, many algorithms minimize the distance vector through a greedy, bring-in-cell approach (Hloucha & Deiters, 1998). Working with fractional coordinates, each component i of the distance vector $\mathbf{d}_f$ is minimized using the nearest-integer function [nint (Hloucha & Deiters, 1998)]:

$$\begin{aligned} \tilde{\mathbf{d}}_{f,i}^{\min} &= \mathbf{d}_{f,i} - \text{nint}(\mathbf{d}_{f,i}) \ \forall i, \\ \tilde{\mathbf{d}}_c^{\min} &= \mathbf{L}\tilde{\mathbf{d}}_f^{\min}, \end{aligned} \quad (3)$$

where $\mathbf{L}$ is the column-space matrix representation of the lattice and $\tilde{\mathbf{d}}_c^{\min}$ is $\tilde{\mathbf{d}}_f^{\min}$ converted to Cartesian coordinates for the mapping determination in equation (1).

While it is a convenient shortcut, the bring-in-cell minimum distance is not generally equivalent to the globally optimized distance: $\tilde{\mathbf{d}}_c^{\min} \neq \mathbf{d}_c^{\min}$ (see Fig. 1*a*). A component-by-component minimization of the distance vector assumes independent basis vectors (no skewness) and neglects potentially closer images that are only considered by exploring all neighboring cells. Occurrence of a distance mismatch depends on the lattice type and compromises the integrity of the mapping determination. The issue becomes particularly elusive in fractional coordinates, where the size and shape of the cell are warped to yield a unit cube as shown in Fig. 1(*b*). The greater the anisotropy of the lattice, the larger the warping. Fig. 1(*c*) illustrates how the tolerance changes between Cartesian and fractional space. In the general case, a spherical tolerance in Cartesian coordinates warps into an ellipsoid in fractional coordinates. Hence, the criteria for successful mappings in fractional space are direction dependent unless the distance is sufficiently small, *i.e.* within the circumscribed sphere of radius ε' (highlighted in orange). Distances within ε' in fractional space always map within ε in Cartesian space, but a robust check (global optimization) is needed for larger distances to account for the extremes of the ellipsoid. Since most distances outside of ε' do not yield

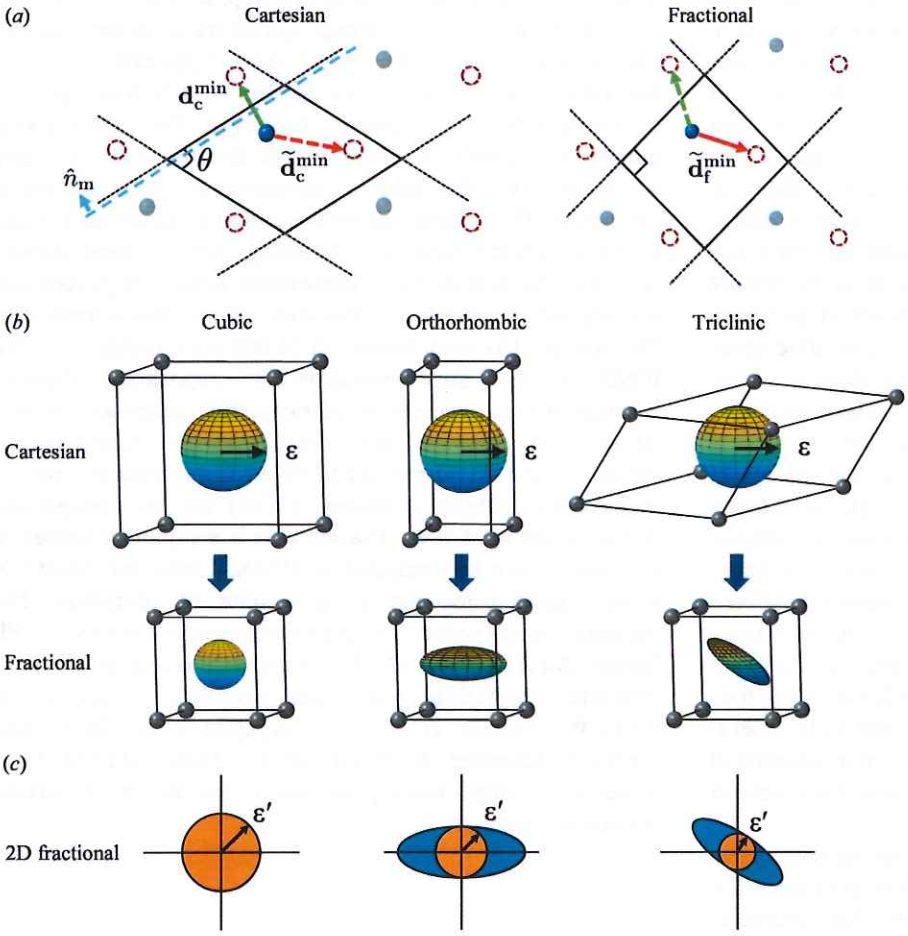

Figure 1
Visualizations of space warping with a basis transformation. (*a*) To validate a candidate mirror operation (described by $\hat{n}_m$) on a crystal (blue atoms), the operation is applied to yield a transformed crystal (hollow orange atoms superimposed on the original crystal). The true minimum distance between the blue and orange atoms is resolved in Cartesian space, indicated by the green $\mathbf{d}_c^{\min}$ vector. However, the bring-in-cell method determines another periodic image to be closer, highlighted by the dashed red vector. The mismatch is obscured in fractional space, where the red vector appears smaller than the green, indicated by $\tilde{\mathbf{d}}_c^{\min}$. (*b*) An atom is placed in the middle of the lattice with a surrounding sphere of radius ε. Mapping occurs when the position of an atom transformed by a symmetry operator is within the sphere. The size and shape of the sphere are warped with a basis transformation (Cartesian to fractional): uniform compression occurs in cubic cells, oblate compression in orthorhombic cells, non-uniform (sheared) compression in triclinic lattices. (*c*) Two-dimensional illustration of how the tolerance (ε) warps in fractional space for cubic, orthorhombic and triclinic lattices. The orange circle with radius ε' in fractional coordinates indicates the bounds of the safe mapping region, independent of direction.

mappings, such a robust check is generally wasteful. Instead, more useful insight can be garnered from Fig. 1(*c*): tolerances sufficiently bounded by the skewness can still yield a proper mapping determination using the inexpensive bring-in-cell algorithm.

The goal is to define an upper tolerance threshold to safely ensure that the bring-in-cell minimum ($\widetilde{\mathbf{d}}_c^{\min}$) and global minimum ($\mathbf{d}_c^{\min}$) yield the same mapping results, in spite of a distance mismatch:

$$\text{map}_{\text{atom}}(\mathbf{d}_c^{\min}) \equiv \text{map}_{\text{atom}}(\widetilde{\mathbf{d}}_c^{\min}) \mid \varepsilon < \left\|\mathbf{d}_c^{\min}\right\|, \quad \forall \mathbf{d}_c \mid \mathbf{d}_c^{\min} \neq \widetilde{\mathbf{d}}_c^{\min}. \tag{4}$$

A mismatch is encountered when the image identified by the bring-in-cell method is not the optimal neighbor; therefore: $\mathbf{d}_c^{\min} \leq \widetilde{\mathbf{d}}_c^{\min}$. A suitable threshold needs to overcome the difference between the two methods for all mismatch possibilities, *i.e.* ε would need to be below $\mathbf{d}_c^{\min}$ or above $\widetilde{\mathbf{d}}_c^{\min}$ to yield a consistent mapping determination. A threshold greater than $\widetilde{\mathbf{d}}_c^{\min}$ is ruled out to ensure that ε is always smaller than the minimum interatomic distance [$d_c^{\text{nn(min)}}$], making it possible to distinguish nearest neighbors. To find a tolerance in the remaining region ($\varepsilon < ||\mathbf{d}_c^{\min}||$), the largest mismatch possible should be addressed directly, which yields the smallest $\mathbf{d}_c^{\min}$ and thus the most restrictive bound on the tolerance. Given the angles between the lattice vectors (α, β, γ), a maximum skewness is defined as

$$\xi_{\max} = \max(\cos\alpha, \cos\beta, \cos\gamma), \tag{5}$$

where the cosine of the angle derives from the normalized, off-diagonal terms of the metric tensor. $\xi_{\max}$ lies in the range [0, 1), where $\xi_{\max} = 0$ characterizes a perfectly orthorhombic cell. A suitable maximum mapping tolerance is heuristically defined as

$$\varepsilon_{\max} = (1 - \xi_{\max}) d_c^{\text{nn(min)}}, \tag{6}$$

which appropriately reduces $d_c^{\text{nn(min)}}$ (an absolute upper bound for the tolerance to maintain resolution between atoms) with increasing skewness. The form of the coefficient $(1 - \cos\theta)$ decays quickly with basis-vector overlap (of the order of θ^2), ensuring a safe enveloping bound. Tolerances well below $\varepsilon_{\max}$ should yield the correct mapping determination with the bring-in-cell approach (in spite of a distance mismatch); otherwise, the global minimization algorithm should be employed:

$$\mathbf{d}_c^{\text{map}} = \begin{cases} \mathbf{L}\widetilde{\mathbf{d}}_f^{\min} & \text{if } \varepsilon \ll \varepsilon_{\max} \\ \min\limits_{n_a,n_b,n_c} (\mathbf{d}_c + n_a\mathbf{L}_a + n_b\mathbf{L}_b + n_c\mathbf{L}_c) & \text{otherwise} \end{cases}. \tag{7}$$

To demonstrate the robustness of $\varepsilon_{\max}$, extreme hypothetical cases are presented in Appendix *C*.

2.2. Adaptive tolerance scheme

While $\varepsilon_{\max}$ offers a practical upper tolerance bound for the choice of the distance minimization algorithm, it offers no insight for choosing a specific tolerance. Of course, there are fundamental constraints, such as the minimum interatomic distance and the precision of the input structure parameters: $\varepsilon_{\text{precision}} < \varepsilon < d_c^{\text{nn(min)}}$, but these can span over several orders of magnitude, throughout which a variety of results are possible. Fig. 2 illustrates the different space groups that may be assigned to AgBr (ICSD No. 56551; http://aflow.org/material.php?id=Ag1Br1_ICSD_56551) with various tolerance choices (the ICSD reports space group No. 11). Interestingly, adjacent space-group regions show non-isomorphic subgroup relations: between space-group Nos. 59 and 11 and between 225 and 166. Of particular concern is the gap highlighted in Fig. 2(*b*) between space-group regions 166 and 59. Not surprisingly, these space groups share no subgroup relations. These gaps represent problematic regions where noise in the structural information interferes with the determination of satisfied symmetry operations, yielding profiles inconsistent with any possible space group. Rather than an *a posteriori* selection of the symmetry elements to include in the analysis, we employ an adaptive tolerance approach. A radial tolerance scan is performed surrounding the initial input tolerance ε_0 to overcome the 'confusion' region, as shown in Fig. 2(*b*). With each adjustment of the tolerance, the algorithm updates and validates all symmetry properties and operations, yielding a globally consistent profile and an effective spatial resolution for the structure.

To fully characterize a structure's symmetry, *AFLOW-SYM* employs two major symmetry procedures. The first calculates the symmetry of the crystal in the *International Tables for Crystallography* (Hahn, 2002; Wondratschek & Müller, 2004; Aroyo, Perez-Mato *et al.*, 2006; Aroyo, Kirov *et al.*, 2006) (ITC) conventional cell, yielding the space group and Wyckoff positions. The second resolves the symmetry profile of the structure in the original (input) representation, including: the lattice point group, reciprocal-lattice point group, factor group, crystal point group, dual of the crystal point group,

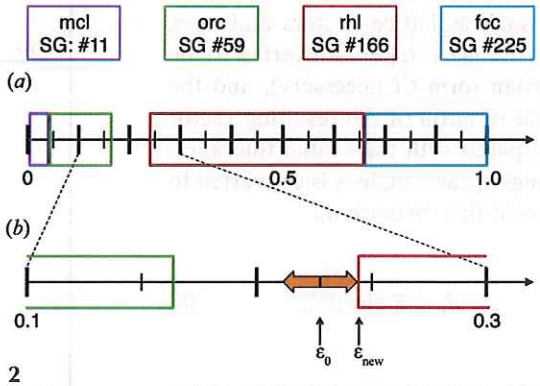

Figure 2
Variation of space group with mapping tolerance for AgBr (ICSD No. 56551) as determined by *AFLOW-SYM*. (*a*) Space groups and tolerance ranges identified are as follows (ascending order): 1.0×10^{-6} to 4.0855×10^{-2} Å is monoclinic (space group No. 11), 4.08556×10^{-2} to 1.64186×10^{-1} Å is orthorhombic (space group No. 59), 2.46281×10^{-1} to 6.69605×10^{-1} Å is rhombohedral (space group No. 166) and 6.69606×10^{-1} to 1.0 Å is face-centered cubic (space group No. 225). (*b*) A gap is highlighted between 1.64186×10^{-1} to 2.46281×10^{-1} Å where no consistent space group is identified. The orange arrows illustrate how the algorithm scans possible tolerances to find the closest consistent space group.

space group, inequivalent and equivalent atoms, and the site symmetry. While both routines can be employed independently, the two are combined in *AFLOW-SYM* by default, affording additional validation schemes to ensure a stricter consistency.

Ultimately, the combination of the tolerance scan and integrated workflow (with robust validation schemes) ensures the automatic determination of a consistent symmetry profile. While the option remains for a user-defined tolerance (with and without the scan), *AFLOW-SYM* heuristically defines two default tolerance values: `tight` ($\varepsilon_{\text{tight}} = d_c^{\text{nn(min)}}/100$) and `loose` ($\varepsilon_{\text{loose}} = d_c^{\text{nn(min)}}/10$). Generally, an expected symmetry profile (perhaps from experiments) can be found in either of the two tolerances. If no tolerance is defined, *AFLOW-SYM* defaults to the tight tolerance. The tolerance chosen for the analysis is compared against ε_{max} to identify the required minimization technique to yield consistent mappings [see equation (7)]. Overall, the *AFLOW-SYM* tolerance scheme has been validated against 54 000 entries from the ICSD, and subsequently applied to all 1.7 million entries stored in the http://www.aflow.org/ repository. The symmetry results can be retrieved from the *AFLOW* repository *via* the *REST-API* (Taylor *et al.*, 2014) or the *AFLUX Search-API* (Rose *et al.*, 2017).

2.3. Tolerance types and conversions

Outside of mapping distances, there are a number of relevant quantities for which an equivalence criterion is required, *e.g.* lattice vectors, axes, angles and symmetry operations. Instead of defining separate tolerances for each, *AFLOW-SYM* leverages the single spatial tolerance, converting quantities to Cartesian distances whenever possible. For vector quantities such as lattice vectors and axes, the difference is taken, converted to the Cartesian form (if necessary), and the Euclidean norm of the resulting vector is compared with the spatial tolerance. For angles, each angle θ_i is converted to a straight-line distance d_i:

$$d_i = \bar{x}_i \sin(\theta_i), \qquad (8)$$

where $\bar{x}_i$ is the average length of the angle-defining vectors in Cartesian space. The two straight-line distances are subtracted and compared with the input spatial tolerance. To compare rotation matrices for a particular lattice, each matrix is transformed into its fractional form, resulting in two integer matrices that can be matched exactly.

2.4. *International Tables for Crystallography* standard representation

One strategy for uncovering a structure's symmetry profile is to convert it to a standard form, such as the one defined by ITC. In this representation, the symmetry operations, space group and Wyckoff positions are well tabulated, mitigating the computational expense involved in combinatorial operation searches. To efficiently explore the possibilities, the algorithm exploits the lattice symmetry to resolve the crystal symmetry, from which the conventional cell is defined. The full workflow is illustrated in Fig. 3.

First, the algorithm finds a primitive representation of the crystal (of which there are many) by exploring possible internal translations forming a smaller lattice (Hahn, 2002). To optimize the search, only the vectors between the least-frequently occurring atomic species are considered. The translation vector should preserve cell periodicity, and the resulting reduced representation should conserve the stoichiometry.

Next, the symmetry of the lattice is determined by calculating the mirror and n-fold rotation operations. The primitive cell is expanded from −1 to 1 in each direction (Le Page, 1987) and combinations of lattice points are considered for defining the following: (i) mirror operations characterized by a plane

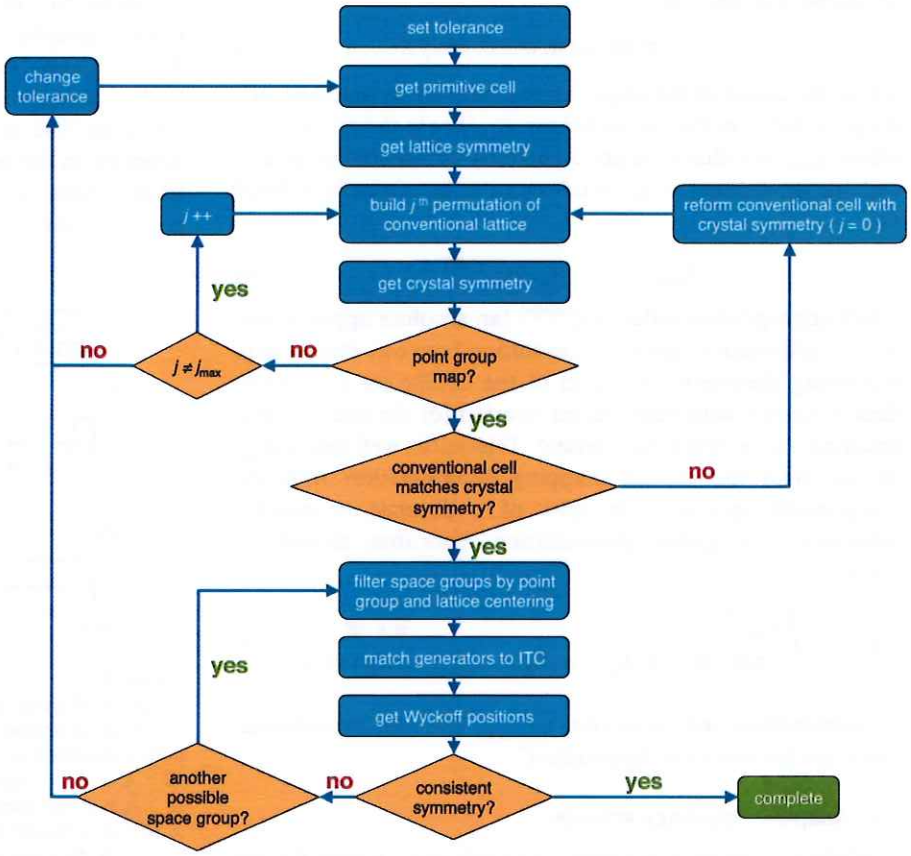

Figure 3
Workflow for the algorithm for converting a structure to the standard representation as defined by *International Tables for Crystallography*. Functions are represented by blue rectangles and validation schemes by orange diamonds.

Table 1
Conventional cell construction rules based on symmetry operations.

Lattice/crystal system	No. of mirrors	No. of n-fold rotations	Conventional cell
Cubic	9	3 (fourfold)	**a**, **b**, **c**: parallel to three equivalent fourfold axes
Hexagonal	7	1 (three-/sixfold)	**c**: parallel to three-/sixfold axis **a**, **b**: parallel to mirror axes ($\|\mathbf{a}\| \equiv \|\mathbf{b}\|$ and $\beta = 120°$)
Tetragonal	5	1 (fourfold)	**c**: parallel to fourfold axis **a**, **b**: parallel to mirror axes ($\|\mathbf{a}\| \equiv \|\mathbf{b}\|$ and $\beta = 90°$)
Rhombohedral	3	1 (three-/sixfold)	**c**: parallel to three-/sixfold axis **a**, **b**: parallel to mirror axes ($\|\mathbf{a}\| \equiv \|\mathbf{b}\|$ and $\beta = 120°$)
Orthorhombic	3	—	**a**, **b**, **c**: parallel to three mirror axes
Monoclinic	1	—	**b**: parallel to mirror axis (unique axis) **a**, **c**: parallel to two (choice of three) smallest translations perpendicular to **b** (Hahn, 2002)
Triclinic	0	—	**a**, **b**, **c**: same as original lattice

(normal $\hat{\mathbf{n}}_{\text{mirror}}$) between two lattice points about which half the lattice points can be reflected onto the other, and (ii) n-fold rotations ($n \in \{2, 3, 4, 6\}$) described by an axis ($\hat{\mathbf{r}}_{n\text{-fold}}$) and angle ($\theta$) such that a rotation about $\hat{\mathbf{r}}_{n\text{-fold}}$ by θ yields an isomorphic mapping of lattice points. The two types of operations are illustrated in Fig. 4.

The cardinality of each operation type defines the lattice system, as detailed in Table 1. If the lattice and crystal systems are the same, the characteristic vectors of the lattice operators ($\hat{\mathbf{n}}_{\text{mirror}}$ and $\hat{\mathbf{r}}_{n\text{-fold}}$) and corresponding lattice points define the lattice vectors of the conventional cell (also outlined in Table 1). For all cases, these lattice vectors are used to construct an initial conventional cell. The aim is to find a conventional cell whose corresponding symmetry operators [tabulated in ITC in Table 11.2.2.1 (Hahn, 2002)] are validated for the crystal, which can have symmetry equal to or less than the lattice. If a mismatch in cardinality is encountered, permutations of the lattice vectors are attempted. Should a mismatch remain after all permutations have been exhausted, the conventional cell is re-formed to reflect the crystal symmetry. The re-formed cell is chosen based on the observed cardinality of the symmetry operations (refer again to Table 1).

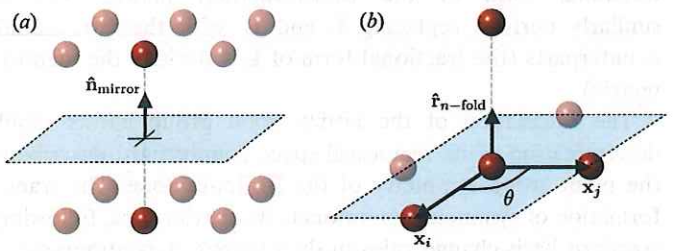

Figure 4
Minimum symmetry identifiers of the lattice system: (*a*) mirror operations, (*b*) n-fold rotations. The resulting lattice vectors are denoted by gray dotted lines.

The resulting crystal point-group set and internal translations (lattice centerings) are then used to filter candidate space groups. To pin down a space group exactly, the symmetry elements of the crystal are matched to the ITC generators, *i.e.* the operations that generate the symmetry-equivalent atoms for the general Wyckoff position (Hahn, 2002). However, a shift in the origin may differentiate the two sets of operators; this is a degree of freedom that should be addressed carefully. The appropriate origin shift should transform the symmetry elements to the ITC generators, thus forming a set of linear equations. Consider two symmetry-equivalent atom positions ($\mathbf{x}$ and $\mathbf{x}'$) in the crystal,

$$\mathbf{x}' = \mathbf{U}\mathbf{x} + \mathbf{t}, \tag{9}$$

where $\mathbf{U}$ and $\mathbf{t}$ are the fixed-point and translation operations, respectively, between the two atoms. An origin shift $\mathcal{O}$ relates these positions to those listed in ITC:

$$\mathbf{x}_{\text{ITC}} = \mathbf{x} + \mathcal{O}, \tag{10}$$

$$\mathbf{x}'_{\text{ITC}} = \mathbf{x}' + \mathcal{O}. \tag{11}$$

Applying $\mathbf{U}$ to equation (10) and subtracting it from equation (11) yields

$$\mathbf{x}'_{\text{ITC}} - \mathbf{U}\mathbf{x}_{\text{ITC}} = \mathbf{x}' + \mathcal{O} - \mathbf{U}\mathbf{x} - \mathbf{U}\mathcal{O}. \tag{12}$$

The ITC translation $\mathbf{t}_{\text{ITC}}$ and the crystal translation $\mathbf{t}$ are related *via*

$$\mathbf{t}_{\text{ITC}} = \mathbf{t} + \mathcal{O} - \mathbf{U}\mathcal{O}. \tag{13}$$

Combining equations (12)–(13) and incorporating equations (10)–(11) produces the following system of equations:

$$(\mathbf{I} - \mathbf{U})\mathcal{O} = \left(\mathbf{t}_{\text{ITC}} - \mathbf{t}\right), \tag{14}$$

where $\mathbf{I}$ is the identity. Equation (14) must be solved for each generator, often resulting in an overdetermined system. Periodic boundary conditions should also be considered when solving the system of equations, as solutions may reside in neighboring cells. If a commensurate origin shift is not found, the next candidate space group is tested.

With the shift into the ITC reference frame, the Wyckoff positions are identified by grouping atoms in the conventional cell into symmetry-equivalent sets. These sets are compared with the ITC standard to identify the corresponding Wyckoff coordinates, site-symmetry designation and letter. The procedure to find the origin shift is similarly applied to determine any Wyckoff parameters (x, y, z). For some space groups, the Wyckoff positions only differ by an internal translation (identical site symmetries), introducing ambiguity in their identification. In these cases, *AFLOW-SYM* favors the Wyckoff scheme producing the smallest enumerated Wyckoff lettering.

XX63

After finding the Wyckoff positions, the algorithm is complete. *AFLOW-SYM* returns the space group, conventional cell and Wyckoff positions in the ITC standard representation.

2.5. Input orientation symmetry algorithm

The standard conventional cell representation described in the previous section affords easy access to the full symmetry profile of the structure. Nevertheless, other representations, such as the *AFLOW* standard primitive representation (Setyawan & Curtarolo, 2010), are often preferred for reducing the computational cost of subsequent calculations/analyses, such as density-functional-theory calculations (Setyawan & Curtarolo, 2010). While conversions are always possible, such as with a Minkowski lattice reduction or as was done to find the standard conventional cell, in practice they introduce errors in the structural parameters, becoming particularly problematic in 'confusion' tolerance regions (Fig. 2) and tolerance-sensitive algorithms, *e.g.* calculations of force constants (Jahnátek *et al.*, 2011; Plata *et al.*, 2017). To mitigate the need for error-accumulating conversions, a general-representation symmetry algorithm is also incorporated in *AFLOW-SYM*. The integration of the two symmetry algorithms affords additional validation schemes that combat 'confusion' tolerance regions and ensures an overall stricter consistency. The full workflow of this algorithm is outlined in Fig. 5. For descriptions of the different symmetry groups, refer to Appendix *A*.

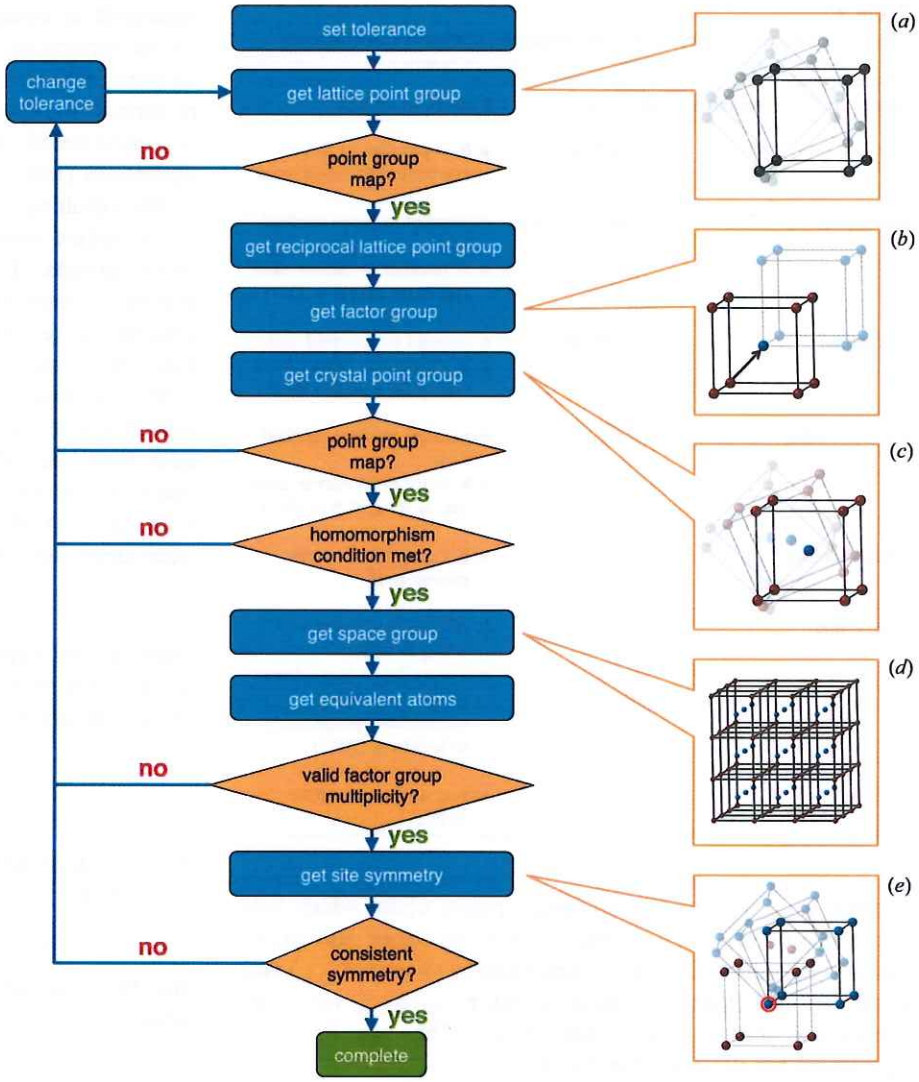

Figure 5
Workflow for the algorithm for calculating the symmetry operations of the system in its original representation. Functions are represented by blue rectangles and validation schemes by orange diamonds.

First, the point group of the lattice is calculated by finding all identical lattice cells of an expanded grid (see §2.7). The unique set of matrices that transform the rotated cells to the original cell define the lattice point group, as depicted in Fig. 5(*a*). The search first considers all lattice points within a radius no smaller than that of a sphere encapsulating the entire unit cell. These points define the candidate lattice vectors (origin to lattice point), and those not of length a, b or c (lattice-vector lengths of the original cell) are eliminated. Next, all combinations of these candidate lattice vectors are considered, eliminating sets by matching the full set of lattice parameters (lattice-vector lengths and angles of the original cell). The transformation matrix is calculated as

$$\mathbf{U}_c = \mathbf{L}(\mathbf{L}')^{-1} \tag{15}$$

where $\mathbf{U}_c$ is the Cartesian form of the transformation (rotation) matrix, $\mathbf{L}$ is the original, column-space matrix representation of the lattice and $\mathbf{L}'$ is the rotated lattice. The fractional form of the transformation matrix ($\mathbf{U}_f$) is similarly derived replacing $\mathbf{L}$ and $\mathbf{L}'$ with their fractional counterparts (the fractional form of $\mathbf{L}$ is trivially the identity matrix).

The calculation of the lattice point group allows rapid determination of its reciprocal-space counterpart, describing the point-group symmetry of the Brillouin zone. The transformation of symmetry operators is straightforward, following standard basis-change rules in dual spaces. A contragredient transformation converts the real-space form of the operator to its reciprocal counterpart, which is trivial for the Cartesian form of the operator (orthogonal matrix):

$$\mathbf{V}_c = (\mathbf{U}_c^{-1})^T = \mathbf{U}_c,$$
$$\mathbf{V}_f = (\mathbf{U}_f^{-1})^T, \quad (16)$$

where $\mathbf{U}_c/\mathbf{U}_f$ and $\mathbf{V}_c/\mathbf{V}_f$ are the Cartesian/fractional forms of the symmetry operator in real and reciprocal spaces, respectively (Sands, 1982).

Next, the coset representatives of the factor group are determined, characterizing the symmetry of the unit cell. These operations are characterized by a fixed-point rotation (lattice point group) and an internal translation that yield an isomorphic mapping among the atoms. The smallest set of candidate translation vectors can be found among atoms of the least frequently occurring species. This symmetry description is represented by Fig. 5(*b*).

The point group of the crystal is then extracted from the coset representatives of the factor groups. By exploiting the homomorphism (or isomorphism for primitive cells) between the factor group and the crystal point group, the internal translations of the coset representatives are removed and the unique elements yield the crystal point group. This is portrayed in Fig. 5(*c*). The dual-space counterpart of the crystal point group is derived by performing the contragredient transformation, as shown in equation (16).

The space-group operations are similarly derived from the coset representatives of the factor group. The space group describes the symmetry of the infinitely periodic crystal, resulting from the propagation of the unit-cell symmetry throughout the lattice. A finite set of space-group operators is generated by applying the lattice translations to each of the coset-representative operations out to a specified radius. The operation is depicted in Fig. 5(*d*).

The coset representatives of the factor group also resolve the symmetry-equivalent atoms (Wyckoff positions). Atoms that are symmetry-equivalent map onto one another through a coset-representative operation. This organization is convenient for calculating the site symmetry of each atom site in the crystal. The site symmetries, or site point groups, are exposed by centering the reference frame onto each atomic site and applying the operations of the crystal point group, as illustrated in Fig. 5(*e*). To expedite this process, the site symmetries are explicitly calculated for all inequivalent atoms. They are then propagated to equivalent atoms with the appropriate change of basis (dictated by the coset representative mapping the inequivalent atom to the equivalent atom).

2.6. Consistency of symmetry

There are a finite number of operation sets that a crystal can exhibit (Giacovazzo *et al.*, 2011). A set of symmetry operations outside of those allowed by crystallographic group theory are attributed to noisy data, thus warranting the adaptive tolerance scan. Numerous symmetry rules are validated throughout the *AFLOW-SYM* routines. The list of consistency checks is:

(i) Point group (lattice/crystal) contains (at the very least) the identity element.

(ii) Point group (lattice/crystal) matches one of 32 point groups.

(iii) Coset representative of the factor group is an integer multiple of the crystallographic point group (homomorphic/isomorphic condition).

(iv) Space-group symbol decomposes into the crystallographic point-group symbol by removing translational components (with the exception of derivative structures).

(v) Number of symmetry-equivalent atoms is divisible by the ratio of the number of operations in the factor and crystal point groups.

(vi) Space-group and Wyckoff positions match ITC conventions (Hahn, 2002).

2.7. Exploring the atomic environment

A description of the local atomic environments in a crystal is required for determining the atom coordinations and atom/lattice mappings. Depending on the cell representation, an expansion is generally warranted for sufficient exploration of the nearest neighbors. Here, an algorithm is outlined for determining the number of neighboring cells to explore in order to capture the local environment within a given exploration radius (r_{sphere}). In *AFLOW-SYM*, the default exploration radius is the largest distance between any two lattice points in a single unit cell. First, the normal of each pair of lattice vectors is calculated and scaled to be of length r_{sphere}, *e.g.* $\mathbf{n}_1 = r_{\text{sphere}}\mathbf{b} \times \mathbf{c}/\|\mathbf{b} \times \mathbf{c}\|$, where $\mathbf{b}$ and $\mathbf{c}$ are lattice vectors. Next, the scaled normals are converted to the basis of the lattice, *e.g.* $\mathbf{n}_1' = \mathbf{L}^{-1}\mathbf{n}_1$, where $\mathbf{L}$ is the column-space matrix representation of the lattice. The magnitude (rounded up to the nearest integer) of the ith component of the $\mathbf{n}_i'$ vector reveals the pertinent grid dimensions (d_1, d_2, d_3). A uniform sphere of radius r_{sphere} centered at the origin fits within a three-dimensional grid spanning $[-d_i, d_i]$.

3. Results

Highlighted here are benchmarks to compare the various standard symmetry packages: *AFLOW-SYM*, *Spglib*, *FINDSYM* and *PLATON*. The results are calculated with the most recent versions available for download: (i) *AFLOW* version 3.1.169, (ii) *Spglib* version 1.10.2.4, (iii) *FINDSYM* version 5.1.0, (iv) *PLATON* version 30118.

The default tolerances are employed as reported by the authors: (i) *AFLOW-SYM*: $\varepsilon_{\text{tight}} = d_c^{\text{nn(min)}}/100$, (ii) *Spglib*: `symprec` $= 1 \times 10^{-5}$ Å, `angle_tolerance` derives from `symprec` [default listed on the web page (Togo, 2017*b*)], (iii) *FINDSYM*: $\varepsilon_{\text{lattice}} = 1 \times 10^{-5}$ Å, $\varepsilon_{\text{atomic position}} = 1 \times 10^{-3}$ Å [default from web interface (Stokes *et al.*, 2017)], (iv) *PLATON*: $\varepsilon_{\text{metric}} = 1.00°$, $\varepsilon_{\text{rotation}} = 0.25$ Å, $\varepsilon_{\text{inversion}} = 0.25$ Å, $\varepsilon_{\text{translation}} = 0.25$ Å (Le Page, 1987).

Alternative tolerance values are also used for *Spglib*, *FINDSYM* and *PLATON*. In general, the alternative tolerances are 100 times the default tolerances, except in the case of *PLATON*, where the default tolerances are divided by 100: (i) *Spglib*: `symprec` $= 1 \times 10^{-3}$ Å, (ii) *FINDSYM*: $\varepsilon_{\text{lattice}} = 1 \times 10^{-3}$ Å, $\varepsilon_{\text{atomic position}} = 1 \times 10^{-1}$ Å, (iii) *PLATON*: $\varepsilon_{\text{metric}} =$

Table 2
Mismatch counts between reported and calculated space groups for entries in the ICSD.

The test set is comprised of 54 015 ICSD entries stored in the http://www.aflow.org/ repository, as of 6 October 2017. The columns indicate the number of entries whose space group, lattice type and crystal family do not match those reported by the ICSD. The results using the user-defined/non-default tolerance values for *Spglib*, *FINDSYM* and *PLATON* are shown in parentheses. For more details, refer to the supporting information.

Package	No. of space-group mismatches	No. of lattice mismatches	No. of crystal system mismatches	No. with space group not found
AFLOW-SYM	834	420	377	0
Spglib	10022 (3389)	9644 (2917)	9523 (2832)	0 (0)
FINDSYM	3540 (1067)	3066 (531)	2982 (483)	127 (156)
PLATON	3000 (1217)	1092 (588)	1083 (486)	195 (1351)†

† Indicates two entries for which the space-group calculation exceeded 48 h.

0.01°, $\varepsilon_{\text{rotation}} = 2.5 \times 10^{-3}$ Å, $\varepsilon_{\text{inversion}} = 2.5 \times 10^{-3}$ Å, $\varepsilon_{\text{translation}} = 2.5 \times 10^{-3}$ Å.

The results from the alternative tolerances are denoted by $^{+}$.

3.1. Accuracy of space-group analyses

The CIF files stored in the ICSD contain information such as the structural parameters and atomic species/positions, as well as the space group (often reported from experiments), publication date and citation. The experimentally reported space-group information provides a unique validation opportunity for the various symmetry packages. The mismatch counts between the reported and calculated space groups are shown in Table 2. The counts are additionally broken down by lattice and crystal system (Fig. 6) to highlight the severity of the mismatch. The full comparison of results is provided in the supporting information, organized in tables by the reported crystal system, with mismatches highlighted in red.

AFLOW-SYM shows the best agreement with the ICSD with a deviation of about 1.5% (reduced to 1.3% if the mismatch is rectified at the loose tolerance). The mismatch is almost halved when comparing only the lattice and crystal systems, suggesting the algorithm found similar/nearby space groups (*e.g.* see Fig. 2). Using their respective default tolerances, *PLATON* performs second best with a 5.6% deviation, followed by *FINDSYM* and *Spglib* with deviations of about 6.6% and 18.5%, respectively. With the alternative tolerances, the overall number of mismatches decreases for each package: *PLATON* reduces to 2.3%, *FINDSYM* reduces to 2.0% and *Spglib* reduces to 6.3%. Table 2 also shows that there are a number of systems for which *FINDSYM* and *PLATON* are unable to identify any space group.

Fig. 6 illustrates the space-group mismatch from each package organized by lattice type. Overall, *AFLOW-SYM* is the most consistent with the ICSD for all lattice types for both the default and alternative tolerances, except for cubic systems where *FINDSYM* has one less mismatch than *AFLOW-SYM* using the alternative tolerance. The default tolerance values certainly play a role in the large deviation count, *e.g.* a tighter tolerance can yield a lower symmetry than expected. This is evident with hexagonal and rhombohedral lattices, where *Spglib* resolves isomorphic subgroups neglecting the three-/sixfold rotations (see the supporting information). However, increases in tolerance do not necessarily yield more consistent space-group determinations. Fig. 6 shows that the default tolerance is more accurate than the alternative tolerance for

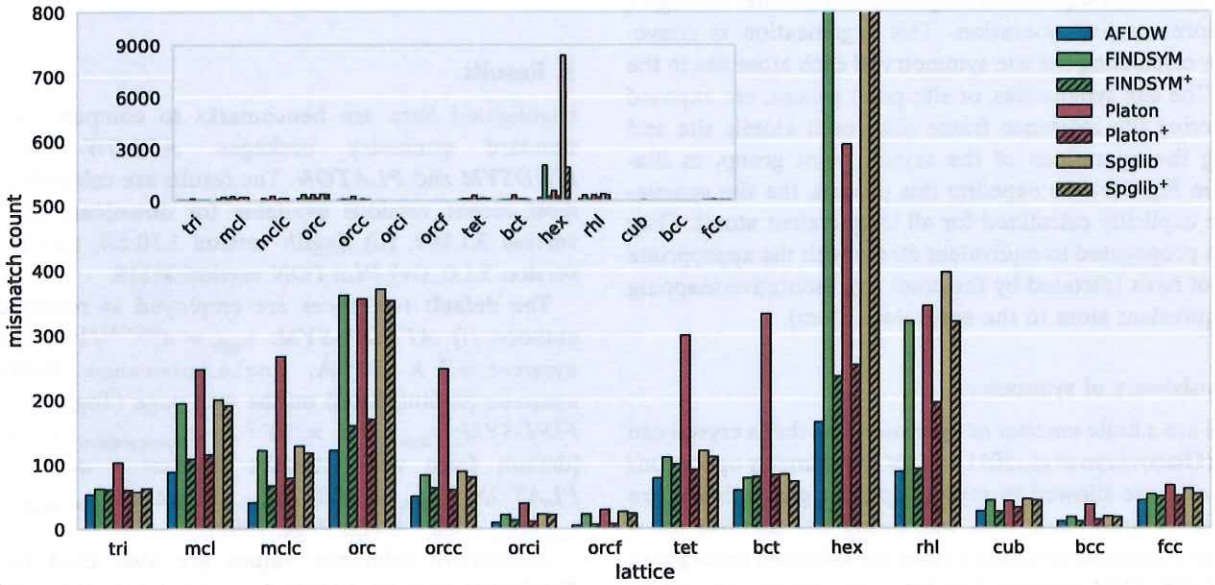

Figure 6
Breakdown of space-group mismatches with the ICSD organized by lattice type. The lattice types are derived from the space-group number reported in the ICSD. The superscript + indicates the results using the user-defined/non-default tolerance values. The lattice abbreviations are as follows: triclinic (tri), monoclinic (mcl), base-centered monoclinic (mclc), orthorhombic (orc), base-centered orthorhombic (orcc), body-centered orthorhombic (orci), face-centered orthorhombic (orcf), tetragonal (tet), body-centered tetragonal (bct), hexagonal (hex), rhombohedral (rhl), cubic (cub), body-centered cubic (bcc), and face-centered cubic (fcc).

XX66

Table 3
List of the symmetry descriptions provided by each of the four packages.

The superlattice analysis refers to the structure symmetry if each atomic site is decorated equally (same atom type), while crystal spin indicates the structure symmetry including the magnetic moment of each atom. Adding the keyword EQUAL to the *Platon* command performs a superlattice analysis.

Symmetry	*AFLOW-SYM*	*Spglib*	*FINDSYM*	*PLATON*
Lattice	√			
Superlattice	√			√ (EQUAL)
Reciprocal lattice	√			
Crystal	√	√	√	√
Crystal spin	√	√	√	

the triclinic (tri) and body-centered tetragonal (bct) systems calculated by *Spglib* and *FINDSYM*, respectively. To guarantee consistent symmetry results, users of *Spglib*, *FINDSYM* and *PLATON* should tune the tolerance for each system. The structure-specific tolerance choice and adaptive tolerance scheme incorporated into *AFLOW-SYM* allow for the automatic calculation of results that are generally consistent with experiments.

Overall, the results indicate the strength of the *AFLOW-SYM* approach. Other packages can reach similar performance to *AFLOW-SYM*, but they require continuous *ad hoc* user adjustments of tolerances, possibly producing results incommensurate with other characteristics of the systems, such as its Pearson symbol. Only the self-consistent approach of *AFLOW-SYM* is ripe for the automation required by autonomous materials design.

3.2. Symmetry characterizations and representations

Of primary concern among the various standard packages is the identification and characterization of crystal symmetry, *i.e.* a symmetry description considering the lattice and basis of atoms. In addition, *AFLOW-SYM* characterizes crystals with a sequence of symmetry-breaking features, including the lattice, superlattice (lattice with a uniform basis), crystal and crystal spin. With the progression of symmetry breaking, each characterization offers a new dimension of physical insight, and is of particular importance for understanding complex phenomena (Matano *et al.*, 2016). The suite of characterizations offered by each package is presented in Table 3.[1] With integration into the automated framework *AFLOW*, new tools and symmetry descriptions will continue to be incorporated. The forums at http://aflow.org/forum/ are the venues for presenting updates and discussing new functionalities. Anticipated future work includes going beyond translationally invariant structures and characterizing disordered/off-stoichiometric structures (Yang *et al.*, 2016; Perim *et al.*, 2016).

[1] Some packages provide more information than listed in Table 3. For example, *PLATON* presents additional useful structural/chemical information such as bonding, coordination, planes and torsions. However, the comparison presented in Table 3 is limited to symmetry information pertaining to space groups.
[2] *FINDSYM* and *PLATON* do provide the general Wyckoff position, although they do not explicitly present the symmetry operators.

Table 4
List of operation representations provided by *AFLOW-SYM* compared with *Spglib*.

The internal translations are only applicable for the coset representative of the factor-group and space-group symmetry operators. Likewise, the lattice translations are only applicable for the space-group symmetry operators.

Operator information	*AFLOW-SYM*	*Spglib*
Operator type	√	
Hermann–Mauguin	√	
Schönflies	√	
Transformation matrix (Cartesian)	√	
Transformation matrix (fractional)	√	√
Generator matrix	√	
so(3) coefficients ($\mathbf{L}_x$, $\mathbf{L}_y$, $\mathbf{L}_z$)	√	
Angle	√	
Axis	√	
Quaternion (vector)	√	
Quaternion (2 × 2 matrix)	√	
Quaternion (4 × 4 matrix)	√	
su(2) coefficients (Pauli)	√	
Inversion Boolean	√	
Internal translation (Cartesian)	√	
Internal translation (fractional)	√	√
Atom index map	√	
Atom type map	√	
Lattice translation (Cartesian)	√	
Lattice translation (fractional)	√	

Furthermore, *AFLOW-SYM* presents the symmetry operations in a wealth of representations. Both *AFLOW-SYM* and *Spglib* explicitly offer representations for the symmetry operations.[2] Table 4 compares the operation representations provided by the two packages. Both provide the unit-cell symmetry operators (coset representatives of the factor group). *AFLOW-SYM* offers the symmetry operations in the rotation-matrix (Cartesian and fractional) and axis–angle, generator and quaternion representations (Karney, 2007; Fritzer, 2001), while *Spglib* only provides the rotation-matrix representation in its fractional form. *AFLOW-SYM* also presents the corresponding mappings for each symmetry operation, almost entirely eliminating the need to reapply the operators for symmetry-reduced analyses such as calculating the force constants (Jahnátek *et al.*, 2011; Plata *et al.*, 2017). Along with the factor-group coset representatives, *AFLOW-SYM* provides the lattice point group, reciprocal-lattice point group, crystal point group, dual of the crystal point group, site point group and space-group symmetry operators. Catering to electronic structure calculations, *AFLOW-SYM* also returns additional symmetry information not explicitly provided by other routines, such as the Pearson symbol, Bravais lattice type and Bravais lattice variation, necessary for constructing the most efficient Brillouin zone (Setyawan & Curtarolo, 2010). The full set of descriptions and representations offered by *AFLOW-SYM* is detailed in Appendix *B*.

4. Using *AFLOW-SYM*

4.1. Input/output formats

AFLOW-SYM reads crystal-structure information from a geometry file containing the lattice vectors and atomic coor-

dinates (coordinate model), which is treated as the *bona fide* representation of the structure. Information can be lost during the transcription of the X-ray diffraction/reflection data to the coordinate model, resulting in a lower-symmetry profile. While a means to verify the two representations offers higher-fidelity symmetry descriptions, the diffraction data are not nearly as accessible as the coordinate-model representation. Furthermore, the geometry file is the *de facto* input format for *ab initio* packages and thus *AFLOW-SYM* resolves the material's symmetry based on this representation.

With *AFLOW-SYM* well integrated into the high-throughput *ab initio* software package *AFLOW*, it can process many standard input file types, including that of the ICSD/CSD (Bergerhoff *et al.*, 1983; Belsky *et al.*, 2002; Groom *et al.*, 2016) (CIF), *VASP* (Kresse & Hafner, 1993, 1994; Kresse & Furthmüller, 1996*a*,*b*) (POSCAR), *QUANTUMESPRESSO* (Giannozzi *et al.*, 2009), *ABINIT* (Gonze *et al.*, 2002) and *FHI-AIMS* (Blum *et al.*, 2009).

Furthermore, all symmetry functions support the JSON object output format. This allows *AFLOW-SYM* to be employed from other programming languages such as Java, Go, Ruby, Julia and Python, facilitating smooth integration into numerous applications and workflows (Supka *et al.*, 2017; Scheffler & Draxl, 2014). These functionalities can be accessed by either the command line or a Python environment. A summary of the output for each command is provided in Appendix *D*2.

4.2. Command-line options

There are three main functions that provide all symmetry information for a given input structure. These functions allow an optional tolerance value (`tol`) to be specified *via* a number or the strings 'tight' or 'loose' corresponding to $\varepsilon_{\text{tight}}$ and $\varepsilon_{\text{loose}}$, respectively. To perform the symmetry analysis of a crystal, the functions are called with the following commands.

`aflow --aflowSYM[=⟨tol⟩] [--print=txt|json] <file`: Calculates and returns the symmetry operations for the lattice point group, reciprocal-lattice point group, coset representatives of the factor group, crystal point group, dual of the crystal point group, site symmetry and space group. It also returns the unique and equivalent sets of atoms.

`aflow --edata[=⟨tol⟩] [--print=txt|json] <file`: Calculates and returns the extended crystallographic symmetry data (crystal, lattice, reciprocal lattice and superlattice symmetry), while incorporating the full set of checks [§2.6, (i)–(vi)] for robust symmetry determination.

`aflow --sgdata[=⟨tol⟩] [--print=txt|json] <file`: Calculates and returns the space-group symmetry of the crystal, while only validating that the symmetry descriptions match with the ITC conventions [§2.6, (vi)].

Square brackets [...] indicate optional arguments. The `--print` flag specifies the output format. The `--aflowSYM` function stores the isometries of the different symmetry groups to their own files `aflow.⟨group⟩.out` or `aflow.⟨group⟩.json`. The ⟨group⟩ labels are as follows: `pgroup` (lattice point group), `pgroupk` (reciprocal-lattice point group), `fgroup` (coset representatives of the factor group), `pgroup_xtal` (crystal point group), `pgroupk_xtal` (dual of the crystal point group), `agroup` (site symmetry) and `sgroup` (space group).

```
from aflow_sym import Symmetry
from pprint import pprint

with open('test.poscar', 'r') as input_file:
  sym = Symmetry(aflow_executable='./aflow')
  output = sym.get_edata(input_file)
  pprint(output)
```

Figure 7
An example Python script that leverages the *AFLOW-SYM* Python module to return a dictionary containing the relevant symmetry information. The optional tolerance (`tol`) and magnetic moment (`magmoms`) arguments can be specified with each method. A copy of this script is available for download in the supporting information.

Crystal spin symmetry functionality is also available in *AFLOW-SYM*. The magnetic moment of each site (collinear or non-collinear) can be specified for each of the commands listed above by adding the magnetic moment flag: [`--magmom=m1,m2,...|INCAR|OUTCAR`]. The magnetic moment information can be specified in three formats: (i) explicitly *via* $m_1, m_2, \ldots, m_n$ in the same order as the input file (or $m_{1,x}, m_{1,y}, m_{1,z}, m_{2,x}, \ldots, m_{n,z}$ for non-collinear), (ii) read from the *VASP INCAR* or (iii) the *VASP OUTCAR*. Magnetic moment readers for other *ab initio* codes will be added in later versions.

4.3. Python environment

Given the recent prevalence of Python programming, we offer a module that employs *AFLOW-SYM* within a Python environment (see Appendix *D*1). It connects to a local *AFLOW* installation and imports the *AFLOW-SYM* results into a `Symmetry` class. A `Symmetry` object is initialized with the code shown in Fig. 7.

By default, the `Symmetry` object searches for an *AFLOW* executable in the `PATH`. However, the location of an *AFLOW* executable can be specified as follows:

```
Symmetry(aflow_executable = 'your_executable').
```

The symmetry object has three built-in methods, which correspond to the command-line calls mentioned previously:

```
get_symmetry(input_file, tol, magmoms)
get_edata(input_file, tol, magmoms)
get_sgdata(input_file, tol, magmoms)
```

Each method requires a Python file handler (`input_file`), while the tolerance (`tol`) and magnetic moments of each site (`magmoms`) are optional arguments.

4.4. *AFLOW-SYM* support

Functionality requests and bug reports should be posted on the *AFLOW* forum http://aflow.org/forum/ under the board 'Symmetry analysis'.

XX68

5. Conclusion

In this article, we present *AFLOW-SYM*, a symmetry platform catered to, but not limited to, high-throughput frameworks.

We address problems stemming from numerical tolerance in symmetry analyses by using a mapping procedure uniquely designed to handle skewed cells and an advanced adaptive tolerance scheme. *AFLOW-SYM* also includes consistency checks of calculated isometries with respect to symmetry principles. These solutions are validated against the experimental data for structures reported by the ICSD. Comparison with other symmetry-analysis suites, *Spglib*, *FINDSYM* and *PLATON*, shows that *AFLOW-SYM* is the most consistent with the ICSD.

For general use of *AFLOW-SYM*, the routines include both a standard text output and a JSON output for easy integration into other computational workflows. Lastly, a comprehensive list of the symmetry descriptions is presented (see Appendix *D*2), illustrating the vast amount of symmetry information available to users of *AFLOW-SYM*.

APPENDIX *A*
Crystallographic symmetry

A1. Mathematical group

A group is an abstract mathematical structure comprised of a set of elements (g) and an operation that combines two elements to form a third (Tinkham, 1964). There are four axioms that a group satisfies:

(1) Closure: the combination of two elements with the operator yields an element that exists in the set; it does not create a new element outside the set.

(2) Associativity: the order of combining elements with the operator is inconsequential given the sequence of operands is unaltered.

(3) Identity: there exists a neutral element (I) that when combined with another element leaves that element unchanged ($gI = g$).

(4) Inverse: for each element g in the set, there exists a corresponding inverse element g^{-1} such that $gg^{-1} = I$.

An abelian group includes the additional axiom of commutativity. These rules are the foundation of group theory and underline the construction of the different symmetry groups.

A2. Point group

A point group is a set of symmetry transformations about a fixed point $\{\mathbf{U}_1, \mathbf{U}_2, \ldots, \mathbf{U}_n\}$ that leave a system invariant.[3] The elements of the group are classified as (i) n-fold rotations, where n describes the rotation order (*i.e.* the number of symmetric points it generates), (ii) inversions and (iii) roto-inversions, which are compound operations comprised of a rotation and inversion. Three-dimensional crystals are confined to one of 32 point groups owing to the crystallographic restriction theorem, which limits the rotation order in a periodic system to two-, three-, four- and sixfold (Hahn, 2002). The 32 crystallographic point groups are categorized into one of seven crystal systems: cubic, hexagonal, trigonal, tetragonal, orthorhombic, monoclinic and triclinic. The classifications are based on the lattice parameters ($a, b, c, \alpha, \beta, \gamma$) of the crystal.

Cubic: $a = b = c, \alpha = \beta = \gamma = 90°$.
Hexagonal/trigonal: $a = b \neq c, \alpha = \beta = 90°, \gamma = 120°$.
Tetragonal: $a = b \neq c, \ \alpha = \beta = \gamma = 90°$.
Orthorhombic: $a \neq b \neq c, \alpha = \beta = \gamma = 90°$.
Monoclinic: $a \neq b \neq c, \alpha = \gamma = 90°, \beta \neq 90°$.
Triclinic: $a \neq b \neq c, \alpha \neq \beta \neq \gamma \neq 90°$.

In crystallography, two types of point groups are of particular importance: the lattice and crystal (vector) point group. Each operates in a different space: the lattice point group characterizes the symmetry of the lattice points (an affine space), while the crystal point group additionally considers the atomic basis and acts on the underlying vector space of the crystal face normals. Fundamentally, the vector space captures the symmetry of the macroscopic crystal (Hahn, 2002). The crystal point-group operations are defined as the linear mappings of the vector space, *i.e.* the unique set of fixed-point transformations of the factor group[4] (Hahn, 2002; Nespolo & Souvignier, 2009). Owing to symmetry breaking from the atomic basis, the cardinality of the crystal point group is at most as large as that of the lattice. Furthermore, the dual (reciprocal) counterparts of the lattice and crystal point group play an important role in electronic structure theory: resolving the symmetries of the Brillouin and irreducible Brillouin zones, respectively. In *AFLOW-SYM*, the output for the lattice, reciprocal lattice, crystal and dual of the crystal point-group operations are labeled `pgroup`, `pgroupk`, `pgroup_xtal` and `pgroupk_xtal`, respectively.

A3. Space group

In periodic systems, translational symmetry gives rise to another mathematical group: the space group. Its elements are comprised of those found in the point group, along with glide (mirror and translation) and screw (rotation and translation) operations. The translational degree of freedom extends the number of unique sets of symmetry operations to 230. The translations of a crystal are divided into lattice translations ($\mathbf{T}$) and internal translations ($\mathbf{t}$):

$$\{\mathbf{U}_1, \mathbf{U}_2, \ldots, \mathbf{U}_n|\mathbf{T} + \mathbf{t}\}. \tag{17}$$

Subsequently, a space group describes the full symmetry of a periodic system. The space-group operations are labeled `sgroup` in *AFLOW-SYM*.

[3] Here, the rotation matrix $\mathbf{U}$ is used to represent the different symmetry groups; however, rotation elements can also be described in axis–angle, matrix-generator and quaternion form.

[4] Without the relevant internal translations (complete coset representatives), the crystal point-group operations do not generally apply in the affine point space (lattice points and atoms), as is the case for non-symmorphic space groups. Conversely, the set of operations that do apply in the point space define the site symmetries.

XX69

A4. Factor group

From the space group, the elements of the factor group are defined as the cosets of the subgroup of lattice translations (**T**):

$$\{\mathbf{I}|\mathbf{0}\}\{\mathbf{I}|\mathbf{T}\}, \{\mathbf{U}_i|\mathbf{t}_i\}\{\mathbf{I}|\mathbf{T}\}, \{\mathbf{U}_j|\mathbf{t}_j\}\{\mathbf{I}, \mathbf{T}\}, \ldots, \quad (18)$$

where $\mathbf{U}_i$ are the point-group operations, $\mathbf{t}_i$ are the associated internal translations and $\boldsymbol{I}$ is the identity. The unit-cell symmetry is exposed *via* the coset representatives:

$$\{\mathbf{I}|\mathbf{0}\}, \{\mathbf{U}_i|\mathbf{t}_i\}, \{\mathbf{U}_j|\mathbf{t}_j\}, \ldots. \quad (19)$$

The coset representatives themselves do not necessarily form a mathematical group, since they violate the closure condition. Repeated application of an internal translation will eventually traverse beyond the unit cell. The unit-cell symmetry elements (coset representatives) are labeled `fgroup` in *AFLOW-SYM*.

In general, there exists a homomorphism between the factor group and the crystal point group, *i.e.* the factor group cardinality is an integer multiple of the crystal point-group cardinality. The multiplicative factor (m) is dictated by the number of internal translations in the system. A crystal in a primitive representation exhibits an isomorphic correspondence ($m = 1$), while non-primitive representations possess the general homomorphic relationship ($m > 1$).

A5. Site point group

The site point group – or site symmetry – describes the point-group symmetry centered on a single site in the crystal, revealing the local symmetry environment. The analysis is performed on each atomic site in the crystal, with symmetry-equivalent atoms (Wyckoff positions) exhibiting the same point-group symmetries. The origin of the fixed-point operations differentiates the site symmetry from the lattice/crystal point group, which are centered on the unit-cell origin. In the finite-difference method for calculating phonons, the unique distortions for a given atomic site are resolved with its site symmetry (Jahnátek *et al.*, 2011; Plata *et al.*, 2017). In *AFLOW-SYM*, the site-symmetry elements are designated by `agroup` ('atomic site group').

A6. Crystal spin symmetry

Introducing the spin degree of freedom can break crystal symmetry. *AFLOW-SYM* includes functionality for a crystal spin (lattice, atoms and spin) description, including the relevant point-group, factor-group, space-group and site-symmetry operations. For magnetic systems, these are the symmetry descriptions employed by *ab initio* packages, such as *VASP* (Kresse & Hafner, 1993, 1994; Kresse & Furthmüller, 1996*a*,*b*). Note that the crystal spin symmetry differs from the magnetic symmetry, which accounts for time-reversal symmetry (spin flips). The magnetic symmetry will be incorporated into *AFLOW-SYM* in a later version.

APPENDIX *B*
Mathematical representation of symmetry

Symmetry elements are characterized into three types of transformation: translation, fixed-point and fixed-point-free (a combination of the two, *i.e.* screw and glide operations) (Hahn, 2002). Translations are generally indicated by 3×1 vectors:

$$\mathbf{t} = \begin{pmatrix} t_1 \\ t_2 \\ t_3 \end{pmatrix}. \quad (20)$$

Fixed-point symmetries O(3) describing rotations, inversions and roto-inversions are represented by rotation matrices. The rotation symmetries SO(3), *i.e.* a subgroup of the orthogonal group O(3), can be represented in three additional forms: axis–angle, matrix-generator and quaternions. *AFLOW-SYM* provides the symmetry operations for rotations in each of these four forms, which are discrete subgroups of the continuous SO(3) group.

B1. Rotation matrix

A rotation matrix describes a transformation between two reference frames. In three dimensions, the symmetry operators are 3×3 square matrices with the following form:

$$\mathbf{U} = \begin{pmatrix} u_{11} & u_{12} & u_{13} \\ u_{21} & u_{22} & u_{23} \\ u_{31} & u_{32} & u_{33} \end{pmatrix}. \quad (21)$$

All transformations are unitary (norm-preserving) and therefore have $\det(\mathbf{U}) = \pm 1$. The matrix representation affords fast computation through use of optimized linear algebra computational packages.

B2. Axis–angle

Rotation operations are also characterized by their axis and angle of rotation. The axis, $\hat{\mathbf{r}} = (r_1, r_2, r_3)$, indicates the direction of the rotation operator, pointing perpendicular to the fixed-point motion. The angle, θ, specifies the magnitude of the rotational motion (following the right-hand rule). The angle and axis components are related to the matrix elements of **U** by

$$\begin{aligned} \theta &= \cos^{-1}\left(\frac{\mathrm{Tr}(\mathbf{U}) - 1}{2}\right), \\ r_d &= [(u_{32} - u_{23})^2 + (u_{13} - u_{31})^2 + (u_{21} - u_{12})^2]^{1/2}, \\ r_1 &= \frac{u_{32} - u_{23}}{r_d}, r_2 = \frac{u_{13} - u_{31}}{r_d}, r_3 = \frac{u_{21} - u_{12}}{r_d}, \end{aligned} \quad (22)$$

where $\mathrm{Tr}(\mathbf{U})$ is the trace of **U**. The axis–angle representation is directly applied to a point **p** *via* Rodrigues' rotation formula

$$\mathbf{p}_{\mathrm{rot}} = \mathbf{p}\cos\theta + (\hat{\mathbf{r}} \times \mathbf{p})\sin\theta + \hat{\mathbf{r}}(\hat{\mathbf{r}} \cdot \mathbf{p})(1 - \cos\theta), \quad (23)$$

where $\mathbf{p}_{\mathrm{rot}}$ is the rotated point. This description highlights the operation order n *via* $n = 360°/\theta$ and identifies the conventional cell lattice vectors, since they are parallel to certain symmetry axes.

XX76

B3. Matrix generator

The Lie group SO(3) grants the use of the corresponding Lie algebra so(3), which are comprised of the infinitesimal matrix generators **G**. The generator is a skew-symmetric matrix that describes the rotation about a symmetry axis, with the following form:

$$\mathbf{G} = \begin{pmatrix} 0 & -r_3 & r_2 \\ r_3 & 0 & -r_1 \\ -r_2 & r_1 & 0 \end{pmatrix}, \tag{24}$$

where r_1, r_2, r_3 are the components of the symmetry unit axis $\hat{\mathbf{r}}$. The identity and inverse elements have no axis; therefore, the generator is not defined and is returned as a zero matrix. While the rotation matrix transforms one reference frame to another, the generator operates about a single axis. The matrix exponential of the generator with the angle maps the operations into the rotation matrix form $[\mathbf{U} = \exp(\theta\mathbf{G})]$. For convenience, *AFLOW-SYM* returns the generator multiplied with the angle $\mathbf{A} = \theta\mathbf{G}$. *AFLOW-SYM* also provides the expansion coefficients of the generator matrix onto the following so(3) basis:

$$\mathbf{G} = x\mathbf{L}_x + y\mathbf{L}_y + z\mathbf{L}_z \tag{25}$$

where

$$\mathbf{L}_x = \begin{pmatrix} 0 & 0 & 0 \\ 0 & 0 & -1 \\ 0 & 1 & 0 \end{pmatrix}, \mathbf{L}_y = \begin{pmatrix} 0 & 0 & 1 \\ 0 & 0 & 0 \\ -1 & 0 & 0 \end{pmatrix}$$
$$\mathbf{L}_z = \begin{pmatrix} 0 & -1 & 0 \\ 1 & 0 & 0 \\ 0 & 0 & 0 \end{pmatrix}. \tag{26}$$

The expansion coefficients x, y and z of this basis set are the unit axis components r_1, r_2 and r_3, respectively.

B4. Quaternion

A quaternion is a mathematical representation of three-dimensional space with both real and imaginary components. Though developed in 1843, the quaternion has only recently gained relevance through the field of computer graphics and modeling. As opposed to using a nine-element 3 × 3 matrix to represent a rotation in space, quaternions have a concise format consisting of four components. The reduced element count increases computational efficiency and thus is particularly suitable for high-throughput frameworks.

Given an axis and angle, the corresponding quaternion representation, $\mathbf{q} = (q_0, q_1, q_2, q_3)$, is

$$\begin{aligned} q_0 &= \cos(\theta/2), \\ q_1 &= r_1 \sin(\theta/2), \\ q_2 &= r_2 \sin(\theta/2), \\ q_3 &= r_3 \sin(\theta/2), \end{aligned} \tag{27}$$

which are equivalent to the Euler parameters. Alternate forms of the quaternion are 2 × 2 and 4 × 4 matrices. The complex 2 × 2 unitary matrix of a quaternion is

$$\mathbf{C} = \begin{pmatrix} q_0 + q_3 i & q_2 + q_1 i \\ -q_2 + q_1 i & q_0 - q_3 i \end{pmatrix}, \tag{28}$$

which is an element of the SU(2) Lie group. The **C** matrix can be expanded onto a basis formed by the Pauli matrices:

$$\boldsymbol{\sigma}_1 = \begin{pmatrix} 0 & 1 \\ 1 & 0 \end{pmatrix}, \boldsymbol{\sigma}_2 = \begin{pmatrix} 0 & -i \\ i & 0 \end{pmatrix}, \boldsymbol{\sigma}_3 = \begin{pmatrix} 1 & 0 \\ 0 & -1 \end{pmatrix}, \tag{29}$$

where multiplying by i $(= \sqrt{-1})$ yields the following decomposition:

$$\mathbf{C} = q_0\mathbf{I} + q_1 i\boldsymbol{\sigma}_1 + q_2 i\boldsymbol{\sigma}_2 + q_3 i\boldsymbol{\sigma}_3. \tag{30}$$

The corresponding Lie algebra, su(2), is (Gilmore, 2008)

$$\mathbf{g} = \frac{i}{2}\begin{pmatrix} r_3 & r_1 - r_2 i \\ r_1 + r_2 i & -r_3 \end{pmatrix}. \tag{31}$$

AFLOW-SYM lists the su(2) generator coefficients expanded on the Pauli matrices

$$\mathbf{g} = x\boldsymbol{\sigma}_1 + y\boldsymbol{\sigma}_2 + z\boldsymbol{\sigma}_3, \tag{32}$$

where the expansion coefficients x, y and z are $(i/2)r_1$, $(i/2)r_2$ and $(i/2)r_3$, respectively. Similar to the SO(3) rotations, the matrix exponential of the su(2) generator **g** with the angle maps the operations into the complex 2 × 2 SU(2) matrix $[\mathbf{C} = \exp(\theta\mathbf{g})]$. The 4 × 4 matrix representation of the quaternion is

$$\mathbf{Q} = \begin{pmatrix} q_0 & q_1 & q_2 & q_3 \\ -q_1 & q_0 & -q_3 & q_2 \\ -q_2 & q_3 & q_0 & -q_1 \\ -q_3 & -q_2 & q_1 & q_0 \end{pmatrix}, \tag{33}$$

which includes all four components of the quaternion vector in a matrix, allowing transformations to be performed through matrix multiplication rather than quaternion algebra. This method is useful for performing operations with other transformations in matrix or vector form, whereas the quaternion vector notation has its own algebra similar to the operations between complex numbers with an additional scalar component (q_0).

B5. Basis transformations of operators

The representations of the symmetry operations are basis dependent and are customarily given with respect to Cartesian or fractional coordinates systems. It is straightforward to transform symmetry operations between these vector spaces *via* a basis change. In matrix notation, the fixed-point operation in Cartesian $(\mathbf{U}_c)$ and fractional $(\mathbf{U}_f)$ coordinates are related *via* the following similarity transformations:

$$\begin{aligned} \mathbf{U}_f &= \mathbf{L}^{-1}\mathbf{U}_c\mathbf{L}, \\ \mathbf{U}_c &= \mathbf{L}\mathbf{U}_f\mathbf{L}^{-1}. \end{aligned} \tag{34}$$

Here, **L** is the column-space form of the lattice vectors:

$$\mathbf{L} = (\mathbf{a} \quad \mathbf{b} \quad \mathbf{c}) = \begin{pmatrix} a_1 & b_1 & c_1 \\ a_2 & b_2 & c_2 \\ a_3 & b_3 & c_3 \end{pmatrix}, \tag{35}$$

XX71

where a_i, b_i and c_i are the corresponding components of the lattice vectors. A translation vector $\mathbf{t}_{c(f)}$ is transformed between Cartesian and fractional coordinates by $\mathbf{t}_f = \mathbf{L}^{-1}\mathbf{t}_c$ and $\mathbf{t}_c = \mathbf{L}\mathbf{t}_f$.

B6. Example representations

An example of a threefold rotation in Cartesian coordinates is shown below in its rotation matrix, axis–angle, matrix-generator, and quaternion vector and matrix representations.

$$\mathbf{U}_{3-\text{fold}} = \begin{pmatrix} 0 & -1 & 0 \\ 0 & 0 & -1 \\ 1 & 0 & 0 \end{pmatrix}$$

$$\hat{\mathbf{r}} = (0.57735, -0.57735, 0.57735)$$

$$\theta = 120^\circ$$

$$\mathbf{A} = \begin{pmatrix} 0.0 & -1.2092 & -1.2092 \\ 1.2092 & 0.0 & -1.2092 \\ 1.2092 & 1.2092 & 0.0 \end{pmatrix}$$

$$\mathbf{q} = (0.5, 0.5, -0.5, 0.5)$$

$$\mathbf{C} = \begin{pmatrix} 0.5 + 0.5i & -0.5 + 0.5i \\ 0.5 + 0.5i & 0.5 - 0.5i \end{pmatrix}$$

$$\mathbf{Q} = \begin{pmatrix} 0.5 & 0.5 & -0.5 & 0.5 \\ -0.5 & 0.5 & -0.5 & -0.5 \\ 0.5 & 0.5 & 0.5 & -0.5 \\ -0.5 & 0.5 & 0.5 & 0.5 \end{pmatrix}.$$

APPENDIX C
Extreme cases of minimal-distance discrepancy between Cartesian and fractional spaces

The bring-in-cell procedure applied to a crystal with lattice parameters $a = b = c = 5$ Å, $\alpha = \gamma = 90°$ and $\beta = 60°$ identifies the minimum distance between the fractional coordinates $(0, 0, 1/2)$ and $(1/2, 0, 0)$ to be $||\widetilde{\mathbf{d}}_c^{\min}|| = 4.3301$ Å, compared with the true minimum of $||\mathbf{d}_c^{\min}|| = 2.5$ Å. A more extreme mismatch occurs if $\beta = 5°$, yielding a minimum of $||\widetilde{\mathbf{d}}_c^{\min}|| = 4.9952$ Å with the bring-in-cell method, differing significantly from the true minimum of $||\mathbf{d}_c^{\min}|| = 0.2181$ Å. Applying the heuristic threshold to the aforementioned skewed examples give bounds of $\varepsilon_{\max} = 1.2130$ Å (with $d_c^{\text{nn(min)}} = 2.4259$ Å) and $\varepsilon_{\max} = 0.0017$ Å (with $d_c^{\text{nn(min)}} = 0.4362$ Å) for $\beta = 60°$ and $\beta = 5°$, respectively. Both thresholds are sufficiently below the true minimum distances – even in the worst cases – validating our choice of the heuristic threshold.

APPENDIX D
AFLOW-SYM details

D1. Python module

The module to run the *AFLOW-SYM* commands referenced in §4.3 is provided in Fig. 8.

D2. Output list

This section details the output fields for the symmetry-group operations, extended crystallographic data (`edata`) and space-group data (`sgdata`) routines. The lists describe the keywords as they appear in the JSON format. Similar keywords are used for the standard text output.

Symmetry operations output

`pgroup`
– *Description*: lattice point-group symmetry operations.
– *Type*: `array of symmetry operator objects`

`pgroupk`
– *Description*: reciprocal-lattice point-group symmetry operations.
– *Type*: `array of symmetry operator objects`

`fgroup`
– *Description*: coset representative of factor-group symmetry operations.
– *Type*: `array of symmetry operator objects`

`pgroup_xtal`
– *Description*: crystal point-group symmetry operations.
– *Type*: `array of symmetry operator objects`

`pgroupk_xtal`
– *Description*: dual of the crystal point-group symmetry operations.
– *Type*: `array of symmetry operator objects`

`sgroup`
– *Description*: space-group symmetry operations out to a given radius.
– *Type*: `array of symmetry operator objects`

`iatoms`
– *Description*: groupings of symmetry-equivalent/unique atoms.
– *Type*: `iatom object`

`agroup`
– *Description*: site- (atom-) symmetry operations (point group).
– *Type*: `array of symmetry operator objects`

Each symmetry group contains an array of symmetry objects, including the operation representations listed in Table 4. The `symmetryoperator` object contains the following:

`Hermann_Mauguin`
– *Description*: Hermann–Mauguin symbol of the symmetry operation.
– *Type*: `string`

`Schoenflies`
– *Description*: Schönflies symbol of the symmetry operation.
– *Type*: `string`

`Uc`
– *Description*: transformation matrix with respect to Cartesian coordinates.
– *Type*: 3 × 3 `array`

```
import json
import subprocess
import os

class Symmetry:

    def __init__(self, aflow_executable='aflow'):

        self.aflow_executable = aflow_executable

    def aflow_command(self, cmd):
        try:
            return subprocess.check_output(
                    self.aflow_executable + cmd,
                    shell=True
                )
        except subprocess.CalledProcessError:
            print "Error aflow executable not found
                ↪ at: " + self.aflow_executable

    def get_symmetry(self, input_file, tol=None,
        ↪ magmoms=None):
        fpath = os.path.realpath(input_file.name)
        command = ' --aflowSYM'
        output = ''

        if tol:
            command += '=' + str(tol)
        if magmoms:
            command += ' --magmom=' + magmoms

        output = self.aflow_command(
            command + ' --print=json --screen_only'
                ↪ + ' < ' + fpath
        )
        res_json = json.loads(output)
        return res_json

    def get_edata(self, input_file, tol=None,
        ↪ magmoms=None):
        fpath = os.path.realpath(input_file.name)
        command = ' --edata'
        output = ''

        if tol:
            command += '=' + str(tol)
        if magmoms:
            command += ' --magmom=' + magmoms

        output = self.aflow_command(
            command + ' --print=json' + ' < ' +
                ↪ fpath
        )
        res_json = json.loads(output)
        return res_json

    def get_sgdata(self, input_file, tol=None,
        ↪ magmoms=None):
        fpath = os.path.realpath(input_file.name)
        command = ' --sgdata'
        output = ''

        if tol:
            command += '=' + str(tol)
        if magmoms:
            command += ' --magmom=' + magmoms

        output = self.aflow_command(
            command + ' --print=json' + ' < ' +
                ↪ fpath
        )
        res_json = json.loads(output)
        return res_json
```

Figure 8
The *AFLOW-SYM* Python module. It includes three symmetry methods (`get_symmetry`, `get_edata` and `get_sgdata`). Each method calls the local *AFLOW* executable to perform the corresponding symmetry analysis and returns the output to a Python dictionary. A copy of this module is available for download in the supporting information.

`Uf`
– *Description*: transformation matrix with respect to fractional coordinates.
– *Type*: 3 × 3 `array`

`angle`
– *Description*: angle corresponding to symmetry operation.
– *Type*: `float`

`axis`
– *Description*: axis of symmetry operation.
– *Type*: 3 × 1 `array`

`generator`
– *Description*: matrix generator of symmetry operation.
– *Type*: 3 × 3 `array`

`generator_coefficients`
– *Description*: matrix-generator expansion coefficients onto $\mathbf{L}_x$, $\mathbf{L}_y$ and $\mathbf{L}_z$ basis.
– *Type*: 3 × 1 `array`

`group`
– *Description*: specifies the group type (`pgroup`, `pgroupk`, `fgroup`, `pgroup_xtal`, `pgroupk_xtal`, `sgroup` and `agroup`).
– *Type*: `string`

XX73

`inversion`
– *Description*: indicates if inversion exists.
– *Type*: `bool`

`quaternion_matrix`
– *Description*: quaternion matrix.
– *Type*: 4 × 4 `array`

`SU2_matrix`
– *Description*: complex quaternion matrix; element of SU(2).
– *Type*: 2 × 2 `array`

`su2_coefficients`
– *Description*: su(2) generator coefficients onto Pauli matrices (σ_1, σ_2 and σ_3).
– *Type*: 3 × 1 `array`

`quaternion_vector`
– *Description*: quaternion vector.
– *Type*: 4 × 1 `array`

`type`
– *Description*: point-group operation type (unity, rotation, inversion or roto-inversion).
– *Type*: `string`

`ctau`
– *Description*: internal translation component in Cartesian coordinates (`fgroup` and `sgroup` only).
– *Type*: 3 × 1 `array`

`ftau`
– *Description*: internal translation component in fractional coordinates (`fgroup` and `sgroup` only).
– *Type*: 3 × 1 `array`

`ctrasl`
– *Description*: lattice translation component in Cartesian coordinates (`sgroup` only).
– *Type*: 3 × 1 `array`

`ftrasl`
– *Description*: lattice translation component in fractional coordinates (`sgroup` only).
– *Type*: 3 × 1 `array`

The `iatom` object contains:
`inequivalent_atoms`
– *Description*: symmetry-distinct atom indices.
– *Type*: `array`

`equivalent_atoms`
– *Description*: groupings of symmetry-equivalent atom indices.
– *Type*: `2Darray`

edata output

`lattice_parameters`
– *Description*: lattice parameters in units of ångstroms and degrees ($a, b, c, \alpha, \beta, \gamma$).
– *Type*: 6 × 1 array
– *Similar to*:
FINDSYM: `Lattice parameters, a, b, c, alpha, beta, gamma`:
PLATON: first six fields in the line containing `CELL`

`lattice_parameters_Bohr_deg`
– *Description*: lattice parameters in units of Bohr and degrees ($a, b, c, \alpha, \beta, \gamma$).
– *Type*: 6 × 1 array

`volume`
– *Description*: real-space cell volume.
– *Type*: `float`
– *Similar to*:
PLATON: last field in the line containing `CELL`.

`c_over_a`
– *Description*: ratio of c and a lattice parameters.
– *Type*: `float`

`Bravais_lattice_type`
– *Description*: Bravais lattice of the crystal (FCC, BCC, CUB, HEX, RHL *etc.*).
– *Type*: `string`

`Bravais_lattice_variation_type`
– *Description*: lattice variation type of the crystal in the *AFLOW* standard (Setyawan & Curtarolo, 2010).
– *Type*: `string`

`Bravais_lattice_system`
– *Description*: Bravais lattice of the crystal.
– *Type*: `string`
– *Similar to*:
PLATON: `CrystalSystem` column in `Cell Lattice` table.

`Pearson_symbol`
– *Description*: Pearson symbol of the crystal.
– *Type*: `string`

`crystal_family`
– *Description*: crystal family.
– *Type*: `string`

`crystal_system`
– *Description*: crystal system.
– *Type*: `string`

`point_group_Hermann_Mauguin`
– *Description*: Hermann–Mauguin symbol corresponding to the point group of the crystal.
– *Type*: `string`
– *Similar to*:
Spglib: `SpglibDataset.pointgroup_symbol`.

`point_group_Schoenflies`
– *Description*: Schönflies symbol for the point group of the crystal.
– *Type*: `string`

`point_group_orbifold`
– *Description*: orbifold of the point group.
– *Type*: `string`

`point_group_type`
– *Description*: point-group type of the crystal.
– *Type*: `string`

`point_group_order`
– *Description*: number of point-group operations describing the crystal.
– *Type*: `int`

XX74

point_group_structure
– *Description*: point-group structure of the crystal.
– *Type*: string

Laue
– *Description*: Laue symbol of the crystal.
– *Type*: string
– *Similar to*:
PLATON: field after the line containing Laue.

crystal_class
– *Description*: crystal class.
– *Type*: string

space_group_number
– *Description*: space-group number.
– *Type*: int
– *Similar to*:
Spglib: SpglibDataset.spacegroup_number.
FINDSYM: field after line containing _symmetry_Int_Tables_number.
PLATON: field after line containing No (number).

space_group_Hermann_Mauguin
– *Description*: Hermann–Mauguin space-group label.
– *Type*: string
– *Similar to*:
Spglib: SpglibDataset.International_symbol.
FINDSYM: field after line containing _symmetry_space_group_name_H–M.
PLATON: field after line containing Space Group H–M.

space_group_Hall
– *Description*: Hall space-group label.
– *Type*: string
– *Similar to*:
Spglib: SpglibDataset.hall_symbol.
FINDSYM: field after line containing _space_group.reference_setting
PLATON: field after line containing Space group – Hall.

space_group_Schoenflies
– *Description*: Schönflies space-group label.
– *Type*: string
– *Similar to*:
Spglib: Spg_get_schoenflies.
FINDSYM: second field after line containing Space Group.
PLATON: field after line containing Schoenflies.

setting_ITC
– *Description*: ITC setting of conventional cell (*AFLOW-SYM* defaults to the first setting that appears in ITC and the hexagonal setting for rhombohedral systems).
– *Type*: int
– *Similar to*:
Spglib: SpglibDataset.choice.

origin_ITC
– *Description*: corresponding origin shift of the crystal to align with the ITC representation.
– *Type*: 3 × 1 array
– *Similar to*:
Spglib: SpglibDataset.choice.
FINDSYM: field after line containing Origin at.
PLATON: field after line containing Origin Shifted to.

general_position_ITC
– *Description*: general Wyckoff position (x, y, z) as indicated by ITC.
– *Type*: 2D array
– *Similar to*:
FINDSYM: field after line containing _space_group_symop_operation_xyz.
PLATON: in the Symmetry Operation(s) table.

Wyckoff_positions
– *Description*: indicates the Wyckoff letter, multiplicity, site symmetry, position (3 × 1 array) and atom name.
– *Type*: array of objects
– *Similar to*:
Spglib: get_symmetry_dataset.wyckoffs (letters only).
FINDSYM: in the loop with _atom prefix.

Bravais_lattice_lattice_type
– *Description*: Bravais lattice of the lattice.
– *Type*: string

Bravais_lattice_lattice_variation_type
– *Description*: lattice variation type of the lattice in the *AFLOW* standard (Setyawan & Curtarolo, 2010).
– *Type*: string

Bravais_lattice_lattice_system
– *Description*: Bravais lattice system of the lattice.
– *Type*: string

Bravais_superlattice_lattice_type
– *Description*: Bravais lattice of the superlattice.
– *Type*: string

Bravais_superlattice_lattice_variation_type
– *Description*: lattice variation type of the superlattice in the *AFLOW* standard (Setyawan & Curtarolo, 2010).
– *Type*: string

Bravais_superlattice_lattice_system
– *Description*: Bravais lattice system of the superlattice.
– *Type*: string

Pearson_symbol_superlattice
– *Description*: Pearson symbol of the superlattice.
– *Type*: string

reciprocal_lattice_vectors
– *Description*: reciprocal-lattice vectors.
– *Type*: 3 × 3 array

reciprocal_lattice_parameters
– *Description*: reciprocal-lattice parameters $(a, b, c, \alpha, \beta, \gamma)$.
– *Type*: 6 × 1 array

reciprocal_volume
– *Description*: reciprocal-cell volume.
– *Type*: float

XX75

reciprocal_lattice_type
– *Description*: Bravais lattice of the reciprocal lattice (FCC, BCC, CUB, HEX, RHL *etc.*).
– *Type*: string

reciprocal_lattice_variation_type
– *Description*: lattice variation type of the reciprocal lattice in the *AFLOW* standard (Setyawan & Curtarolo, 2010).
– *Type*: string

reciprocal_lattice_system
– *Description*: lattice system of the reciprocal lattice.
– *Type*: string

standard_primitive_structure
– *Description*: *AFLOW* standard primitive crystal structure representation.
– *Type*: structure object

standard_conventional_structure
– *Description*: *AFLOW* standard conventional crystal structure representation.
– *Type*: structure object

wyccar
– *Description*: ITC conventional crystal structure representation.
– *Type*: structure object
– *Similar to*:
Spglib: Spg_standardize_cell(to_primitive=0).
FINDSYM: after Space Group line.

The structure object lists the following information regarding the crystal structure:

title
– *Description*: geometry file title.
– *Type*: string

scale
– *Description*: scaling factor of lattice vectors.
– *Type*: float

lattice
– *Description*: row-space representation of lattice vectors (**a**, **b**, **c**).
– *Type*: 3 × 3 array floats

species
– *Description*: list of atomic species in crystal.
– *Type*: array of strings

number_each_type
– *Description*: number of atoms for each distinct atomic species.
– *Type*: array of ints

coordinates_type
– *Description*: indicates the coordinate representation ('Cartesian' or 'direct').
– *Type*: string

atoms
– *Description*: atom information.
– *Type*: array of atom objects

where the atom object contains

name
– *Description*: atomic species name.
– *Type*: string

occupancy
– *Description*: site occupancy.
– *Type*: float

position
– *Description*: Cartesian or fractional coordinate.
– *Type*: 3 × 1 array

sgdata output. The output from this function is a subset of edata containing the space-group and Wyckoff-position information.

Funding information

Funding for this research was provided by: U.S. Department of Defense through the National Defense Science and Engineering Graduate (NDSEG) Fellowship Program (to David Hicks); National Science Foundation (grant No. DGF1106401 to Corey Oses); Office of Naval Research (grant No. N00014-17-1-2090 to Stefano Curtarolo); Alexander von Humboldt-Stiftung (award to Stefano Curtarolo).

References

Agapito, L. A., Curtarolo, S. & Buongiorno Nardelli, M. (2015). *Phys. Rev. X*, **5**, 011006.
Aroyo, M. I., Kirov, A., Capillas, C., Perez-Mato, J. M. & Wondratschek, H. (2006). *Acta Cryst.* A**62**, 115–128.
Aroyo, M. I., Perez-Mato, J. M., Capillas, C., Kroumova, E., Ivantchev, S., Madariaga, G., Kirov, A. & Wondratschek, H. (2006). *Z. Kristallogr.* **221**, 15–27.
Baur, W. H. & Tillmanns, E. (1986). *Acta Cryst.* B**42**, 95–111.
Belsky, A., Hellenbrandt, M., Karen, V. L. & Luksch, P. (2002). *Acta Cryst.* B**58**, 364–369.
Bergerhoff, G., Hundt, R., Sievers, R. & Brown, I. D. (1983). *J. Chem. Inf. Model.* **23**, 66–69.
Blum, V., Gehrke, R., Hanke, F., Havu, P., Havu, V., Ren, X., Reuter, K. & Scheffler, M. (2009). *Comput. Phys. Commun.* **180**, 2175–2196.
Buerger, M. J. (1947). *J. Chem. Phys.* **15**, 1–16.
Carrete, J., Mingo, N., Wang, S. & Curtarolo, S. (2014). *Adv. Funct. Mater.* **24**, 7427–7432.
Curtarolo, S., Hart, G. L. W., Buongiorno Nardelli, M., Mingo, N., Sanvito, S. & Levy, O. (2013). *Nat. Mater.* **12**, 191–201.
Curtarolo, S., Setyawan, W., Hart, G. L. W., Jahnátek, M., Chepulskii, R. V., Taylor, R. H., Wang, S., Xue, J., Yang, K., Levy, O., Mehl, M. J., Stokes, H. T., Demchenko, D. O. & Morgan, D. (2012). *Comput. Mater. Sci.* **58**, 218–226.
Fritzer, H. P. (2001). *Spectrochim. Acta A Mol. Biomol. Spectrosc.* **57**, 1919–1930.
Giacovazzo, C., Monaco, H. L., Artioli, G., Viterbo, D., Milanesio, M., Ferraris, G., Gilli, G., Gilli, P., Zanotti, G. & Catti, M. (2011). *Fundamentals of Crystallography*, 3rd ed. Oxford University Press.
Giannozzi, P., Baroni, S., Bonini, N., Calandra, M., Car, R., Cavazzoni, C., Ceresoli, D., Chiarotti, G. L., Cococcioni, M., Dabo, I., Dal Corso, A., de Gironcoli, S., Fabris, S., Fratesi, G., Gebauer, R., Gerstmann, U., Gougoussis, C., Kokalj, A., Lazzeri, M., Martin-Samos, L., Marzari, N., Mauri, F., Mazzarello, R., Paolini, S., Pasquarello, A., Paulatto, L., Sbraccia, C., Scandolo, S., Sclauzero, G., Seitsonen, A. P., Smogunov, A., Umari, P. & Wentzcovitch, R. M. (2009). *J. Phys. Condens. Matter*, **21**, 395502.

XX76

Gilmore, R. (2008). *Lie Groups, Physics, and Geometry*. Cambridge University Press.
Gonze, X., Beuken, J.-M., Caracas, R., Detraux, F., Fuchs, M., Rignanese, G. M., Sindic, L., Verstraete, M., Zerah, G., Jollet, F., Torrent, M., Roy, A., Mikami, M., Ghosez, P., Raty, J.-Y. & Allan, D. C. (2002). *Comput. Mater. Sci.* **25**, 478–492.
Groom, C. R., Bruno, I. J., Lightfoot, M. P. & Ward, S. C. (2016). *Acta Cryst.* B**72**, 171–179.
Hahn, Th. (2002). Editor. *International Tables for Crystallography*, Vol. A, *Space-group symmetry*. Dordrecht: Kluwer Academic publishers.
Hart, G. L. W., Curtarolo, S., Massalski, T. B. & Levy, O. (2013). *Phys. Rev. X*, **3**, 041035.
Hart, G. L. W. & Forcade, R. W. (2008). *Phys. Rev. B*, **77**, 224115.
Herbstein, F. H. & Marsh, R. E. (1982). *Acta Cryst.* B**38**, 1051–1055.
Hloucha, M. & Deiters, U. K. (1998). *Mol. Simul.* **20**, 239–244.
Jahnátek, M., Levy, O., Hart, G. L. W., Nelson, L. J., Chepulskii, R. V., Xue, J. & Curtarolo, S. (2011). *Phys. Rev. B*, **84**, 214110.
Jain, A., Hautier, G., Moore, C. J., Ping Ong, S., Fischer, C. C., Mueller, T., Persson, K. A. & Ceder, G. (2011). *Comput. Mater. Sci.* **50**, 2295–2310.
Karney, C. F. F. (2007). *J. Mol. Graphics Modell.* **25**, 595–604.
Kresse, G. & Furthmüller, J. (1996*a*). *Comput. Mater. Sci.* **6**, 15–50.
Kresse, G. & Furthmüller, J. (1996*b*). *Phys. Rev. B*, **54**, 11169–11186.
Kresse, G. & Hafner, J. (1993). *Phys. Rev. B*, **47**, 558–561.
Kresse, G. & Hafner, J. (1994). *Phys. Rev. B*, **49**, 14251–14269.
Le Page, Y. (1987). *J. Appl. Cryst.* **20**, 264–269.
Levy, O., Chepulskii, R. V., Hart, G. L. W. & Curtarolo, S. (2010). *J. Am. Chem. Soc.* **132**, 833–837.
Levy, O., Hart, G. L. W. & Curtarolo, S. (2010*a*). *Phys. Rev. B*, **81**, 174106.
Levy, O., Hart, G. L. W. & Curtarolo, S. (2010*b*). *J. Am. Chem. Soc.* **132**, 4830–4833.
Levy, O., Jahnátek, M., Chepulskii, R. V., Hart, G. L. W. & Curtarolo, S. (2011). *J. Am. Chem. Soc.* **133**, 158–163.
Marsh, R. E. & Herbstein, F. H. (1983). *Acta Cryst.* B**39**, 280–287.
Matano, K., Kriener, M., Segawa, K., Ando, Y. & Zheng, G. (2016). *Nat. Phys.* **12**, 852–854.
Mehl, M. J., Hicks, D., Toher, C., Levy, O., Hanson, R. M., Hart, G. L. W. & Curtarolo, S. (2017). *Comput. Mater. Sci.* **136**, S1–S828.
Nath, P., Plata, J. J., Usanmaz, D., Al Rahal Al Orabi, R., Fornari, M., Buongiorno Nardelli, M., Toher, C. & Curtarolo, S. (2016). *Comput. Mater. Sci.* **125**, 82–91.
Nath, P., Plata, J. J., Usanmaz, D., Toher, C., Fornari, M., Buongiorno Nardelli, M. & Curtarolo, S. (2017). *Scr. Mater.* **129**, 88–93.
Nespolo, M. & Souvignier, B. (2009). *Z. Kristallogr.* **224**, 127–136.
Perim, E., Lee, D., Liu, Y., Toher, C., Gong, P., Li, Y., Simmons, W. N., Levy, O., Vlassak, J. J., Schroers, J. & Curtarolo, S. (2016). *Nat. Commun.* **7**, 12315.
Plata, J. J., Nath, P., Usanmaz, D., Carrete, J., Toher, C., de Jong, M., Asta, M. D., Fornari, M., Buongiorno Nardelli, M. & Curtarolo, S. (2017). *Npj Comput. Mater.* **3**(45), 45.
Rose, F., Toher, C., Gossett, E., Oses, C., Buongiorno Nardelli, M., Fornari, M. & Curtarolo, S. (2017). *Comput. Mater. Sci.* **137**, 362–370.
Saal, J. E., Kirklin, S., Aykol, M., Meredig, B. & Wolverton, C. (2013). *JOM*, **65**, 1501–1509.
Sands, D. E. (1982). *Vectors and Tensors in Crystallography*. Reading, Massachusetts: Addison-Wesley.
Scheffler, M., Draxl, C. & Computer Center of the Max-Planck Society & Garching (2014). The *NoMaD* repository. http://nomad-repository.eu.
Setyawan, W. & Curtarolo, S. (2010). *Comput. Mater. Sci.* **49**, 299–312.
Spek, A. L. (2003). *J. Appl. Cryst.* **36**, 7–13.
Stokes, H. T. (1995). *Ferroelectrics*, **164**, 183–188.
Stokes, H. T., Campbell, B. J. & Hatch, D. M. (2017). *FINDSYM*. http://stokes.byu.edu/iso/findsym.php.
Stokes, H. T. & Hatch, D. M. (2005). *J. Appl. Cryst.* **38**, 237–238.
Supka, A. R., Lyons, T. E., Liyanage, L. S. I., D'Amico, P., Al Rahal Al Orabi, R., Mahatara, S., Gopal, P., Toher, C., Ceresoli, D., Calzolari, A., Curtarolo, S., Buongiorno Nardelli, M. & Fornari, M. (2017). *Comput. Mater. Sci.* **136**, 76–84.
Taylor, R. H., Rose, F., Toher, C., Levy, O., Yang, K., Buongiorno Nardelli, M. & Curtarolo, S. (2014). *Comput. Mater. Sci.* **93**, 178–192.
Tinkham, M. (1964). *Group Theory and Quantum Mechanics*. New York, New York: McGraw-Hill, Inc.
Togo, A. (2017*a*). *Spglib – spglib 1.10.1 documentation*. https://atztogo.github.io/spglib/.
Togo, A. (2017*b*). *Crystal symmetry – Phonopy v.1.12.6*. https://atztogo.github.io/phonopy/symmetry.html.
Toher, C., Oses, C., Plata, J. J., Hicks, D., Rose, F., Levy, O., de Jong, M., Asta, M. D., Fornari, M., Buongiorno Nardelli, M. & Curtarolo, S. (2017). *Phys. Rev. Mater.* **1**, 015401.
Toher, C., Plata, J. J., Levy, O., de Jong, M., Asta, M. D., Buongiorno Nardelli, M. & Curtarolo, S. (2014). *Phys. Rev. B*, **90**, 174107.
Wondratschek, H. & Müller, U. (2004). Editors. *International Tables for Crystallography*, Vol. A1, *Symmetry relations between space groups*. Heidelberg: Springer.
Yang, K., Oses, C. & Curtarolo, S. (2016). *Chem. Mater.* **28**, 6484–6492.

XX77